Report No. CDOT-DTD-R-98-7

Colorado Study on Transfer and Development Length of Prestressing Strand in High Performance Concrete Box Girders

Daniel E. Cooke
P. Benson Shing
Dan M. Frangopol
Department of Civil, Environmental,
& Architectural Engineering
University of Colorado
Boulder, CO 80309

University of Colorado Research Series No. CU/SR-97/4
Final Report
April, 1998

Prepared in cooperation with the
U.S. Department of Transportation
Federal Highway Administration

The contents of this report reflect the views of the author who is responsible for the facts and the accuracy of the data presented herein. The contents do not necessarily reflect the official views of the Colorado Department of Transportation or the Federal Highway Administration. This report does not constitute a standard, specification, or regulation.

REPORT DOCUMENTATION PAGE

FORM APPROVED
OMB NO. 0704-0188

1. AGENCY USE ONLY (Leave Blank)	2. REPORT DATE	3. REPORT TYPE AND DATES COVERED
	July, 1998	Final Report

4. TITLE AND SUBTITLE

Colorado Study on Transfer and Development Length of Prestressing Strand in High Performance Concrete Box Girders

5. FUNDING NUMBERS

6. AUTHORS(S)

Daniel E. Cooke, P. Benson Shing, Dan M. Frangopol

7. PERFORMING ORGANIZATION NAME(S) AND ADDRESS(S)

University of Colorado
Dept. Of Civil, Environmental and Architectural Engineering
Boulder, Colorado 80309-0428

8. PERFORMING ORGANIZATION REPORT NUMBER

CU/SR-97/4

9. SPONSORING/MONITORING AGENCY NAME(S) AND ADDRESS(S)

Colorado Department of Transportation
4201 E. Arkansas Ave.
Denver, Colorado 80222

10. SPONSORING/MONITORING AGENCY REPORT NUMBER

CDOT-DTD-R-98-7

11. SUPPLEMENTARY NOTES

Prepared in Cooperation with the U.S. Department of Transportation, Federal Highway Administration

12a. DISTRIBUTION/AVAILABILITY STATEMENT

No Restrictions: This report is available to the public through the National Technical Information Service. Springfield, VA 22161

12b. DISTRIBUTION CODE

13. ABSTRACT (Maximum 200 words)

Results of an investigation on the transfer and development lengths of Grade 270,15.2 mm (0.6 in) diameter prestressing strands spaced at 51 mm (2 in) on center in high performance concrete are presented. Three box girders with composite topping slabs were tested. These girders were 381 mm (15 in) wide, 553 mm (21.75 in) high, including the topping slab, and 10,400 mm (411 in) long. The compressive strength, moduli of elasticity and rupture, split cylinder strength, and shrinkage were measured at different ages. Compressive strength for the main girder section was approximately 54 Mpa (7.8 ksi) at release, and 77 Mpa (11 ksi) at the time of development length tests, while the topping slab concrete was approximately 57 Mpa (8.3 ksi). The girders were pretensioned using nine strands with a strand stress immediately before release of about 1407 Mpa (204 ksi). The strand was supplied by a single manufacturer. Pullout tests were conducted on samples of prestressing strand, and strand slip at stress transfer was measured. Transfer length was determined by measuring concrete surface strain with mechanical strain gages. Strain profiles were constructed from these measurements, and the 95% Average Maximum Strain Plateau method was used to determine the transfer length at each girder end. The development length was measured using an iterative testing process involving six flexural tests. Each girder was loaded to failure at a distance from the girder end equal to the estimated development length. The estimated development length was revised after each test until the required development length was found. Deflections, strand slip, concrete surface strain, and applied load were monitored. The development length for these girders was determined to be approximately 1524 mm (60 in). The ACI/AASHTO formulas over-estimate the transfer length of the girders by 18%, and the development length by 53%. The average maximum pullout force attained in the strand pullout tests was 215 kN (48 kips). The average strand slip at stress transfer was 1.49 mm (0.059 in).

14. SUBJECT TERMS

High Performance Concrete | Transfer Length | Pullout Test
Development Length | Prestressing Strand

15. NUMBER OF PAGES

168

16. PRICE CODE

17. SECURITY CLASSIFICATION OF REPORT	18. SECURITY CLASSIFICATION OF THIS PAGE	19. SECURITY CLASSIFICATION OF ABSTRACT	20. LIMITATION OF ABSTRACT
Unclassified	Unclassified	Unclassified	

ABSTRACT

In this report, results of an investigation on the transfer and development lengths of Grade 270, 15.2 mm (0.6 in.) diameter prestressing strands spaced at 51 mm (2 in.) on center in a hex close packed pattern in high performance concrete are presented. Three box girders with composite topping slabs were tested. These girders were 381 mm (15 in.) wide, 553 mm (21.75 in.) high, including the topping slab, and 10,400 mm (411 in.) long.

The compressive strength, modulus of elasticity, modulus of rupture, split-cylinder strength, creep, and shrinkage of the girder concrete were measured at different ages. Concrete compressive strength for the main girder section was approximately 54 MPa (7.8 ksi) at release and 77 MPa (11 ksi) at the time of development length tests, while the strength of the topping slab concrete was approximately 57 MPa (8.3 ksi) at the time of development length tests. The girders were pretensioned using nine strands with a strand stress just before release of about 1407 MPa (204 ksi). The strand was supplied by a single manufacturer. Pullout tests were conducted on samples of prestressing strand and strand slip at stress transfer was measured.

Transfer length was determined by measuring concrete strain at the concrete surface with a mechanical strain gage. Strain profiles were constructed from these measurements and the 95% Average Maximum Strain Plateau method was used to

determine the transfer length at each end of a girder. The average transfer length for these girders was determined to be 593 mm (23.4 in.).

The development length was measured using an iterative testing process involving six flexural tests. Each end of a girder was loaded to failure at a distance from the end of the girder equal to the estimated development length. The estimated development length was revised after each test until the required development length was found. Deflections, strand slip, concrete surface strain, and applied load were monitored throughout each test. The development length for these girders was determined to be approximately 1524 mm (60 in.).

The ACI/AASHTO formulas for transfer and development length overestimate the transfer length of the girders by 18% and the development length by 53%. The average maximum pullout force attained in the strand pullout tests was 215 kN (48 kips). The average strand slip measured at stress transfer was 1.49 mm (0.059 in.).

ACKNOWLEDGMENTS

This study was sponsored by the Federal Highway Administration as part of a Colorado showcase project on the use of high performance concrete for prestressed concrete bridge girders. The assistance and input provided by Susan Lane, Donald Magura, Gail Kelley, and Matthew Greer of the Federal Highway Administration in this project are gratefully acknowledged.

Mark Leonard of the Colorado Department of Transportation was instrumental in the coordination and execution of this project. Michael McMullen of the Colorado Department of Transportation was responsible for the design of the test girders.

The writers appreciate the invaluable assistance of Nat Jansen of the Federal Highway Administration, and Werner Hutter and David Price of the Colorado Department of Transportation in the instrumentation of the test girders, and the help of Sam Scupham, Mike Meiggs, Ann Grooms, and Keith Ostrander, undergraduate students at the University of Colorado, in carrying out the experimental work. The technical advice provided by Donald Logan of Stresscon on strand pullout tests is also appreciated.

The girders were fabricated at Rocky Mountain Prestress in Denver, Colorado. The writers would like to thank the personnel at Rocky Mountain Prestress for their patience and help in the fabrication process. Special thanks to Howard Knapp of Rocky Mountain Prestress for his assistance and cooperation.

TABLE OF CONTENTS

LIST OF FIGURES

LIST OF TABLES

1. INTRODUCTION

1.1 BACKGROUND AND PROBLEM STATEMENT

During the last 40 years, prestressed concrete has seen increasing use in structural design, particularly in bridge structures. Prestressed concrete offers substantial benefits to the bridge designer, especially in spanning long distances and maintaining a large span-to-depth ratio. Over the years, these abilities have been enhanced by the use of higher strength concrete and larger diameter, higher strength prestressing strands.

The force in prestressing strand is transferred to the concrete in pretensioned members by bond between the strand and the concrete. Increases in concrete strengths, strand diameters, and strand strengths have led to greater strand forces, and thus, increased demand on the bond. For safe and effective use of these new materials, the nature of the bond must be fully understood.

In 1988, the Federal Highway Administration (FHWA) issued a memorandum which required that the required development length be increased to 1.6 times the development length stipulated in the AASHTO Specifications [1]. Additionally, the minimum spacing of strands must be four times the strand diameter and the use of 15.2 mm (0.6 in.) diameter strand was disallowed. These requirements were instituted because the AASHTO formulas are based on tests using lower strength materials and

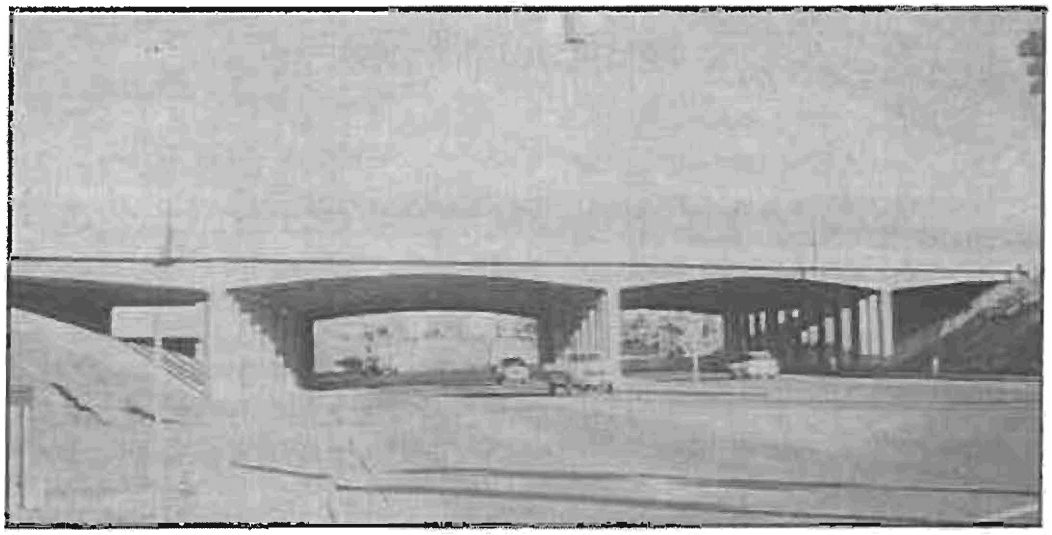

Figure 1.1 - Existing Bridge at I-25 over Yale Avenue

smaller strand diameters and because recent test results had led to the questioning of the conservatism of these formulas.

As a result of this memorandum, a number of research programs were initiated to investigate the bond, and transfer and development length in prestressed concrete. This study was initiated in April, 1996, as part of a larger project being carried out by the Colorado Department of Transportation (CDOT) in conjunction with the University of Colorado (CU).

The project involves the replacement of the existing bridge at Interstate 25 over Yale Avenue in Denver, Colorado with a new design utilizing high performance concrete (HPC) and Grade 270, 15.2 mm (0.6 in.) diameter prestressing strands in side-by-side box girders. The existing 65 m (215 ft.) long, four-span, cast-in-place, T-girder bridge, shown in Figure 1.1, is structurally deficient. This bridge is being replaced by a two-span bridge, as shown in Figure 1.2, utilizing side-by-side, precast, pretensioned box girders with a composite deck. This program was sponsored by

FHWA as one of the nationwide showcase projects on the use of HPC in bridge structures.

The box girders, shown in Figure 1.3, are 1700 mm (66.9 in.) wide by 750 mm (29.5 in.) deep and are pretensioned with Grade 270, 15.2 mm (0.6 in.) diameter prestressing strands spaced at 51 mm (2 in.) on center. The concrete strength for these

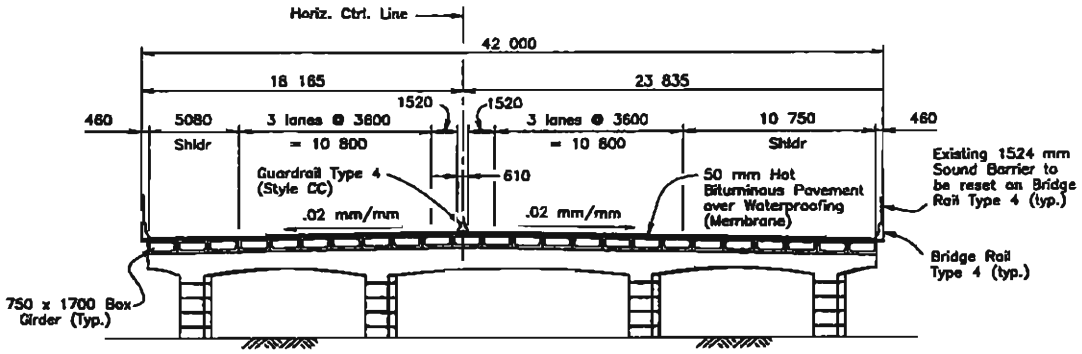

Typical Transverse Section

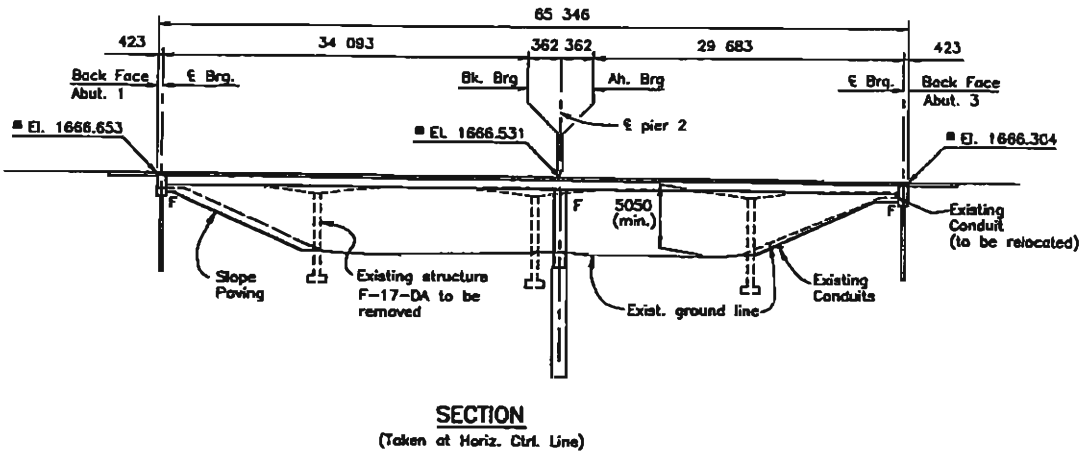

Longitudinal Section

Figure 1.2 - Replacement Bridge

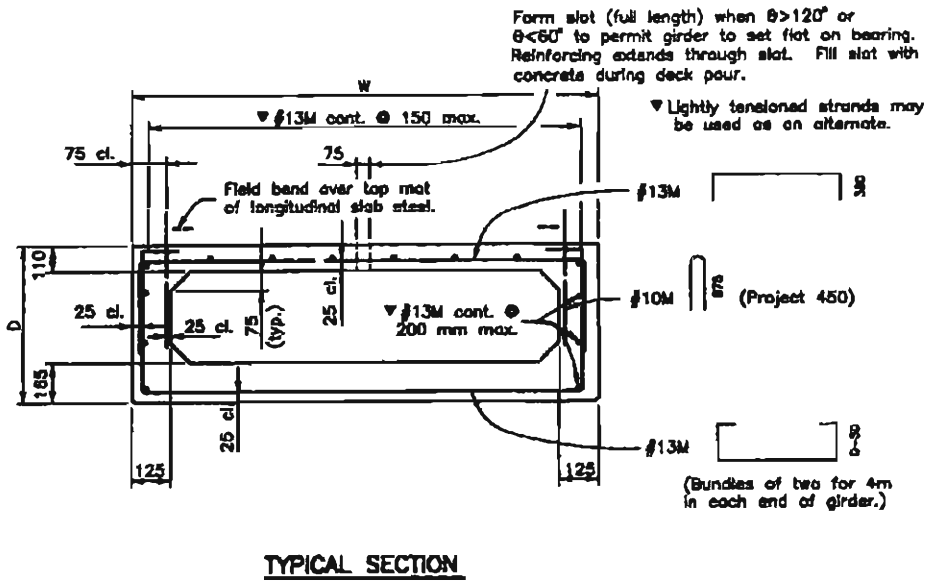

Figure 1.3 - New Bridge Girder (Strands in Bottom Flange not Shown)

girders was specified to be 45 MPa (6.5 ksi) at transfer and 69 MPa (10 ksi) at 56 days after casting. The use of high performance concrete and large diameter strand was necessary to achieve the desired long spans while maintaining a high span-to-depth ratio. The maximum span-to-depth ratio of the bridge girders is about 40. The use of high performance concrete was also desirable from a durability standpoint. The concrete for the topping slab was specified to have a compressive strength of 40 MPa (5,800 psi).

A number of girders and portions of the deck of the completed bridge will be instrumented to measure temperature and strain variations, and to determine the behavior of the superstructure under prestress loss, creep, shrinkage, temperature changes, and dead and live loads.

1.2 OBJECTIVES AND SCOPE OF THIS STUDY

At the time this project was initiated, the use of 15.2 mm (0.6 in.) diameter strand at 51 mm (2 in.) spacing was prohibited by FHWA unless there was experimental verification demonstrating the adequacy of the transfer and development length provided. This test program was conducted to satisfy this requirement.

The primary objective of this study was to demonstrate the adequacy of the transfer length and development length of the strands to be used in the prestressed concrete bridge girders in the new bridge mentioned previously. Specifically, pursuant to FHWA's objectives, this project was intended to provide data for the transfer length and development length of 15.2 mm (0.6 in.) diameter strands at 51 mm (2 in.) spacing in a high strength (10 ksi) concrete. A secondary objective was to verify the instrumentation techniques to be used in the actual bridge.

Three girders of identical designs were cast for use in the testing program. These girders, designed by CDOT, were scaled down versions of the actual girders to be used in the bridge. The strand size and spacing, concrete strengths, and strand stresses at the ultimate flexural capacity were approximately the same as those in the actual girders. Both ends of the girders were instrumented at the time of casting to determine the transfer length. The girders were tested to failure in an iterative process to determine the development length.

1.3 ORGANIZATION OF REPORT

Chapter 2 of this report provides background information on theories and other studies pertaining to transfer and development length of pretensioned members. In Chapter 3, the test program is described in detail. The results of the tests are presented in Chapter 4. In Chapter 5, the test results are discussed and compared to the values calculated with the formulas given in the AASHTO Specifications [1] and with formulas developed in previous research. A summary of this study and the conclusions drawn from it are presented in Chapter 6.

2. TRANSFER AND DEVELOPMENT LENGTH

In a prestressed concrete member, the prestressing force is transferred to the concrete through the bond between the strand and concrete. The bond length necessary for this transfer is termed the transfer length. The total embedment length of strand required to develop the maximum flexural capacity at a critical section of a member is termed the development length.

Previous research has indicated that a number of variables can affect the transfer and development length. To date, no comprehensive theory has been developed which can accurately account for the influence of all of these variables. However, many empirical and semi-empirical design equations have been proposed to assess transfer and development length.

In this chapter, previous research on transfer and development length of prestressing strands is reviewed. First, early research and development of the ACI and AASHTO formulas for transfer and development length are presented. Results of later research and concerns raised about the conservatism of these formulas are then discussed. Finally, design equations proposed by different researchers are summarized.

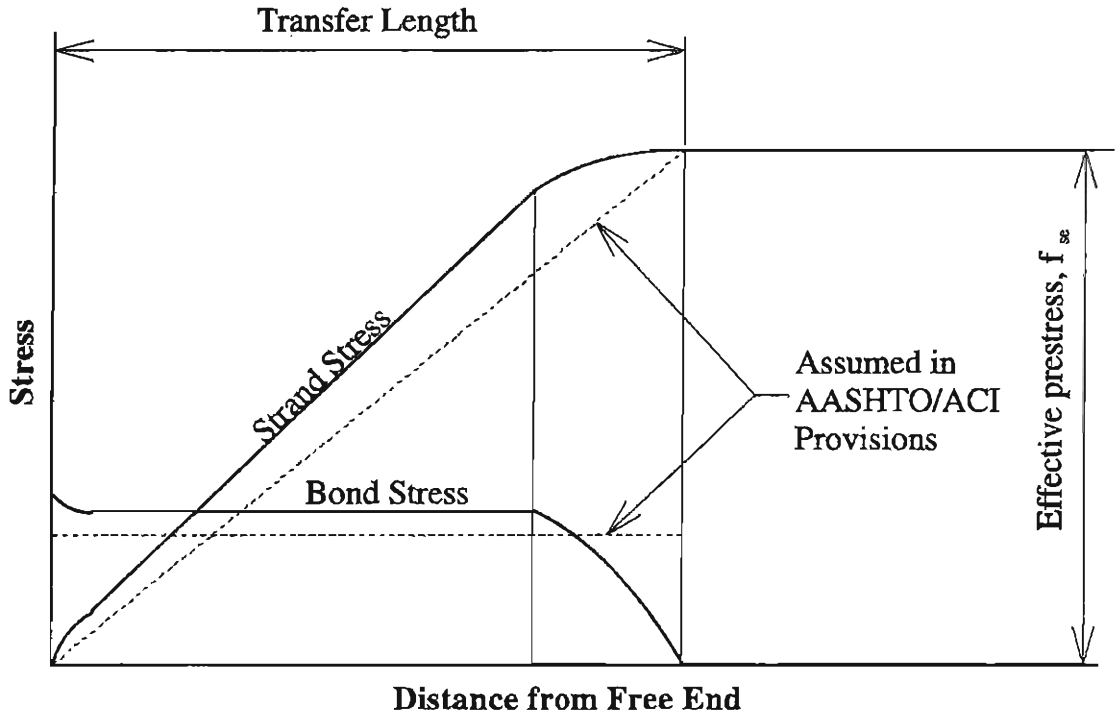

Figure 2.1 - Steel and Bond Stresses in the Transfer Region

2.1 BASIC CONCEPTS

2.1.1 Transfer Bond Stress and Length

Transfer length, shown in Figure 2.1, is the embedment length of strand over which the prestress force is transferred to the concrete. The length of embedded strand required to transfer this force depends on the bond stress developed between the strand and the concrete.

Bond stress in the transfer region is developed primarily through mechanical interlock and frictional resistance [11]. These mechanisms develop when the strand slips relative to the concrete. Upon release of the prestressing force, slip occurs throughout the transfer region, destroying any chemical adhesion which may have

developed between the strand and the concrete. The magnitude of this slip varies from zero at the end of the transfer region to a maximum at the free end of the strand.

Frictional resistance is enhanced through mechanical interlock and radial expansion of the strand. Radial expansion of the strand occurs as a result of Poisson's effect and develops in proportion to the reduction in stress the strand experiences from the jacking force. Upon transfer of prestress, strand stress is reduced in the transfer zone due to slip and the elastic shortening of the beam. This reduction in stress leads to radial expansion of the strand. The concrete resists this expansion, leading to the development of radial stress and, thus, enhancement of the frictional forces between the concrete and the strand.

At the free end of the strand, the entire prestress is lost, and the strand tends to return to its original unstressed diameter. This results in the development of significant frictional resistance. It is referred to as Hoyer effect. The reduction in stress and, thus, the radial expansion of the strand decreases as the end of the transfer region is approached. Therefore, the contribution to frictional resistance from this effect is reduced as the end of the transfer region is approached.

Mechanical interlock is developed due to the helical shape of prestressing strand. If the strand is restrained from twisting throughout the concrete, resisting forces, similar to those developed by the deformations provided on ordinary reinforcing bars, develop along the interface between the outer wires of a strand and the concrete. The frictional resistance developed at the free end of the strand due to

radial expansion arrests twisting of the strand. Thus, mechanical interlock forces are able to develop throughout the transfer region.

The actual variation of bond stress in the transfer region is difficult to characterize precisely. However, based on experimental data, a generally accepted model for the variation of bond stress in the transfer region has been developed [1, 2, 11].

As shown in Figure 2.1, bond stress is a maximum near the free end of the strand where resistance due to radial expansion of the strand and mechanical interlock are fully effective. As the resistance due to radial expansion of the strand decreases, the bond stress drops off to an approximately constant value. Near the end of the transfer region, slip and bond stresses drop to a value of zero.

Strand stress is directly related to bond stress through equilibrium and can, thus, be inferred from the bond stress distribution. As shown in Figure 2.1, strand stress increases progressively from zero at the free end of the strand to the effective prestress at the end of the transfer region. Steel stress varies approximately linearly with distance throughout most of the transfer region, with nonlinear regions at the beginning and the end of the transfer region due to the changes in bond stress.

2.1.2 Flexural Bond Stress and Length

Flexural bond length, shown in Figure 2.2, is defined as the length of prestressing strand beyond the transfer zone that is required to anchor the strand sufficiently to develop the maximum strand stress at ultimate flexural failure. This

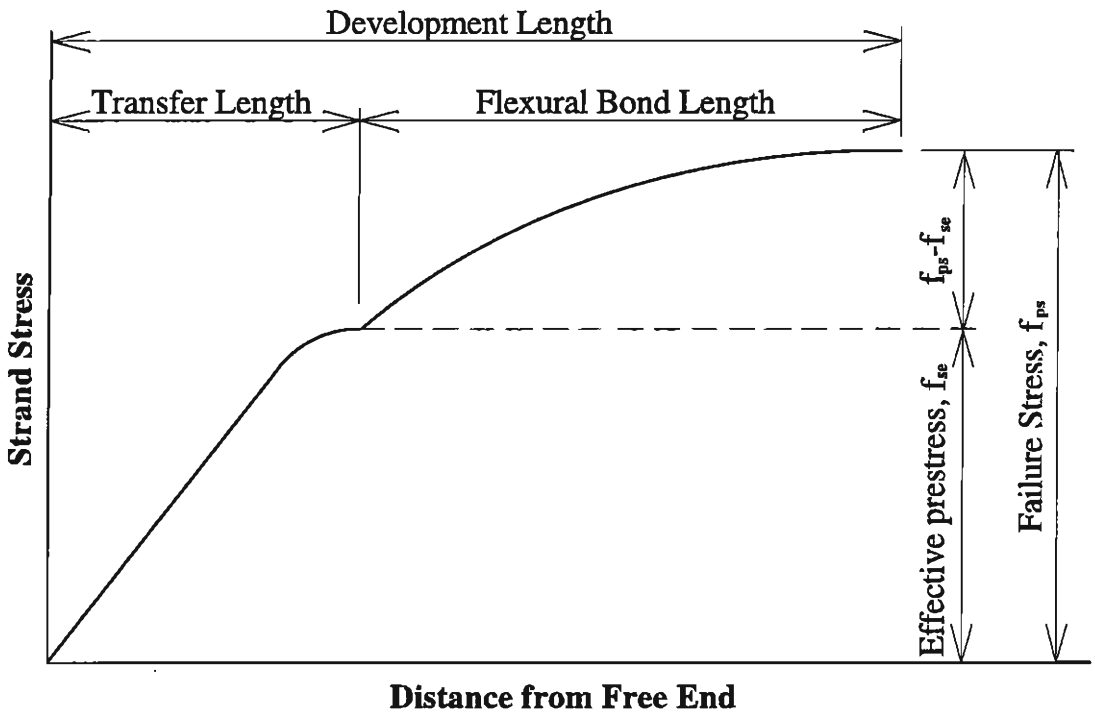

Figure 2.2 - Strand Stresses at Bond Failure

length depends on the flexural bond stress developed between the strand and the concrete.

As load is applied to a member, strand tension and flexural bond stress increases. Before concrete cracking occurs, the increase in bond stress is typically very small and no slip occurs in the flexural bond length region [11]. Thus, chemical adhesion contributes to the bond in this region.

Upon the appearance of a crack, there is a transfer of stress from the concrete to the strand in the cracked region. The bond stress demand increases dramatically in this region. Upon reaching the limiting bond stress value, localized strand slip occurs, which leads to a redistribution and relief of these high bond stresses over a greater length of strand [11].

Chemical adhesion is destroyed in the localized slip region, and mechanical interlock and frictional resistance are responsible for maintaining the bond stress. Furthermore, because strand stress in a cracked region is greater than the initial prestress, the strand shrinks in diameter, and frictional resistance due to radial expansion of the strand is reduced.

As the load continues to increase, flexural cracking propagates towards the ends of the member and flexural bond stresses continue to increase. This progression has been characterized as a wave of flexural bond stresses moving towards the ends of the specimen [11].

If the external loading on a member is large enough, the member will fail in shear or flexure, or the increase in flexural bond stress will reach the transfer region. Bond stress in the transfer region is considered to be at the limiting bond stress value. Thus, if bond stress is further increased, due to the flexural bond stress, the limiting bond stress value will be exceeded in the transfer region and a general bond failure will occur.

Previous studies have noted that, in addition to flexural cracking, web shear cracking can lead to bond failure [8, 16]. It is not clear, however, whether the ultimate failures observed were introduced by shear failure leading to bond failure or, conversely, bond failure leading to shear failure [5]. However, theoretically, any cracks which propagate into the strand anchorage zone at the strand level could lead to a sufficient increase in bond stress to precipitate a general bond failure.

The assumed state of strand stress just before general bond failure is shown in Figure 2.2. The strand stress is assumed to vary along a smooth curve from the effective prestress at the end of the transfer region to the maximum strand stress at failure at the critical section. In reality, the flexural bond stress may be significantly higher in cracked regions. However, this variation is smoothed out, to some extent, by strand slip and the accompanying redistribution of bond stress.

2.1.3 Development Length

Development length is defined as the total embedment length of strand required to develop the maximum flexural capacity at a critical section of a member. It is calculated as the sum of the transfer length and the flexural bond length, as shown in Figure 2.2.

2.1.4 Parameters affecting Transfer and Development Length

Transfer and development length are affected by a number of parameters. These parameters include:

- Strand diameter
- Spacing of strand
- Manufacturing process of strand
- Surface condition of strand
- Strand stress
- Strength, consistency, and degree of consolidation of concrete around strand

- Concrete cover
- Confinement steel
- Type of release
- Type of loading
- Time dependent effects

The parameters which are thought to have the greatest influence on transfer and development length are discussed in more detail below.

2.1.4.1 Strand Diameter

Experimental results indicate that transfer and development length tends to increase in an almost linear manner with increases in strand diameter, d_b [8, 10, 11, 16, 18, 19]. This relationship can be demonstrated theoretically by setting the force in the steel equal to the total bond force over the embedment length as follows.

$$\mu l_e \Sigma_o = f_s A_s \qquad (2\text{-}1)$$

in which μ is the average bond stress over the embedment length, l_e, Σ_o is the perimeter of the strand, f_s is the strand stress at l_e, and A_s is the area of the strand.

Substituting πd_b for the strand perimeter, $\pi d_b^2/4$ for the strand area, and solving for the embedment length, one has

$$l_e = \frac{f_s}{4\mu} d_b \qquad (2\text{-}2)$$

Thus, for a given bond strength and steel stress, the required embedment length is linearly proportional to the strand diameter.

2.1.4.2 Manufacturing Process of Steel

The manufacturing process used to produce prestressing strand has been considered as the main contributor to the variation of strand bonding capacity [13]. The lubricant used and lay of the strand are thought to contribute the most variability to bonding capacity. Differences in the lay of the strand can affect mechanical interlock, while the lubricant used can affect frictional resistance.

2.1.4.3 Surface Condition of Strand

Strand condition at the time of casting has been shown to significantly influence bonding capacity [6, 8, 10, 11, 12]. In the process of manufacturing and installing strand, the strand surface can be contaminated by various chemicals. These chemicals include various stearates left over from the manufacturing process and various form release agents used in casting of prestressed members. Uncoated strand may also rust if not protected from weathering. The resulting surface conditions can have a significant effect on the adhesion and friction developed between strand and concrete and can, thus, severely affect bond capacity. Generally, a rusted, relatively contaminant free strand will develop a greater bond stress than an unrusted, contaminated strand. Additionally, epoxy coated strand with embedded grit, will typically sustain higher bond stress than an uncoated strand [6, 13].

2.1.4.4 Strength, Consistency, and Degree of Consolidation of Concrete Around Strands

The quality of the concrete used in a member has a significant effect on the bond developed between the concrete and the strand. Higher strength concrete has

demonstrated higher bond stress capacity than lower strength concrete [12, 16]. This appears to stem from the higher stiffness of the concrete and its greater capacity to resist high shear forces at the concrete to strand interface. The concrete must be in good contact with the strand and of consistent quality to develop the bond mechanisms discussed previously. Thus, higher bond capacity is achieved with increased consistency and degree of consolidation of the concrete around the strands [3, 4].

2.1.4.5 Type of Release

The manner in which prestress is released, gradual or sudden, has been shown to significantly affect transfer length. Typically, sudden release, by flame or saw cutting, results in a 20% to 30% longer transfer region than that obtained using a gradual release method [12].

2.1.4.6 Strand Stress

The steel stress at transfer of prestress clearly affects the required transfer length. With increases in steel stress, for a given bond stress, the transfer region must also increase in length to maintain equilibrium. This relationship is evident in Eq. (2-2) where, for a given bond stress and strand diameter, the required embedment length is directly proportional to the strand stress.

The strand stress at failure affects the required flexural bond length. As strand stress increases, bond stress demand increases, while strand diameter and, thus,

frictional resistance decreases. The increasing bond stress demand and decreasing frictional resistance lead to a longer flexural bond length requirement.

2.2 EARLY RESEARCH

2.2.1 Study by Janney

In1954, Janney published the results of one of the pioneering studies on the nature of bond in prestressed concrete [11]. In this study, Janney developed methods for measuring transfer and flexural bond in specimens which are still used today. He also proposed a theoretical model for transfer length and a generally accepted theory for flexural bond stress behavior.

Janney's experimental program consisted of two test series. The first investigated transfer bond, and the second investigated flexural bond. In each series, concrete prisms of varying strength were cast and prestressed with wire or strand of varying diameters.

2.2.1.1 Transfer Bond Model

To measure transfer bond stresses, strains along the length of each prism were measured after prestress release. From these measurements, the variation of strand stress and transfer bond stress with length was deduced.

As part of this investigation, Janney also proposed an approximate model for the variation of transfer bond stress, which is presented in the following.

The transfer bond model developed by Janney assumes that transfer bond is affected by friction only and is based on an elastic thick-walled cylinder analogy. The following derivation is adapted from Janney's report.

A reduction of tension at any point along a pretensioned wire, which is free to expand, from an initial value f_{s0} to a value f_s will result in an increment of radius as follows.

$$\Delta r_1 = r(f_{s0} - f_s)\frac{\nu_s}{E_s} \qquad (2\text{-}3)$$

in which ν_s is Poisson's ratio of the wire, E_s is the elastic modulus of the steel, and r is the radius of the wire.

However, if the wire is surrounded by concrete, the actual increase in radius must be compatible with the radial displacement of the concrete. When the concrete section is large in comparison with the wire radius, the elastic theory of a thick-walled cylinder gives the following change of the wire radius due to the radial stress imposed by the surrounding concrete.

$$\Delta r = r\sigma_r \frac{1+\nu_c}{E_c} \qquad (2\text{-}4)$$

in which σ_r is the radial stress in the wire, ν_c is Poisson's ratio of the concrete, and E_c is the elastic modulus of the concrete. The radial stress in the wire is equal to the contact pressure between the steel and concrete and can be found by the following equation.

$$\sigma_r = \frac{\Delta r_1 - \Delta r}{r(1-\nu_s)} E_s = \frac{(f_{s0} - f_s)\nu_s - \sigma_r(1+\nu_c)\frac{E_s}{E_c}}{(1-\nu_s)} \qquad (2\text{-}5)$$

which results in

$$\sigma_r = \frac{(f_{s0} - f_s)\nu_s}{(1-\nu_s)+(1+\nu_c)\frac{E_s}{E_c}} \qquad (2\text{-}6)$$

From equilibrium, the bond stress at any point, μ, is

$$\mu = \frac{df_s}{dl}\frac{r}{2} \qquad (2\text{-}7)$$

If the bond is entirely due to friction, it is directly related to σ_r by the coefficient of friction ϕ. This leads to

$$\mu = \phi\sigma_r \qquad (2\text{-}8)$$

Substituting Eq. (2-8) in Eq. (2-7) yields

$$dl = \frac{r}{2\phi\sigma_r} df_s \qquad (2\text{-}9)$$

Substituting σ_r from Eq. (2-6) into the above equation and integrating it with the boundary condition that f_s=0 at l=0, one obtains

$$l = \frac{-r\left[(1-\nu_s)+(1+\nu_c)\frac{E_s}{E_c}\right]\ln\frac{f_{s0}-f_s}{f_{s0}}}{2\phi\nu_s} \qquad (2\text{-}10)$$

or

$$\ln\frac{f_{s0}-f_s}{f_{s0}} = -\frac{2\phi\nu_s l}{r\left[(1-\nu_s)+(1+\nu_c)\frac{E_s}{E_c}\right]} \qquad (2\text{-}11)$$

Equation (2-11) is plotted in Figure 2.3 for various values of the friction coefficient, ϕ, with f_{s0} = 1407 MPa (204 ksi), r = 7.6 mm (0.3 in.), ν_s = 0.29, ν_c = 0.15, E_s = 197879 MPa (28700 ksi), and E_c = 34474 MPa (5000 ksi). The shape of these curves is similar to experimentally observed stress transfer distributions.

As Janney pointed out, this model has several shortcomings and is only useful as a qualitative model of transfer bond stress behavior. The primary problems with this model stem from the use of friction as the only bond mechanism and the assumption of elastic behavior.

For prestressing wire, friction is undoubtedly the largest contributor to bond strength in the transfer region. However, for prestressing strand, it is generally agreed that mechanical interlock contributes a significant portion of the transfer bond strength and that this contribution cannot be neglected.

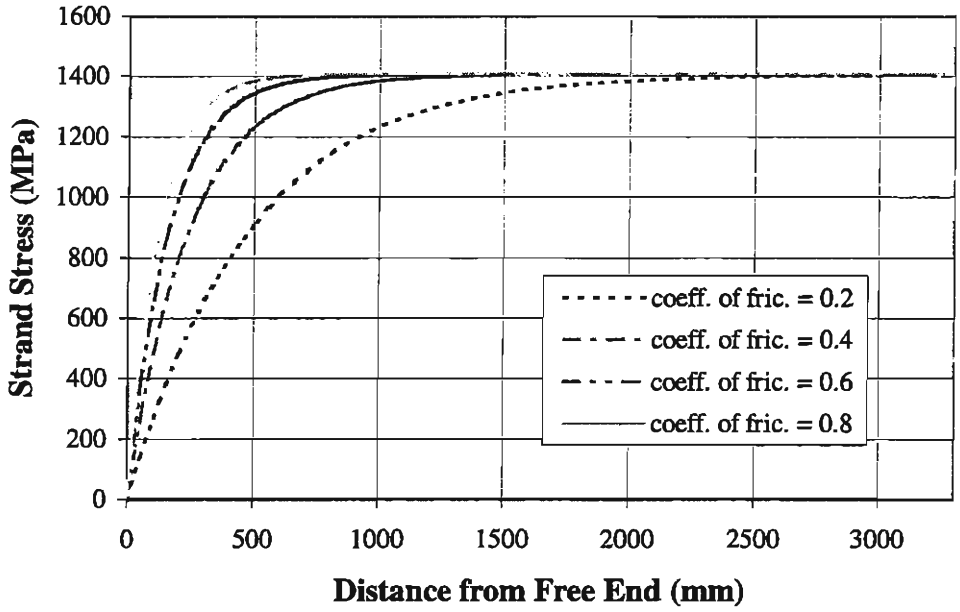

Figure 2.3 - Theoretical Stress Transfer Distribution for 15.2 mm (0.6 in.) Diameter Strand

Additionally, the assumption of elastic concrete behavior is violated for much of the first portion of the transfer region. For example, with the parameters used to generate the curves in Figure 2.3, Eq. (2-6) leads to

$$\sigma_r = 0.0382(f_{s0} - f_s)$$

At the end of a member, where the entire prestress of 1407 MPa (204 ksi) is released, the resulting radial compression, σ_r, is 53.7 MPa (7.8 ksi). For elastic conditions and small wire diameter, the tangential tension in the concrete at the interface would be approximately equal to the radial compression of 53.7 MPa (7.8 ksi), which is well beyond the elastic limit of concrete in tension. Thus, this theory would not be expected to model the bond stress in an accurate manner for a significant portion of the transfer region.

2.2.1.2 Flexural Bond

To measure flexural bond stresses, short beam specimens were loaded to failure by Janney using centerpoint loading [11]. Strand strain was measured at selected points along the strand using electrical strain gages. From these measurements, average flexural bond stresses at failure were deduced along the length of the specimens.

The results of these tests indicate that, as the load increases, flexural bond stresses increase and progress towards the end of the beam in a wave-like fashion. Janney assumed that if this wave of flexural bond stress reached the transfer region before flexural failure occurred, a general bond failure along the strand length would occur. This theory was subsequently confirmed by Hanson and Kaar and is the commonly accepted model for flexural bond stress behavior today [10].

2.2.2 Study by Hanson and Kaar

In 1959, Hanson and Kaar published the results of their study of flexural bond in pretensioned beams [10]. The objectives of their investigation were to develop a theory of bond action predicting ultimate strength in bond and to study the influence of various factors on bond performance of prestressing strand. The test program involved the investigation of the flexural bond strengths in 47 beam specimens prestressed with Grade 250 strand. Strand diameters of 6.4, 9.5, and 12.7 mm (0.25, 0.375, and 0.5 in.) were used in the study. Concrete strengths at 28 days ranged from 35 MPa (5.0 ksi) to 54 MPa (7.8 ksi).

Each specimen was instrumented with strain gages and tested to failure. Steel strains during testing were continuously recorded and were converted to steel stresses for use in the analysis of flexural bond stresses.

Hanson and Kaar calculated the average flexural bond stresses for their test specimens and derived equations to predict bond stress at general bond failure. Based on this model, they were able to suggest minimum embedment lengths to develop full strand strength at failure.

Average flexural bond stresses were calculated based on equilibrium. Setting the force in the strands equal to the force due to bond stresses yields

$$\mu l_e \Sigma_o = f_s A_s \qquad (2\text{-}12)$$

in which all the terms have been defined previously.

Solving for the average bond stress, μ, yields

$$\mu = \frac{f_s A_s}{l_e \Sigma_o} \qquad (2\text{-}13)$$

Applying this equation to their experimental results, they were able to calculate the average bond stress at general bond slip for each of the embedment lengths tested. Their results for the 12.7 mm (0.5 in.) diameter strand used in their study are shown in Figure 2.4.

Equation (2-13), with the appropriate values for A_s and Σ_o and with f_s equal to the ultimate strand stress, was also used to calculate the average bond stress required to develop the ultimate strength of a particular strand for particular embedment

lengths. The values derived by Hanson and Kaar for the 12.7 mm (0.5 in.) diameter strand used in their study are plotted as the heavy line in Figure 2.4.

Hanson and Kaar then attempted to find the variation of the flexural bond stress immediately prior to general bond failure. The average transfer bond stress was assumed equal to 2.8 MPa (400 psi) for any strand diameter and the flexural bond stress curve was assumed to be smooth with a peak value of 2.8 MPa (400 psi) at the end of the transfer region. The average transfer bond stress of 2.8 MPa (400 psi) was based on prior tests performed at the Portland Cement Association. Based on these assumptions, they derived a curve which represented the lower limiting values of bond stress at general slip versus distance from the end of the transfer region for all strand diameters. Using this curve, they were able to calculate the average bond stress over a particular embedment length at which general bond slip would occur. These values have been plotted for various embedment lengths to form the curve shown in Figure 2.4 as a thin line.

In Figure 2.4, the embedment length at which the thin and the heavy lines intersect is the minimum required embedment length for 12.7 mm (0.5 in.) diameter strand if the ultimate strength of the strand is to be developed before general bond failure occurs. Hanson and Kaar derived similar curves for each strand diameter investigated and recommended minimum embedment lengths based on the embedment lengths at which the respective curves intersected. For Grade 250 strand which is gradually released, initially prestressed to about 1034 MPa (150 ksi), and embedded in concrete with a compressive strength of about 36 MPa (5.5 ksi), they

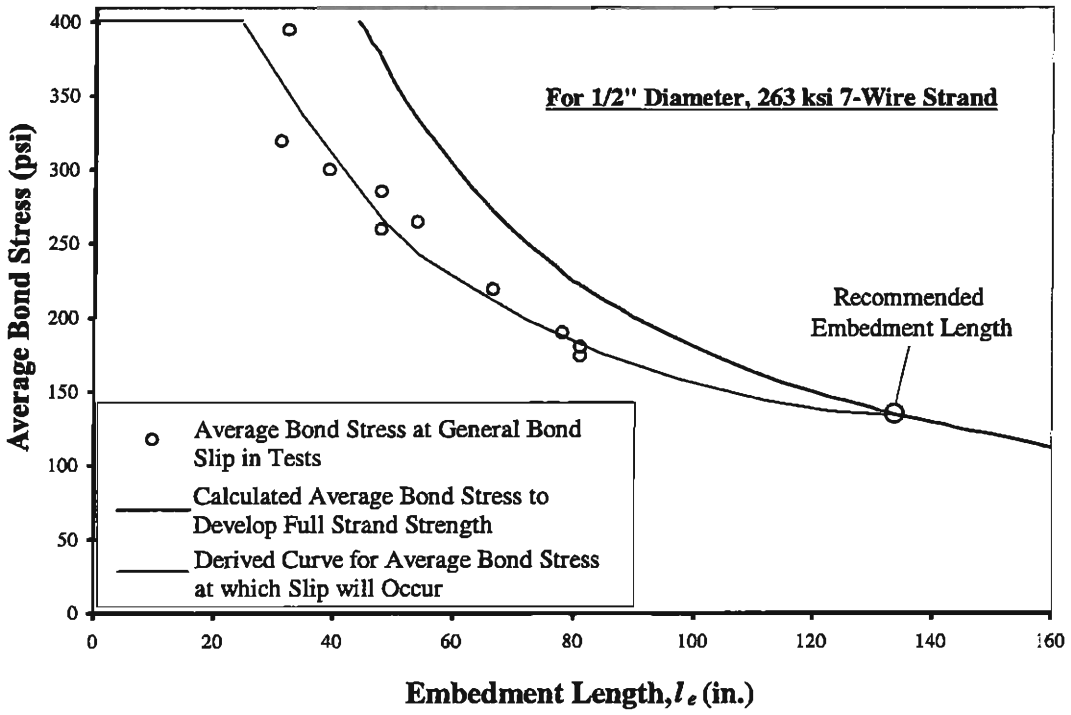

Figure 2.4 - Variation of Average Bond Stress with Embedment Length (1 in. =25.4 mm; 1 psi = 6.89x10^3 Pa)

suggested minimum embedment lengths of 1778 mm (70 in.) for 6.4 mm (0.25 in.) strand, 2692 mm (106 in.) for 9.5 mm (0.375 in.) strand, and 3404 mm (134 in.) for 12.7 mm (0.5 in.) strand. These values are significantly larger than those obtained using the current ACI expressions for development length, which are based, in part, on this study.

2.2.3 Study by Kaar, LaFraugh, and Mass

In 1963, Kaar et al. published the results of their study on the influence of concrete strength on strand transfer length [12]. The test program involved the investigation of the transfer lengths of 18 beam specimens prestressed with stress relieved Grade 250 strand. Strand diameters of 6.4, 9.5, 12.7, and 15.2 mm (0.25,

0.375, 0.5, and 0.6 in.) were used in the study. Concrete strengths at 28 days ranged from 11 MPa (1.6 ksi) to 38.6 MPa (5.6 ksi).

Strains were measured along the length of each specimen and used to deduce the transfer length. Average transfer lengths of 267, 572, 876, and 889 mm (10.5, 22.5, 34.5, and 35 in.) were reported for strand diameters of 6.4, 9.5, 12.7, and 15.2 mm (0.25, 0.375, 0.5, and 0.6 in.), respectively.

Using these results, the authors concluded that transfer length varies approximately linearly with strand diameter. The slope of this line, for an effective prestress of 1207 MPa (175 ksi), was equivalent to a uniform bond stress of approximately 1.7 MPa (250 psi). It should be noted that this bond stress is significantly lower than the value of 2.8 MPa (400 psi) cited in the study by Hanson and Kaar [10]. The authors also concluded that concrete strength had no significant influence on transfer length. This contradicts other studies [12,16].

2.3 ACI/AASHTO EQUATIONS

The current ACI and AASHTO equations for transfer and development length are essentially identical. The expressions were derived by Mattock and are based primarily on the test results of Hanson and Kaar [10], and Kaar et al. [12]. The expressions developed were first introduced in the 1963 edition of the ACI-318 Building Code, and were subsequently adopted in the AASHTO specifications in 1973.

2.3.1 Transfer Length

The expression for transfer length, as presented in the AASHTO Specifications [1] and ACI-318 [2], is

$$L_t = \frac{f_{se}}{3} d_b \qquad (2\text{-}14)$$

in which L_t is the transfer length in inches, f_{se} is the effective prestress in ksi, and d_b is the nominal strand diameter in inches.

This expression for transfer length was derived using the average transfer bond stress of 2.76 MPa (400 psi) reported by Hanson and Kaar in their 1959 study. Although Hanson and Kaar did not provide specific published results to support this value, Mattock felt that this value was reasonable.

Using this information, and the fact that the transfer bond force must be equal to the force in the prestressing steel, one has

$$\mu \Sigma_o L_t = A_s f_{se} \qquad (2\text{-}15)$$

where

μ = average bond stress = 2.76 MPa (0.4 ksi)
Σ_o = actual circumference of 7-wire prestressing strand = $\frac{4\pi d_b}{3}$
L_t = transfer length
A_s = actual area of Grade 250 prestressing strand = $0.725\frac{\pi d_b^2}{4}$
d_b = nominal strand diameter
f_{se} = effective prestress

The constant, 0.725, in the expression for A_s is the ratio of the actual area of Grade 250 strand to the area of a circle of the same nominal diameter. Substituting the above values into Eq. (2-15) yields

$$0.4\left(\frac{4\pi d_b}{3}\right)L_t = 0.725\left(\frac{\pi d_b^2}{4}\right)f_{se} \qquad (2\text{-}16)$$

Solving Eq. (2-16) for the transfer length, L_t, yields

$$L_t = \frac{f_{se}}{2.94}d_b \approx \frac{f_{se}}{3}d_b \qquad (2\text{-}17)$$

which is the current ACI/AASHTO formula for transfer length. As shown in Figure 2.2, this equation implies that bond stress is constant and that steel stress increases linearly in the transfer region.

Using the effective prestress of approximately 1030 MPa (150 ksi) in Hanson and Kaar's specimens, Eq. (2-17) simplifies to L_t=50d_b. This is the origin of the simplified expression recommended by both the ACI Code and the AASHTO Specifications for the calculation of transfer length.

Mattock compared Eq. (2-17) to results from Kaar et al.'s study as well as to the results of tests sponsored by the American Association of Railroads. He concluded that the equation represented the average values from these studies reasonably well. It is important to note, however, that this equation was meant to be an estimate of the average transfer length, and not a conservative lower bound.

2.3.2 Development Length

The expression for development length, as presented in the AASHTO and ACI codes, is

$$L_d = \frac{f_{se}}{3}d_b + (f_{ps} - f_{se})d_b \qquad (2\text{-}18)$$

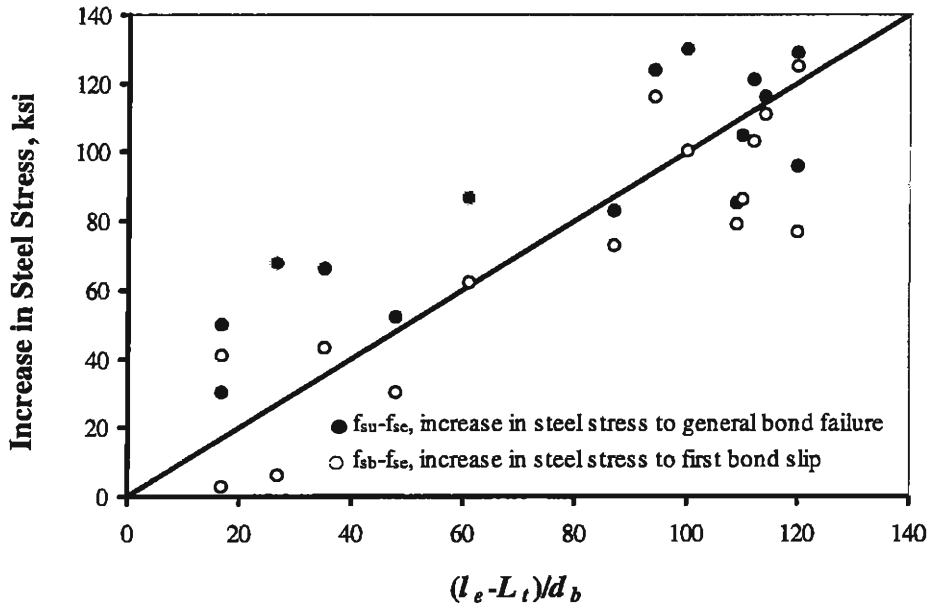

Figure 2.5 - ACI Flexural Bond Length Equation and Data from Hanson and Kaar [20] (1 ksi = 6.89 MPa)

in which L_d is the development length in inches, f_{ps} is the stress in ksi in the strands at the nominal flexural capacity, and all other terms are as defined previously.

This expression is based on a reappraisal of Hanson and Kaar's data and data obtained from the American Association of Railroads. Figure 2.5 shows the data points obtained by Hanson and Kaar for increases in steel stress above effective prestress at first slip and general bond failure plotted against the flexural embedment length, (l_e-L_t), divided by the strand diameter.

From the data in Figure 2.5, Mattock derived the following equation.

$$f_{ps} - f_{se} = \left(\frac{L_d - L_t}{d_b} \right) \qquad (2\text{-}19)$$

In his opinion, this equation was a reasonable mean line for the points representing first bond slip without being overly conservative at larger embedment lengths [20]. Substituting the expression for transfer length from Eq. (2-17), and solving for the development length leads to Eq. (2-18).

Although this expression was based primarily on the work of Hanson and Kaar, it yields significantly shorter embedment lengths than those recommended by them. These differences occur primarily because Hanson and Kaar used conservative lower bound expressions in developing their recommendations, while ACI has chosen to use a less conservative expression [20].

Although this expression was not derived on the basis of measured bond stresses in the flexural bond region, it is instructive to derive the average bond stress implied by it. Following the logic of the transfer length derivation above, the equilibrium expression for the flexural bond length is

$$\mu_b\left(\frac{4\pi d_b}{3}\right)L_b = 0.725\left(\frac{\pi d_b^2}{4}\right)\left(f_{ps} - f_{se}\right) \qquad (2\text{-}20)$$

in which μ_b is the average bond stress over the length of the flexural bond region. Solving for L_b yields

$$L_b = \left(\frac{3\times 0.725}{16\mu_b}\right)\left(f_{ps} - f_{se}\right)d_b \qquad (2\text{-}21)$$

In the ACI/AASHTO formula, the term $(3\times 0.725)/(16\mu_b)$ is unity, implying a constant flexural bond stress of $\mu_b \approx 136$ psi. The assumption of a constant bond stress implies that, for a given effective prestress, the flexural bond length is only a

function of the failure stress and the strand diameter. Technically, because Grade 270 strand is about 6% larger in cross-sectional area than Grade 250 strand of the same nominal diameter, the equations for transfer and development length became invalid when the industry switched to the use of Grade 270 strand. However, due to the apparently small influence of such a factor, no changes have been made in the codes.

2.4 LATER RESEARCH

Since the ACI equations were adopted in 1963, use of high strength strand with larger diameters in high strength concrete has become common. Questions were raised about the validity of the equations with respect to these new materials. Consequently, many studies were completed in an effort to address these concerns. A number of researchers found that the equations were unconservative not only for these new materials, but also for the materials used in the research which led to the current design equations [6, 15, 22].

In 1988, because of these results, FHWA issued a memorandum which required that development length be increased to 1.6 times the development length specified by AASHTO Eq. (9-32) [1]. Additionally, the minimum spacing of strands must be four times the strand diameter and the use of 15.2 mm (0.6 in.) diameter strand was disallowed. The new requirements stimulated further research into the development length issue. In 1996, based on the results of these recent studies, the restriction on the use of 15.2 mm (0.6 in.) diameter strand was lifted. However, the

development length requirement is still in effect. Important research related to this issue is presented in more detail in the following sections.

2.4.1 Study by Martin and Scott

In 1976, Martin and Scott re-evaluated data from Hanson and Kaar's and Kaar et al.'s test programs [15]. This program was initiated primarily to address concerns about recent bond failures which seemed to indicate that the ACI provisions for development length were unconservative. They also addressed design of members with short spans, where the required embedment length could not be developed.

Using failure stress versus embedment length data from Hanson and Kaar's study, they derived bi-linear curves for the variation of the maximum allowable strand stress at failure, f_{ps}, with respect to distance along the member. For a distance, l, from the end of a member less than $80d_b$, they proposed the following equation.

$$f_{ps} \leq \frac{l}{80d_b}\left(\frac{135}{d_b^{1/6}}+31\right) \qquad (2\text{-}22)$$

in which f_{ps} is in ksi and d_b is in inches. The value of $80d_b$ is their recommended value for the transfer length. This value appears to be a conservative estimate from the results of Kaar et al. [12].

For l greater than $80d_b$, they recommended the following equation.

$$f_{ps} \leq \frac{135}{d_b^{1/6}}+\frac{0.39l}{d_b} \qquad (2\text{-}23)$$

These equations were intended to give the designer a means of designing members where there is insufficient embedment length to satisfy the ACI provisions.

Substituting values for nominal strand diameter and using a failure stress of 1586 MPa (230 ksi) yields their recommended values for development length. They recommended values of 1016, 1778, and 2540 mm (40, 70, and 100 in.) for 6.4, 9.5, and 12.7 mm (0.25, 0.375, and 0.5 in) diameter strands, respectively. Due to their conservative use of Hanson and Kaar's data, these values are significantly more conservative than those recommended by ACI.

2.4.2 Study by Zia and Mostafa

In 1977, Zia and Mostafa, under a PCI Fellowship program, completed a literature survey addressing the conflict between Martin and Scott's conclusions and previous research conclusions [22]. Transfer length data was compiled from nine previous studies for strand sizes from 6.44 mm (0.25 in) to 19 mm (0.75 in) and concrete compressive strengths from 11 MPa (1.6 ksi) to 77 MPa (11.2 ksi). Development length data was compiled from Hanson and Kaar's study [10].

Zia and Mostafa performed a linear regression analysis on the compiled data in an effort to deduce an equation for transfer length. This analysis yields

$$L_t = \left[1.5 \left(\frac{f_{si}}{f'_{ci}} \right) d_b \right] - 4.6 \qquad (2\text{-}24)$$

in which f_{si} is the initial prestress in psi, f'_{ci} is the concrete strength at the time of transfer in psi, and d_b is the nominal strand diameter in inches. This equation provides

similar results to ACI's equation for smaller strand diameters, with increasing conservatism for greater strand sizes.

Zia and Mostafa re-evaluated Hanson and Kaar's test data. They concluded that the actual embedment lengths required to develop the ultimate strength of the strands were considerably shorter than those recommended by Hanson and Kaar. This led Zia and Mostafa to derive a new equation for development length.

In developing this equation, they assumed that the strand stress varied from f_{se}, the effective prestress, to f_{ps}, the stress in the strand at ultimate flexural failure, within the flexural bond region. Based on equilibrium of bond and strand forces,

$$L_b = \frac{(f_{ps} - f_{se})}{4\mu} d_b \qquad (2\text{-}25)$$

in which L_b is the length of the flexural bond region, and μ is the average bond stress within L_b.

An average flexural bond stress of 1600 Pa (233 psi) was derived from Hanson and Kaar's data. This bond stress was derived based on a cylindrical element of the same nominal diameter as a Grade 250 strand. For design purposes, an average bond stress of 1380 Pa (200 psi) was recommended by Zia and Mostafa, which led to the following recommended equation for flexural bond length:

$$L_b = \frac{(f_{ps} - f_{se})}{4(0.2)} d_b = 1.25(f_{ps} - f_{se})d_b \qquad (2\text{-}26)$$

This expression is identical to the ACI formula, with the exception of the factor of 1.25. In the ACI formula, for Grade 250 strands, with the assumption of a

cylindrical element of the same nominal diameter as the strand, an average bond stress, μ, of 1724 Pa (250 psi) is implied [22]. Thus, Zia and Mostafa's use of an average bond stress of 1380 Pa (200 psi) leads to a 25% increase in the required flexural bond length.

Combining Eqs. (2-24) and (2-26) results in their recommended equation for development length as follows.

$$L_d = 1.5\frac{f_{si}}{f'_{ci}}d_b - 4.6 + 1.25(f_{ps} - f_{se})d_b \qquad (2\text{-}27)$$

in which all terms are as defined previously. This equation yields development lengths about 25% greater than those given by the ACI expression.

Both Martin and Scott and Zia and Mostafa concluded that the ACI equation was unconservative. However, because there is little new experimental data available to support their conclusions, none of the proposed changes have been addressed in the codes.

2.4.3 Study by Cousins, Johnston and Zia

In 1990, Cousins et al. published the results of an experimental program investigating transfer and development length of epoxy coated and uncoated strand [6]. This research program investigated transfer and development lengths for 9.5, 12.7, and 15.2 mm (0.375, 0.5, and 0.6 in.) diameter epoxy coated and uncoated prestressing strand.

The average measured transfer lengths for uncoated 9.5, 12.7, and 15.2 mm (0.375, 0.5, and 0.6 in.) diameter strands were $91d_b$, $100d_b$, and $93d_b$, respectively, with an initial concrete compressive strength of about 29 MPa (4.1 ksi). These results are as much as 65% greater than that required by ACI.

The average measured development lengths for uncoated 9.5, 12.7, and 15.2 mm (0.375, 0.5, and 0.6 in.) diameter strands were 1448, 3023, and 3353 mm (57, 119, and 132 in.), respectively. These results are as much as 113% greater than that required by ACI. These results, along with Martin and Scott's and Zia and Mostafa's findings, raised serious concerns, and led to the issuance of the 1988 FHWA memorandum [9].

In addition to their experimental results, Cousins et al. proposed analytical models for transfer length and flexural bond length. The following derivations are adapted from their paper [6].

2.4.3.1 Transfer Length Model

Within the transfer length, the steel stress is assumed to vary from zero to the effective prestress. The bond stress is related to the steel stress by the following equation.

$$\mu = \frac{df_s}{dl}\left(\frac{A_s}{\pi d_b}\right) \qquad (2\text{-}28)$$

For small displacements of the strand relative to the concrete, bond stress is considered proportional to slip. The region where this proportionality occurs is termed the elastic zone. Outside of the elastic zone, the bond stress is assumed to maintain a

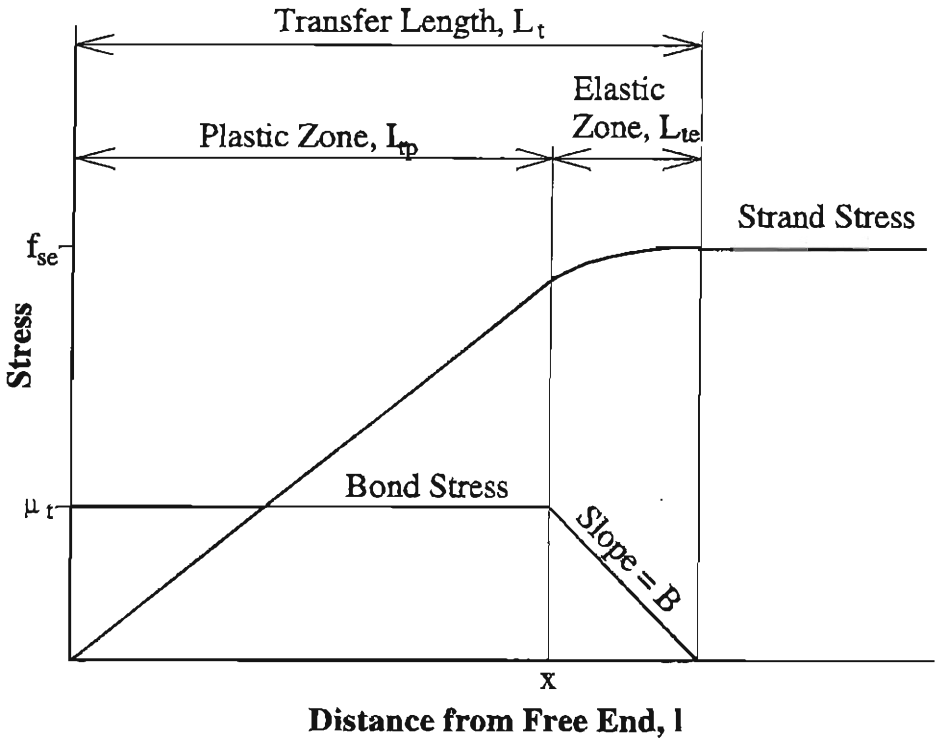

Figure 2.6 - Assumptions of Transfer Length Model [6]

maximum, or limiting, value. The region where this upper limit is maintained is termed the plastic zone. Figure 2.6 shows a plot of the idealized bond stress with the elastic and plastic zones defined.

The length of the elastic zone can be derived as

$$L_{te} = \frac{\mu_t}{B} \tag{2-29}$$

Based on Eq. (2-28), the steel stress, f_s, at point x in Figure 2.6 is

$$f_s = f_{se} - 0.5\left(\frac{\mu_t^2}{B}\right)\left(\frac{\pi d_b}{A_s}\right) \tag{2-30}$$

Furthermore, the area under the μ versus l curve in the plastic zone multiplied by the strand perimeter is equal to the prestress force, F_s, at x, i.e.,

$$F_s = f_s A_s = L_{tp}\pi d_b \mu_t \tag{2-31}$$

Solving Eq. (2-31) for L_{tp}, the length of the plastic zone, and substituting Eq. (2-30) for f_s yields

$$L_{tp} = \frac{f_s A_s}{\pi d_b \mu_t} = \frac{f_{se} A_s}{\pi d_b \mu_t} - 0.5\left(\frac{\mu_t}{B}\right) \qquad (2\text{-}32)$$

With Eqs. (2-29) and (2-32), the equation for the transfer length is

$$L_t = L_{te} + L_{tp} = \frac{f_{se} A_s}{\pi d_b \mu_t} + 0.5\left(\frac{\mu_t}{B}\right) \qquad (2\text{-}33)$$

This equation for transfer length does not explicitly account for the concrete compressive strength, f'_{ci}, at transfer. However, previous research has suggested that bond strength is proportional to $\sqrt{f'_{ci}}$. Thus, μ_t can be expressed as $\mu'_t\sqrt{f'_{ci}}$ in psi. The equation for transfer length then becomes

$$L_t = \frac{f_{se} A_s}{\pi d_b \mu'_t \sqrt{f'_{ci}}} + 0.5\left(\frac{\mu'_t \sqrt{f'_{ci}}}{B}\right) \qquad (2\text{-}34)$$

To calculate transfer lengths, Cousins et al. derived values for μ'_t and B from experimental data. They found that the values of μ'_t for uncoated strand ranged from 3.8 to 11.2, with an average of 6.7 and a median of 6.85. They recommended using μ'_t equal to 6.7 for design calculations. The value of B varied widely. However, the elastic zone made up an average of only 13% of the total transfer length. They recommended using an average value of 300 psi/in (0.0814 MPa/mm) for design calculations. Using the recommended values and substituting $0.77\left(\pi d_b^2/4\right)$ for the strand area and $(4/3)(\pi d_b)$ for the strand perimeter yields

$$L_t = \frac{21.5 f_{se} d_b + 0.0112 f'_{ci}}{\sqrt{f'_{ci}}} \qquad (2\text{-}35)$$

The factors 0.77 and 4/3 used in the above derivation account for the difference between the actual area and perimeter of a Grade 270 strand and those of a cylindrical element with the same nominal diameter.

With Eq. (2-35), transfer lengths for different diameters of uncoated strand were calculated. From this, ratios of measured to calculated transfer length were computed. The average ratio of measured to calculated transfer length was 1.01 with a standard deviation of 0.26. The above equation was also compared to equations proposed previously by other researchers and to the ACI equation. Overall, their equation yielded the best correlation to experimental data.

2.4.3.2 Development Length Model

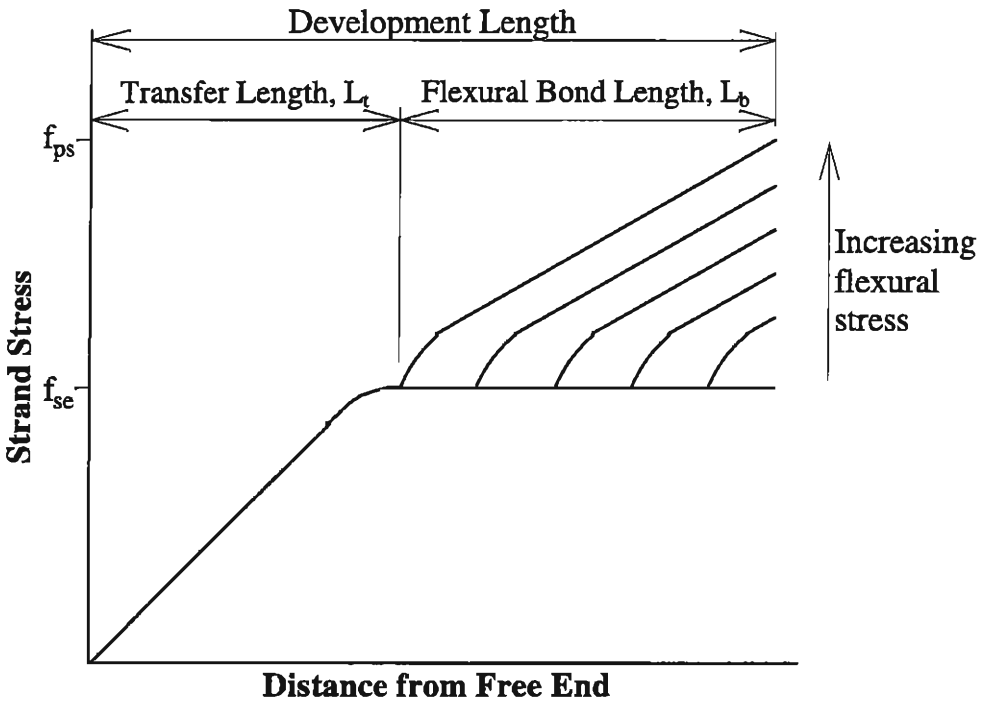

Figure 2.7 - Assumptions of Development Length Model [6]

As Janney first proposed, with increases in applied load, the stress in the strand increases and propagates towards the end of the transfer region. If the flexural bond stress "wave" reaches the transfer region, a general bond slip occurs. Figure 2.7 shows a diagram of this behavior, and the assumptions used in this model.

The flexural bond length is assumed to have elastic and plastic zones similar to those defined in the transfer length model. However, because the elastic region was considered to be relatively short, the entire flexural bond length can be assumed plastic.

At failure, the increase in strand force would be resisted by the plastic bond stress, μ_d, over the flexural bond length. Equilibrium of forces over the flexural bond length yields

$$\left(f_{ps} - f_{se}\right)A_s = \left(\mu_d\right)\pi d_b L_b \qquad (2\text{-}36)$$

The flexural bond length, L_b, is then

$$L_b = \left(f_{ps} - f_{se}\right)\left(\frac{A_s}{\mu_d \pi d_b}\right) \qquad (2\text{-}37)$$

This expression is identical to that derived by Zia and Mostafa in Eq. (2-25). Substituting the relation $\mu_d = \mu_d' \sqrt{f_c'}$ into Eq. (2-37) yields

$$L_b = \left(f_{ps} - f_{se}\right)\left(\frac{A_s}{\mu_d' \sqrt{f_c'}\,\pi d_b}\right) \qquad (2\text{-}38)$$

Combining Eqs. (2-34) and (2-38) gives the following expression for the development length:

$$L_d = \frac{f_{se}A_s}{\pi d_b \mu_t' \sqrt{f_{ci}'}} + 0.5\left(\frac{\mu_t' \sqrt{f_{ci}'}}{B}\right) + \left(f_{ps} - f_{se}\right)\left(\frac{A_s}{\pi d_b \mu_d' \sqrt{f_c'}}\right) \qquad (2\text{-}39)$$

In this expression, the plastic bond stress parameters, μ'_t and μ'_d, are assumed to be inherently different because of the different bond mechanisms in each zone.

To calculate development lengths, Cousins et al. derived values for μ_d' from experimental data. The values of μ_d' for uncoated strand ranged from 0.9 to 2.6. They felt that these values varied more than would be desirable. However, based on their analysis, they recommended using μ_d' equal to 1.32 for design calculations. Values for f_{ps} were calculated using Eq. (18-3) in the ACI Code [2].

Using the recommended values and substituting $0.77\left(\pi d_b^2 / 4\right)$ for the strand area and $(4/3)(\pi d_b)$ for the strand perimeter yields

$$L_d = \frac{21.5 f_{se} d_b + 0.0112 f_{ci}'}{\sqrt{f_{ci}'}} + \frac{142.0 d_b}{\sqrt{f_c'}}\left(f_{ps} - f_{se}\right) \qquad (2\text{-}40)$$

Using Eq. (2-40), development lengths for different diameters of uncoated strand were calculated. From this, ratios of measured to calculated development length were derived. The ratios of measured to calculated development length ranged from 0.76 to 1.18. The above equation was also compared to equations proposed by previous researchers and to the ACI provision. Overall, their equation yielded the most conservative results; however, the results still showed poor correlation to the experimental data. Based on this, Cousins et al. concluded that the development

length model required more experimental verification before it would be suitable for design use.

2.4.4 Study by Shahawy, Issa, and Batchelor

In 1992, Shahawy et al. authored a paper on strand transfer length based on their research at the Florida Department of Transportation [19]. In this paper, results of an experimental and analytical investigation of the transfer length of 12.7 mm (0.5 in.) and 15.2 mm (0.6 in.) diameter prestressing strands in full-scale AASHTO girders are presented. The main variables in this program were the size of the prestressing strand, percentage of shielded strands, and web shear reinforcement ratio.

Elastic and plastic zones, conforming to the model used by Cousins, Johnston, and Zia [6], were observed in the strain measurements for transfer length. Average measured transfer lengths for 12.7 and 15.2 mm (0.5 and 0.6 in.) diameter strands in girders with unshielded strands were $60d_b$ and $57d_b$ respectively. These values are somewhat higher than the ACI value of $50d_b$, but significantly lower than those reported in previous research.

Results of this study also indicated that the FHWA memorandum prohibiting the use of 15.2 mm (0.6 in.) diameter strand at 51 mm (2 in.) spacing was overly conservative. The 51 mm (2 in.) spacing, used in several of the girders tested, did not result in any significant cracking or deterioration in the girders.

The transfer length results were compared with analytical predictions by Zia and Mostafa [22], Cousins, Johnston, and Zia [6], ACI, and with $(f_{si}/3)d_b$. Shahawy et

al. concluded that the use of the equation $(f_{si}/3)d_b$, the ACI equation with the effective prestress, f_{se}, replaced by the initial prestress, f_{si}, resulted in the best correlation to their results. Based on this, they recommended the following equation for transfer length:

$$L_t = \left(\frac{f_{si}}{3}\right) d_b \qquad (2\text{-}41)$$

This equation is somewhat more conservative than the ACI expression, typically giving values closer to $60d_b$.

2.4.5 Study by Mitchell et al.

In 1993, Mitchell et al. reported the results of their testing program at McGill University [16]. Twenty-two precast, pretensioned beam specimens were tested to determine the influence of concrete strength on the transfer length and development length of prestressing strand. The main variables investigated in the study were concrete compressive strength and strand diameter. Concrete compressive strength at 28 days varied from 31 to 89 MPa (4.5 ksi to 12.9 ksi). Strand diameters of 9.5, 12.7, and 15.7 mm (0.375, 0.5, and 0.62 in.) were used in the study.

The results of this study showed a definite decrease in transfer and development length with increasing concrete strength. These results agree with previous research which has indicated this correlation [6, 22].

The average measured transfer lengths for 15.7 mm (0.62 in.) diameter strand were $48d_b$ and $31d_b$ for initial concrete compressive strengths of 21 MPa (3.0 ksi) and 48 MPa (7.0 ksi), respectively. These results are close to or significantly lower than

values predicted by the ACI formula. It must be noted, however, that the prestress was released gradually in these specimens and that the transfer lengths measured would likely have been longer if the prestress was released suddenly.

Approximate development lengths for 15.7 mm (0.62 in.) diameter strand were 1854 mm (73 in.) and 762 mm (30 in.) for concrete compressive strengths at 28 days of 31 MPa (4.5 ksi) and 65 MPa (9.4 ksi), respectively. Again, these values are well below those given by the ACI formula.

Based on the clear correlation to concrete compressive strength seen in their results, new equations were derived for transfer and development length.

The researchers used the transfer length equation recommended by Zia and Mostafa [22] as a basis for their derivation of a transfer length equation. Incorporating new constants to fit their transfer length results yielded the following expression:

$$L_t = 0.33 f_{si} d_b \sqrt{\frac{3}{f'_{ci}}} \qquad (2\text{-}42)$$

Reflecting the study results, this equation typically gives somewhat shorter transfer lengths than the ACI formula.

The authors also derived the following equation for development length, incorporating a factor for concrete compressive strength:

$$L_d = 0.33 f_{si} d_b \sqrt{\frac{3}{f'_{ci}}} + \left(f_{ps} - f_{se}\right) d_b \sqrt{\frac{4.5}{f'_c}} \qquad (2\text{-}43)$$

This equation also typically gives somewhat shorter development lengths than the ACI formula.

Both of these equations, as pointed out by the authors, apply only to the condition of gradual prestress release. These equations will typically be unconservative for cases where prestress release is sudden.

2.4.6 Study by Deatherage, Burdette, and Chew

In 1994, Deatherage et al. reported the results of their PCI sponsored experimental program conducted at the University of Tennessee at Knoxville [8]. Twenty full-scale AASHTO Type I beams were tested to identify the effect of strand size and spacing on the transfer and development length of prestressing strand. Strand diameters of 12.7, 13.3, 14.3, and 15.2 mm (0.5, 0.5 special, 0.563, and 0.6 in.) were used in the study. Strand spacings of $4.0d_b$ and $3.5d_b$ were evaluated.

In this study, specimens prestressed with 15.2 mm (0.6 in.) diameter strands had shorter transfer and development lengths than those prestressed with the smaller diameter strands. These results contradict the general assumption that transfer and development length increases with strand diameter. The authors felt that an increase in mechanical bond, due to differences in 15.2 mm (0.6 in.) diameter strand configuration, might have been responsible for these short transfer lengths. This behavior was also noted by Hanson and Kaar [10], Mitchell et al.[16], and Cousins et al. [6]. The authors also concluded that a reduction of strand spacing to $3.5d_b$ appeared to have no adverse effects on specimen performance, supporting the conclusions of Shahawy et al. [19].

The average measured transfer lengths for 12.7, 14.3, and 1.2 mm (0.5, 0.563, and 0.6 in) diameter strands were $64d_b$, $62d_b$, and $40d_b$ respectively, for initial concrete compressive strengths between 23 MPa (3.4 ksi) and 38 MPa (5.6 ksi). The results for 12.7 mm and 14.3 mm (0.5 in. and 0.563 in.) diameter strand are somewhat higher than values calculated using the ACI formula. However, the results for 15.2 mm (0.6 in.) diameter strands are significantly lower than those calculated using the ACI formula.

Approximate development lengths for 12.7, 14.3, and 15.2 mm (0.5, 0.563, and 0.6 in.) diameter strand were 2032, 2667, and 2159 mm (80, 105, and 85 in.) respectively, for concrete compressive strengths at 28 days between 36 MPa (5.2 ksi) and 55 MPa (8.0 ksi). These values are all greater than those given by the ACI expression, and are not entirely consistent with the results from previous research.

The transfer length equation proposed by Shahawy et al., Eq. (2-41), conservatively fit the results of this study. Thus, they supported its use.

Based on a review of previous flexural bond length data, the researchers felt that the ACI equation for development length was unconservative. The flexural bond length was found to be underestimated by approximately 42%. Consistent with these findings, the following equation for development length was proposed.

$$L_d = \frac{f_{si}}{3} d_b + 1.50\left(f_{ps} - f_{se}\right)d_b \qquad (2\text{-}44)$$

The proposed equation increases the development length by increasing the transfer length and by applying a multiplier of 1.5 to the flexural bond length. This

large increase in development length is not consistently supported by data from prior research, and the authors conclude that further work is needed to refine this equation.

2.4.7 Study by Buckner

In 1995, Buckner published the results of an independent review, commissioned by the Federal Highway Administration (FHWA), of recent research on the transfer and development length of prestressing strands [5]. The objectives of this study were to conduct a review of literature related to transfer and development length of seven-wire pretensioning strand, to rationalize discrepancies among conclusions drawn from various studies, and to recommend equations for strand transfer and development length.

Buckner reanalyzed the data from these studies and found a number of discrepancies in the methods used for data gathering, analysis, and reduction. He found that many of the differences in the results reported could be explained by these discrepancies.

In analyzing methods used for determining transfer length, Buckner found that many different methods were used in the research projects reviewed. Transfer length is typically determined from a measured set of strains along the specimen length. In the transfer region, the strains increase more or less linearly with distance until they reach some point where strains tend to remain constant with distance. Differences in determining the transfer length occurred primarily in the method of determining

where this "plateau" began, and thus where the transfer region ended. The methods employed were typically very subjective.

In an attempt to identify a rational method for measuring transfer length, he recommended the use of the 95% constant strain method [21]. This method still requires a subjective determination of the average magnitude of the strain plateau, termed the 100% average strain plateau. It, however, eliminates much of the subjectiveness found in other methods. Once the 100% average strain plateau is defined, a line representing the 95% average strain plateau can be deduced. The distance at which this line intersects the line through the measured data points is defined as the transfer length.

Additionally, Buckner identified several factors which introduce errors into the measured strains. Errors are introduced into the measured data by instrument error, shear lag, and strains introduced by the self-weight of the member. The combined effect of these errors is thought to result in about a 10% increase in measured transfer length. Buckner argued that the use of 95% of the strain plateau, rather than the 100% strain plateau, lessens the apparent transfer length by approximately 10%.

Buckner analyzed these effects and other discrepancies in reported results extensively and concluded that the current ACI equation for transfer length is unconservative and inappropriate for current practice. Based on analysis of recent test results, Buckner supports the use of Eq. (2-41), recommended by Deatherage et al. [8] and Shahaway et al. [19], for the calculation of the transfer length.

Buckner felt that transfer length should be expected to vary widely due primarily to the observed wide variation in concrete elastic modulus at transfer. To support this, he cited several studies which demonstrate a correlation between transfer length and elastic modulus at transfer. Despite this expected variation, Buckner felt that Eq. (2-41) was representative of mean values of transfer length which could be expected for Grade 270 strands and was adequate for design.

In evaluating development length results, Buckner once again found many discrepancies in the methods of testing, data gathering, and data analysis. His most significant conclusion was that flexural bond length should be a function of strain in the strand at failure, rather than a linear function of the strand stress at failure. This concept of relating flexural bond length to failure strain is not employed in either the ACI/AASHTO equation or any of the proposed equations.

This concept stems from the change in behavior of prestressing strand near ultimate and its effect on the mechanical bond developed. Prestressing strand exhibits approximately linear stress-strain behavior up to yield, after which any increase in stress results in a progressively larger increase in strain. Strand stress at member failure is commonly above yield, and thus, exhibits non-linear stress-strain behavior. Mechanical bond is thought to decrease as the strand stretches and contracts radially. Thus, bond capacity would seem to decrease with increases in strand strain. As bond capacity decreases, a greater length of embedded strand is required to maintain equilibrium. Therefore, the flexural bond length should depend on strand strain at

ultimate. Buckner supports this conclusion by demonstrating correlation between strand strain at failure and reported flexural bond lengths in previous studies.

Based on this concept, Buckner has recommended the following equation for development length.

$$L_d = \left(\frac{f_{si}}{3}\right)d_b + \lambda\left(f_{ps} - f_{se}\right)d_b \qquad (2\text{-}45)$$

in which λ is taken as $(0.6+40\varepsilon_{ps})$, with a lower bound of 1.0 and an upper bound of 2.0, and ε_{ps} is the strain corresponding to the strand stress at failure, f_{ps}. All other terms are as defined previously.

The assumed maximum value of $\lambda = 2.0$ corresponds to the ASTM specified minimum elongation of 0.035 for prestressing strand. A lower bound of $\lambda = 1.0$ applies to cases in which strand strains at failure are equal to or less than 0.01. This corresponds to a reinforcing index close to the maximum permitted by the codes.

Use of this equation results in development lengths which can be significantly more conservative than those calculated with the current ACI formula. The relative increase in required development length is determined by the ultimate strand strain at failure, which in turn depends on, among other things, member depth, reinforcement ratio, and concrete compressive strength.

Buckner noted that there is clear evidence of increase in strand bond capacity with increase in concrete compressive strength. However, he felt that insufficient data

existed in the literature to warrant the inclusion of a factor for concrete compressive strength in the proposed equations.

Buckner's conclusions were questioned by some researchers, with perhaps the most compelling comments coming from Logan [14]. Logan listed several possible reasons for disparities in reported values which Buckner did not address.

1. There is no minimum standard for bond capacity of prestressing strand produced by the various manufacturers. Based on an extensive series of tests using the Moustafa Pullout Method (see following section), there is a wide variation in the bond capacity of strand from different manufacturers. Thus, transfer length and development length could vary widely depending on the particular strand used. None of the tests reviewed in Buckner's report included a standard measurement of the bond capacity of the strand used in the test specimens. Without this correlation, one cannot compare the results from each study on a standardized basis.

2. The degree of suddenness of release of prestress is difficult to quantify and has a significant effect on the transfer length. This makes transfer length results from each study difficult to compare.

3. Based on Logan's comments, a significant portion of the disparities seen in previously reported results could stem from variables which were not addressed or measured. This makes a meaningful comparison of these results impossible. Logan suggested that all future testing should include a

standard measurement of the bond capacity of the strands used in order to facilitate future correlation of test results. Two methods of measuring bond quality of strand are discussed in Section 2.6.

2.5 SUMMARY OF PREVIOUS RESEARCH

A summary of the equations proposed by various researchers on the transfer and development length, and of experimentally determined values of development length for 15.2 mm (0.6 in.) diameter strand is shown in Table 2.1.

Table 2.1 - Equations for Transfer and Development Length and Reported Development Length Values for 15.2 mm (0.6 in.) Diameter Strand

Authors	Year	Proposed Equation for Transfer Length	Proposed Equation for Development Length	Reported values of L_d
ACI 318	1963	$\frac{f_{se}}{3}d_b$	$\frac{f_{se}}{3}d_b+\left(f_{ps}-f_{se}\right)d_b$	NA
Martin & Scott	1976	$80d_b$	NA	NA
Zia and Mostafa	1977	$\left[1.5\left(\frac{f_{si}}{f'_{ci}}\right)\right]-4.6$	$1.5\frac{f_{si}}{f'_{ci}}d_b-4.6+1.25\left(f_{ps}-f_{se}\right)d_b$	NA
Cousins et al.[1]	1990	$\frac{21.5f_{se}d_b+0.0112f'_{ci}}{\sqrt{f'_{ci}}}$	$\frac{21.5f_{se}d_b+0.0112f'_{ci}}{\sqrt{f'_{ci}}}+\frac{142d_b}{\sqrt{f'_c}}\left(f_{ps}-f_{se}\right)$	$220d_b$
Shahawy et al.	1992	$\left(\frac{f_{si}}{3}\right)d_b$	NA	NA
Mitchell et al.[2]	1993	$0.33f_{si}d_b\sqrt{\frac{3}{f'_{ci}}}$	$0.33f_{si}d_b\sqrt{\frac{3}{f'_{ci}}}+\left(f_{ps}-f_{se}\right)d_b\sqrt{\frac{4.5}{f'_c}}$	$122d_b$[3] $50d_b$
Deatherage et al.	1994	$\left(\frac{f_{si}}{3}\right)d_b$	$\frac{f_{si}}{3}d_b+1.50\left(f_{ps}-f_{se}\right)d_b$	$142d_b$
Buckner	1995	$\left(\frac{f_{si}}{3}\right)d_b$	$\left(\frac{f_{si}}{3}\right)d_b+\lambda\left(f_{ps}-f_{se}\right)d_b$ $1.0\le\left[\lambda=\left(0.6+40\varepsilon_{ps}\right)\right]\le 2.0$	NA

Note: All transfer and development length equations yield results in inches and the stress is in psi (1 in.=25.4 mm; 1 psi = $6.89x10^3$ Pa).

(1) Applies to uncoated strands only
(2) Prestress was released gradually
(3) For 28 day concrete compressive strengths of 31 and 65 MPa (4.5 and 9.4 ksi) respectively

2.6 CHARACTERIZATION OF BOND QUALITY

Several studies have attempted to develop simple methods for quantifying bond quality of strand. Two of the most promising methods, slip theory and pullout testing, are discussed in the following sections.

2.6.1 Slip Theory

In 1976, Anderson and Anderson [3] reported the results of tests on 36 prestressed hollow core slab specimens. The objective of this program was to evaluate the ability of such specimens to meet the transfer and development length criteria set out in the ACI Code. Additionally, a theory was developed which relates initial measured end slip to the quality of the bond between the strand and the concrete. Comparison to results of their tests showed that this theory, herein termed the slip theory, could adequately predict the ability of a specimen to develop the required transfer and flexural bond stresses to achieve the flexural capacity.

As mentioned previously, upon prestress release, the strand slips relative to the concrete in the transfer region. The total slip can be measured at the end of the specimen, and is referred to as end slip. The slip theory is founded on the assumption that the magnitude of the end slip a strand experiences upon release of prestress is an indicator of the quality of the bond between the strand and the concrete [3, 4]. Therefore, it is also directly related to the required transfer length and development length.

Prior to the release of the prestressing force, the strand stress induced by the jacking force is denoted as f_{so}. After release, the strand stress in the transfer region decreases, and is assumed to vary from zero at the beginning of the transfer region to the initial prestress, f_{si}, at the end of the transfer region. Thus, the strand experiences a change in stress varying from f_{so} at the free end of the strand to $(f_{so}-f_{si})$ at the end of the transfer region. Hence, the change in steel strain varies from f_{so}/E_s at the free end of the strand to $(f_{so}-f_{si})/E_s$ at the end of the transfer region. Since slip occurs only in the transfer region, the strain increment in the strand is identical to that in the concrete at the end of the transfer region during stress transfer. Thus, we can assume that the concrete also experiences a change in strain varying from zero at the free end of the strand to $(f_{so}-f_{si})/E_s$ at the end of the transfer region. This implies that there is a differential strain increment between the strand and the concrete varying from f_{so}/E_s at the free end of the strand to zero at the end of the transfer region. The integral of this differential strain increment, $(\Delta\varepsilon_s-\Delta\varepsilon_c)$, over the transfer length is equal to the cumulative slip between the strand and the concrete and is, thus, equal to the end slip. If the variation of the differential strain increment is linear, then the end slip, δ, can be found with the following equation.

$$\delta = \int_0^{L_t} (\Delta\varepsilon_s - \Delta\varepsilon_c) dl = \int_0^{L_t} \left(\frac{f_{so}}{E_s} - \frac{f_{so} l}{E_s L_t} \right) dl = \frac{L_t f_{so}}{2E_s}$$

Solving for L_t yields

$$L_t = \frac{2\delta E_s}{f_{so}} \qquad (2\text{-}46)$$

in which all the terms are defined previously.

When the transfer length obtained from this equation is less than that obtained by the ACI equation, the ACI equation is assumed to govern.

Furthermore, the initial strand slip can also be related to the flexural bond length, L_b, by introducing the following assumption.

$$L_b = \alpha L_t \qquad (2\text{-}47)$$

in which α is a factor which can be derived from the ACI equations in the following manner.

$$\alpha = \frac{L_{b,ACI}}{L_{t,ACI}} = \frac{\left(f_{ps} - f_{se}\right)d_b}{\frac{f_{se}}{3}d_b} = \frac{3\left(f_{ps} - f_{se}\right)}{f_{se}} \qquad (2\text{-}48)$$

Using Eqs. (2-46), (2-47), and (2-48), and the relation that $L_d = L_t + L_b$, the following equation can be derived for the development length:

$$L_d = \frac{2\delta E_s}{f_{so}}\left[\frac{3\left(f_{ps} - f_{se}\right)}{f_{se}} + 1\right] \qquad (2\text{-}49)$$

A maximum allowable end slip criterion can then be obtained by setting Eq. (2-46) equal to the ACI formula for transfer length. The resulting expression is

$$\delta_{max} = \frac{\left(f_{so} f_{se}\right)}{6E_s} d_b \qquad (2\text{-}50)$$

in which f_{se}, f_{so}, and E_s are in ksi, and d_b is in inches. Members with end slips greater than this value are expected to require transfer and development lengths greater than those calculated by the ACI provisions. Instead of using the above equation directly, Anderson and Anderson suggested the following equation based on an empirical fit to their test results.

$$\delta_{max} = \frac{f_{si} d_b}{950} \qquad (2\text{-}51)$$

A number of different test programs using prestressed hollow core slabs have clearly demonstrated that the magnitude of the end slip at transfer can indicate the quality of the bond developed between the strand and the concrete [3, 4, 14].

However, this theory is probably unsuitable for accurately predicting the transfer and development length of a member. The assumption of a linear variation of steel stress with distance in the transfer region is not entirely accurate. Additionally, the use of the ACI equations to evaluate the ratio of transfer to development length would appear to be questionable as the validity of these equations has been challenged by recent test results.

2.6.2 Pullout Tests

The direct tension pullout test, developed by Moustafa, is very simple to execute and has been shown to be a reliable indicator of bond quality in prestressed concrete members [13, 14]. In a pullout test, lengths of unstressed prestressing strand are cast into a concrete block at regular spacings, and, after two days of curing, are pulled out by a hydraulic ram. The force required to pull the strand out of the concrete can then be correlated to the bond quality of the strand. Presumably, any strand which meets a minimum pullout strength criterion can provide the bond strength expected in the ACI code.

A research program investigating the bond capacity of prestressing strand from different manufacturers was recently completed by Logan [13]. The objective of

this test program was to correlate the untensioned pullout capacity of a strand to its transfer and development length. This program was a follow-up to several previous test programs performed by Logan.

In the test program, samples of 12.7 mm (0.5 in.) diameter prestressing strand from six different manufacturers were cast into concrete test blocks according to the Moustafa pullout test procedure [13].

Using strand from the same six manufacturers, prestressed concrete beams were also cast for transfer and development length testing. Transfer length was determined by applying Eq. (2-46), derived by Anderson and Anderson [3], to measured end slip values from each of the specimens. Development length capacity was determined by loading each beam, at the ACI predicted development length, to failure. Members were categorized by whether they failed by bond, signifying insufficient bond capacity, or in flexure.

Strand samples with pullout strength exceeding 160 kN (36 kips) showed satisfactory performance. In the beam flexural tests, these strand groups exhibited the desired flexural failure mode in all tests. These groups had an average transfer length of $29d_b$, which is significantly lower than the ACI prediction.

Strand samples with pullout strengths less than 53.4 kN (12 kips) were unable to meet the performance expected in the ACI transfer and development length formulas. In the beam flexural tests, these strand groups exhibited general bond failure in every test. These strands had an average transfer length of $58d_b$, which is

twice the average transfer length of the strand group that had pullout strengths exceeding 160 kN (36 kips). Additionally, for the strands with low pullout strengths, the end slips were seen to increase dramatically over time.

These results are in agreement with the conclusions of earlier studies by Logan et al. as well as the conclusions from tests conducted in 1974 by Moustafa. Based on these results, Logan has recommended that all strand be prequalified using the direct tension pullout test, and that a minimum pullout strength of 160 kN (36 kips), with an embedment of 457 mm (18 in.), be met for any 12.7 mm (0.5 in.) diameter strand used in a member. The results of these tests support Logan's assertion that some of the significant differences in earlier research results could be attributed to the manufacturing processes of different strands.

3. TEST PROGRAM

3.1 SCOPE OF TEST PROGRAM

Three pretensioned box girder specimens of identical designs were fabricated for testing. The girders were made of high performance, 69 MPa (10 ksi), concrete with a 40 MPa (5.8 ksi) composite topping slab. They were pretensioned with nine 15.2 mm (0.6 in.) diameter prestressing strands spaced at 51 mm (2 in.) on center.

The primary objective of the test program was to measure the transfer and development lengths for these girders. In particular, the effects of using 15.2 mm (0.6 in.) diameter prestressing strand at 51 mm (2 in.) spacing in high performance concrete (HPC) were investigated.

In this chapter, the design and fabrication of the girder specimens is discussed. Additionally, the instrumentation and procedures used in the testing program are presented.

3.2 SPECIMEN DESIGN AND DESIGNATION

3.2.1 Girder Design

The girder specimens, designed by CDOT, were reduced scale models of the box girders to be used in the upcoming bridge replacement project at Interstate 25. The scaling was determined such that the test girders would have the same performance as the actual bridge girders in terms of the stresses at the top and bottom

of the section, the percentage of the compression region provided by the topping slab, and the strain in the prestressing strands at flexural failure.

The final specimen design is shown in Figure 3.1. Each girder specimen consisted of a box section with a composite topping slab. The girder section was prestressed with nine Grade 270, seven-wire, 15.2 mm (0.6 in.) diameter strands at 51 mm (2 in.) spacing. The prestress immediately before release was specified to be 1,407 MPa (204 ksi). High-strength concrete was specified for the main box section. This concrete was to have a design concrete compressive strength of 45 MPa (6.5 ksi) at prestress release and 69 MPa (10 ksi) at 56 days. The design concrete compressive strength for the topping slab was 40 MPa (5.8 ksi) at 28 days.

A span length of 10.2 m (33.4 ft.) was chosen to insure that development length testing could be carried out on both ends of each girder. The total length of each girder was 10.4 m (34.25 ft.). Based on a review of prior research, the maximum development length expected for the girders was approximately 3.4 m (11 ft.). Presumably, with the chosen span, failure of the first end at this embedment length would leave sufficient strand embedment length to permit testing of the second end.

The girders were also designed for the high shear forces expected during development length testing. Development length testing requires the application of a point load, at the expected development length, sufficient to cause flexural failure. The minimum expected development length, based on prior research was 1.5 m (4.9 ft.). The application of an ultimate load so close to the end of a member is not typical in service and would typically result in a shear failure. To prevent this type of failure

during testing, it was necessary to provide the maximum shear reinforcement allowed by the AASHTO Specifications [1].

The reinforcement ratio of these specimens was 0.0071, which was close to the maximum allowable reinforcement ratio of 0.0079 in accordance with the AASHTO Specifications [1]. This results in a strand strain at ultimate flexural capacity of approximately 0.011, which is well below the guaranteed minimum strand elongation of 0.035. As mentioned in Section 2.1.4, members with low strand strains at failure may have shorter development lengths than similar members with higher strand strains at failure. However, the strand strain at failure in the test girders is reflective of the actual bridge girders modeled by the test specimens.

A minimum concrete cover of 25 mm (1.0 in.) was specified for all reinforcement. Presumably, this small amount of concrete cover simulated the worst case for concrete splitting or cracking due to close strand spacing and high prestress forces. However, 254 mm (10 in.) long solid end blocks and heavy anchorage zone reinforcement were provided according to standard CDOT design practice.

The calculated moment capacity of the girders, using the specified material properties, are presented in Table 3.1 for later comparison to experimental values.

Table 3.1 - Design Moment Capacity of Test Girders

M_n by AASHTO Specification *kN-m (kip-ft.)*	**M_n by Strain Compatibility** *kN-m (kip-ft.)*
839 (619)	872 (644)

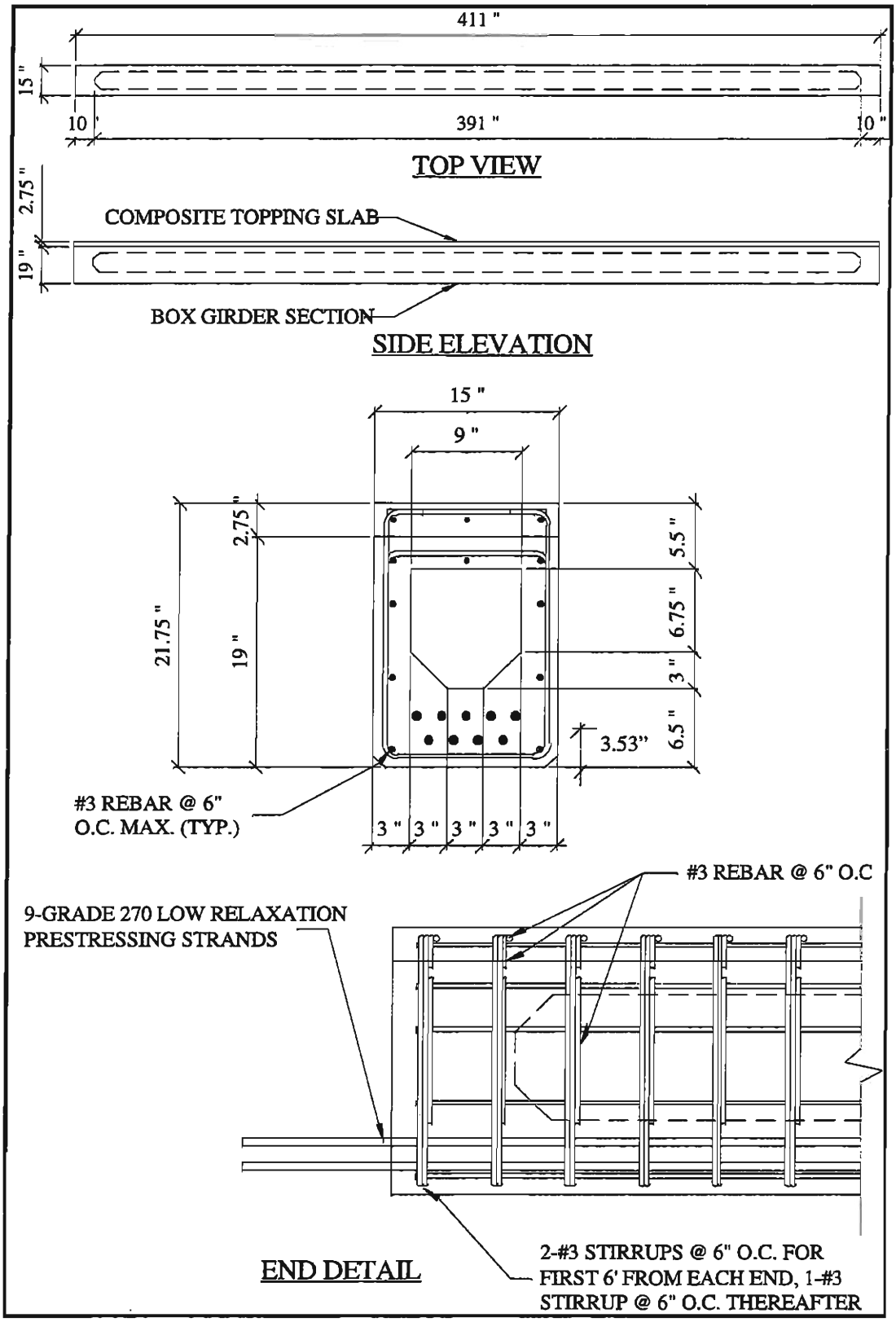

Figure 3.1 - Test Specimen (1 in. =25.4 mm)

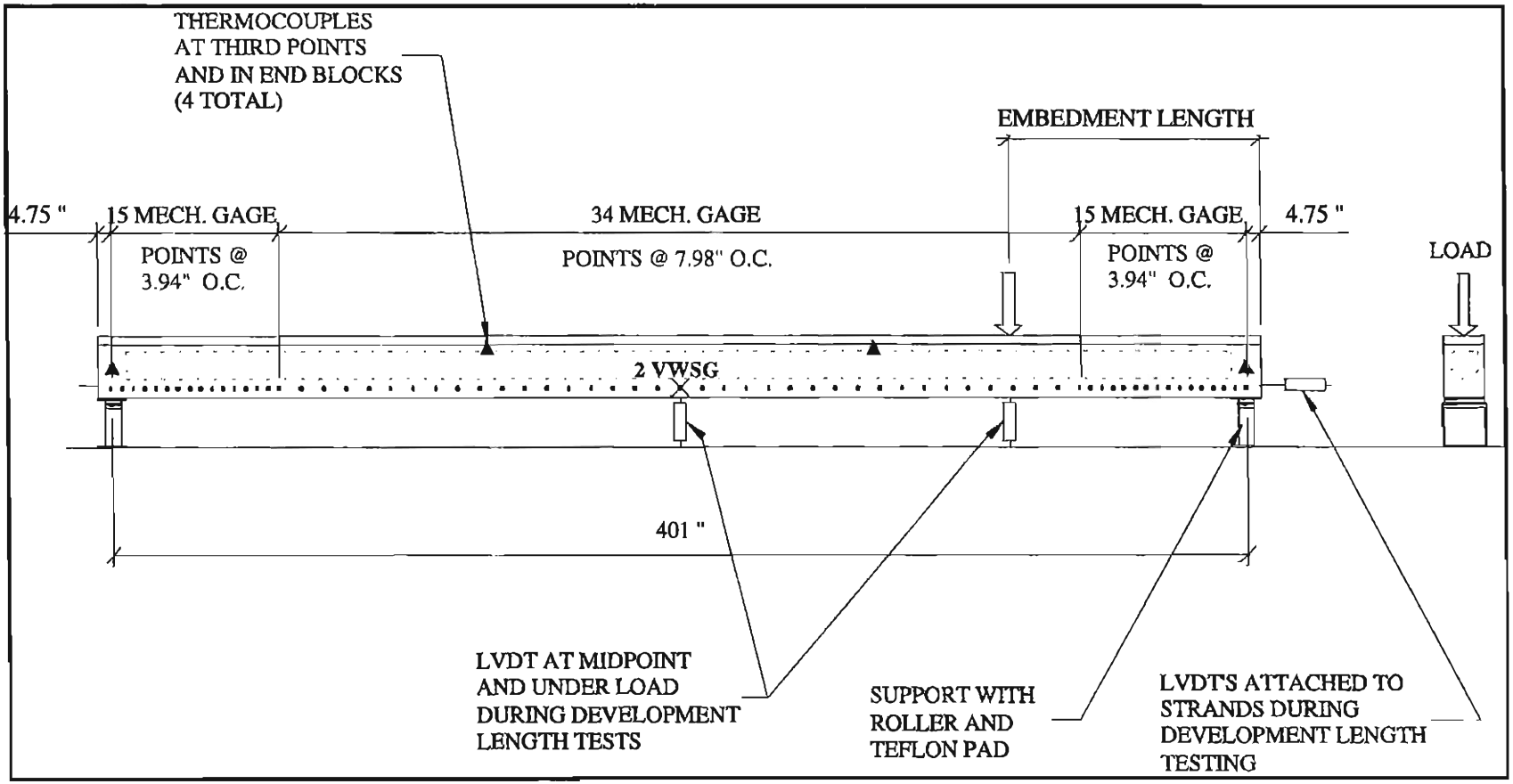

Figure 3.2 - Test Setup and Instrumentation (1 in. = 25.4 mm)

3.2.2 Specimen Designation

Each girder was designated numerically, 1, 2, or 3, with the ends of the girder labeled east (E) and west (W). Measurements pertaining to each girder are designated first by girder number, and when applicable, by girder end.

3.3 TEST SETUP AND PROCEDURE

The instrumentation and procedures used in the experimental program are discussed in the sections below.

3.3.1 Transfer Length Measurement

Transfer length was determined by measuring strains along the concrete surface with a Whittemore gage. This gage had a 200 mm (7.87 in.) gage length and was used to measure strain at various times during the test program. As shown in Figure 3.3, threaded target points were cast into both sides of each girder at the same level as the tendon center of gravity. As shown in Figure 3.2, these target points were located at 100 mm (3.94 in.) spacing over the first 1600 mm (63 in.) from each end of a girder, and at 200 mm (7.87 in.) spacing for the rest of the girder.

Measurements were taken immediately before and after prestress release, immediately before and after topping slab casting, at 14 and 28 days after girder casting, and just before each development length test. Measurements were delivered to a portable electronic device as they were read, and were ultimately uploaded to a personal computer for transfer length analysis. These measurements were also used to calculate the prestress losses along the length of each girder.

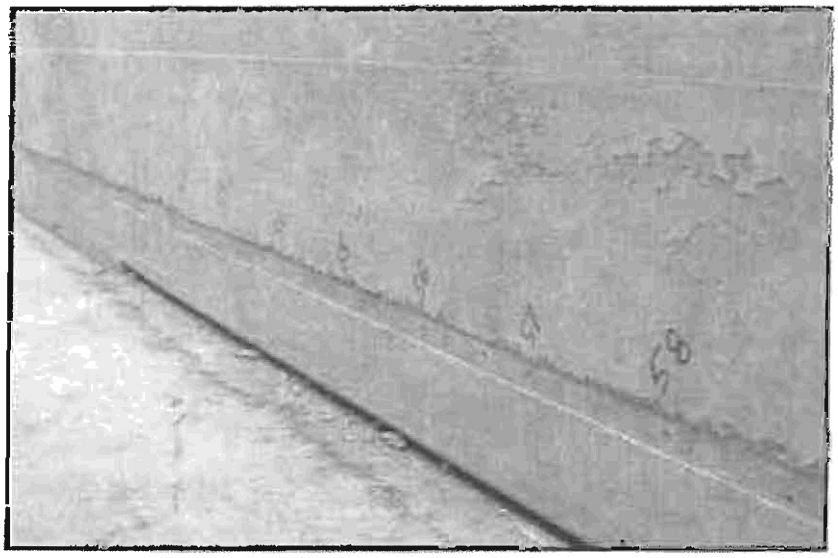

Figure 3.3 - Embedded Target Points

The mechanical gage measurements were verified by strain readings from two vibrating wire strain gages (VWSG's) placed in each girder at the span midpoint. They were located at the strand center of gravity with each gage offset 63.5 mm (2.5 in.) from the centerline of the girder cross section. The gages were attached to a portable data acquisition device where measurements were recorded for each girder at various intervals up to the day of development length testing.

3.3.2 Development Length Tests

Development length was determined using an iterative process. For each test, an estimate of the development length for the member was made. The member was then loaded to failure, using a point load at a distance from the end of the member equal to the estimated development length. Based on whether a bond or flexural compression failure occurred, the estimate of development length would be revised. The occurrence of a flexural failure would indicate that sufficient embedment length

existed to develop the failure stress in the strands, and thus the actual development length was shorter than the previous estimate. Conversely, the occurrence of a bond failure would indicate that the actual development length was likely to be greater than the previous estimate. With the revised estimate of development length, a new test would be conducted with the new embedment length. This process would be continued until the development length was found.

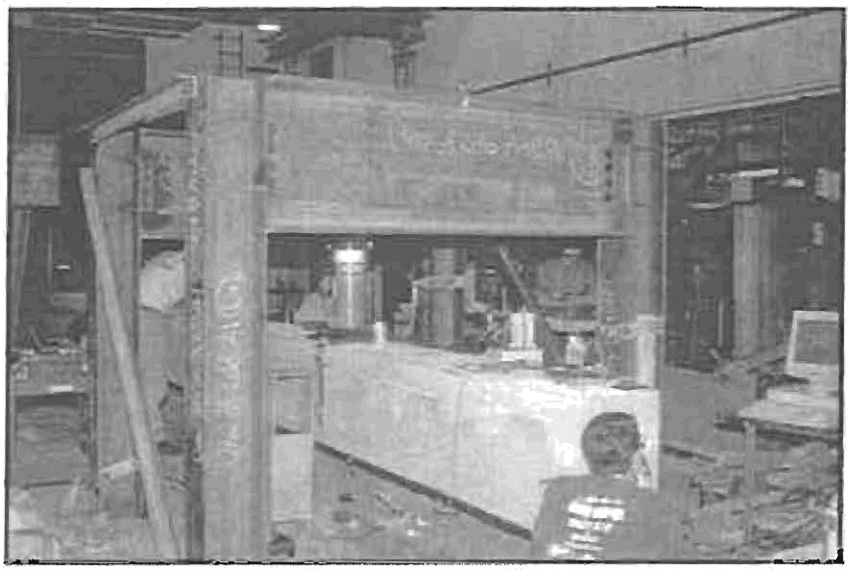

Figure 3.4 - Development Length Test Setup

After eliminating extreme values from previous research data, we estimated that our development length would most probably fall between 1.47 m and 4.22 m (4.83 ft. and 9.67 ft.). The average of these experimental values was calculated to be 2.16 m (7.08 ft.), which was used as our first estimate of development length. The embedment lengths at which each test was eventually conducted are shown in Table 3.2.

Table 3.2 - Development Length Tests

Test Designation	Test Date	Embedment Length mm (in.)
1-E	10/2/96	2159 (85)
1-W	10/11/96	2057 (81)
2-W	10/21/96	1918 (76)
2-E	10/28/96	1651 (65)
3-E	11/4/96	1524 (60)
3-W	11/11/96	1497 (59)

The development length tests were performed in the Structures Laboratory at the University of Colorado at Boulder. In each test, only the embedment length was varied. For each test, the specimen was simply supported on specially fabricated supports as shown in Figure 3.2. These supports allowed rotation of the girder ends through a roller arrangement. Teflon pads placed between the girder and the support also allowed for free displacement of the girder end.

As shown in Figure 3.4, a point load was applied at a distance from the end of the girder equal to the current estimated development length using a 890 kN (200 kip) capacity Power Team hydraulic jack. The jack was controlled using a manually operated switch attached to a Power Team electric pump. During each test, the applied load, deflections at midspan and under the load, concrete strain at the tendon center of gravity, and strand slip were measured.

An inline pressure sensor was used to record applied load. This device was attached to a data acquisition system connected to a personal computer. All measurements were then converted to engineering units using Labview, a commercial data acquisition program.

Linear voltage differential transducers (LVDT's) were used to measure both strand slip and deflection. As shown in Figure 3.5, LVDT's were attached to each strand at the girder end being tested to detect strand slip. These LVDT's were constantly monitored in an effort to detect impending bond failure. LVDT's were also attached to the girder at midspan and beneath the load point to measure deflection during the tests. These LVDT's were attached to the data acquisition system and read at various intervals. The deflection measurements were also verified by dial gages placed under the girder at midspan and at the load point.

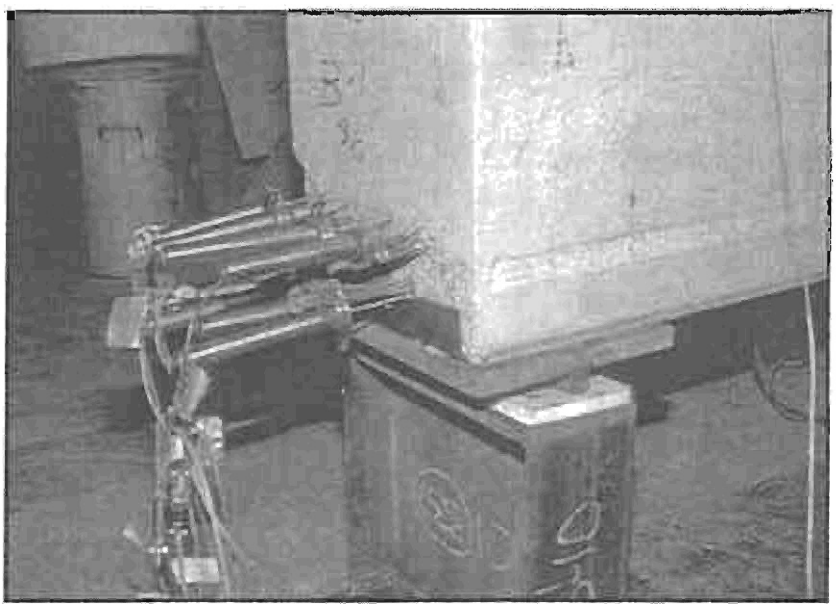

Figure 3.5 - LVDT's Attached to Strands During Tests

Concrete strain at the tendon center of gravity was measured at selected load intervals using a Whittemore gage. However, because only small changes in strain occurred at the far end, only the strain between the midspan and the end of the girder being tested was measured. These readings were loaded into a personal computer and used to calculate the approximate variation of strand stress during testing.

3.3.3 Other Measurements

3.3.3.1 Camber

Bolts were attached to one side of each girder, near each end, at the level of the center of gravity of the girder section before prestress release. Fishing line was stretched tight between these bolts and a reference mark was made on the girder at midspan. To measure camber, a steel ruler was used to measure the distance between the reference mark and the fishing line, whose tension was maintained constant. Camber was measured for each girder immediately after prestress release, immediately before and after the topping slab casting, 14, and 28 days after girder casting, and on the day of development length testing.

3.3.3.2 End Slip at Transfer

Strand slip measuring devices developed at FHWA's Turner-Fairbanks Highway Research Center were attached to the strands near the ends of each girder before prestress release. These devices were essentially a section of aluminum C-channel which was clamped to the strand at approximately 90 mm (3.5 in.) from the end face of the girder. As shown in Figure 3.6, a Brown & Sharpe Digit-Cal Mark IV

caliper was used to measure the distance from one leg of the C-channel to the girder. Measurements were taken immediately before and after prestress release.

Figure 3.6 - Measurement of End Slip

3.3.3.3 Pullout Tests

Pullout tests were performed according to the Mostafa method mentioned in Chapter 2. As shown in Figure 3.8, a total of 8 strand samples approximately 1.83 m (6 ft.) long were embedded to a depth of 457 mm (18 in.) in a 610 mm (24 in.) deep by 914 mm (36 in.) long by 610 mm (24 in.) wide concrete block. The concrete was the same as that used in the girder box sections. Two such blocks were cast and allowed to air cure for two days before commencement of pullout testing.

As shown in Figure 3.7, the strands were pulled out of the concrete using an Enerpac center-hole hydraulic ram. The ram was set on a specially fabricated support which prevented compressive stresses from developing in the concrete immediately adjacent to the strand being tested. The strand was threaded through the ram, a strand

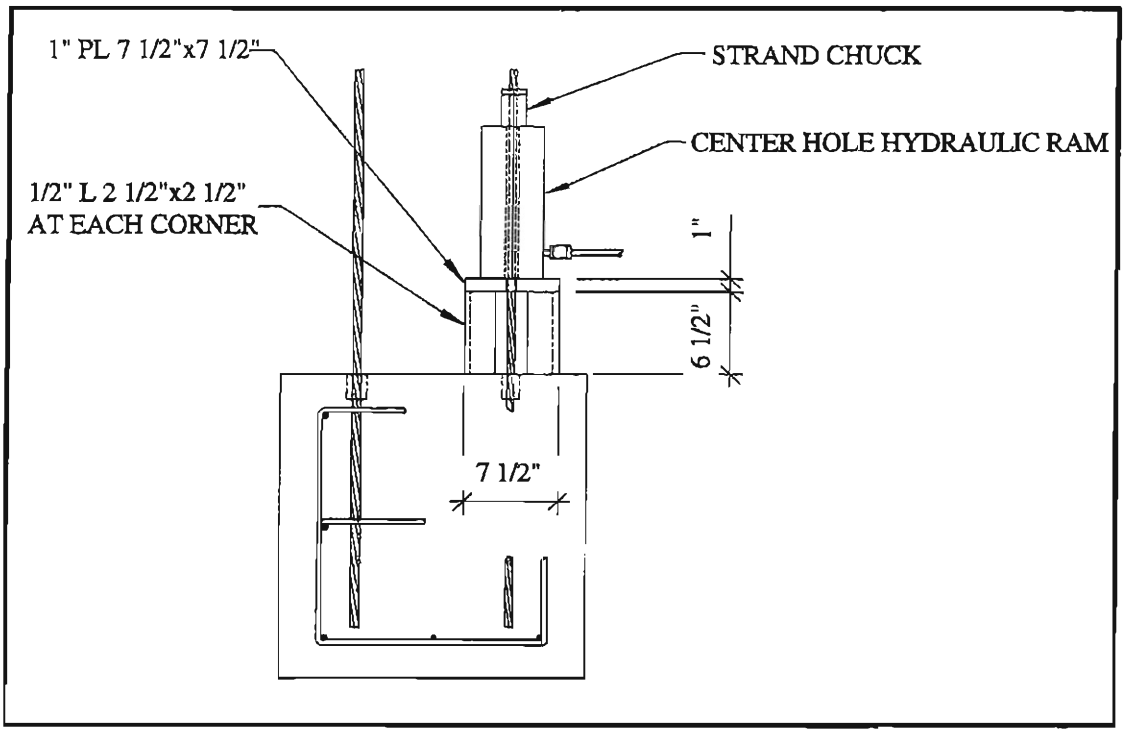

Figure 3.7 - Pullout Test Setup (1 in. = 25.4 mm)

chuck was affixed to it, and load was applied by a hand pump until the strand could not sustain further load increase. The maximum load, the load at first slip, and the total pullout distance at the maximum load were recorded manually for each strand tested.

3.3.3.4 Heat of Hydration

Four thermocouples were placed in each girder, one at each third point of the span, and one centered in each end block. Immediately after girder casting, these devices were read every 30 minutes for approximately one week. These measurements were recorded and used to gauge the temperature changes in the

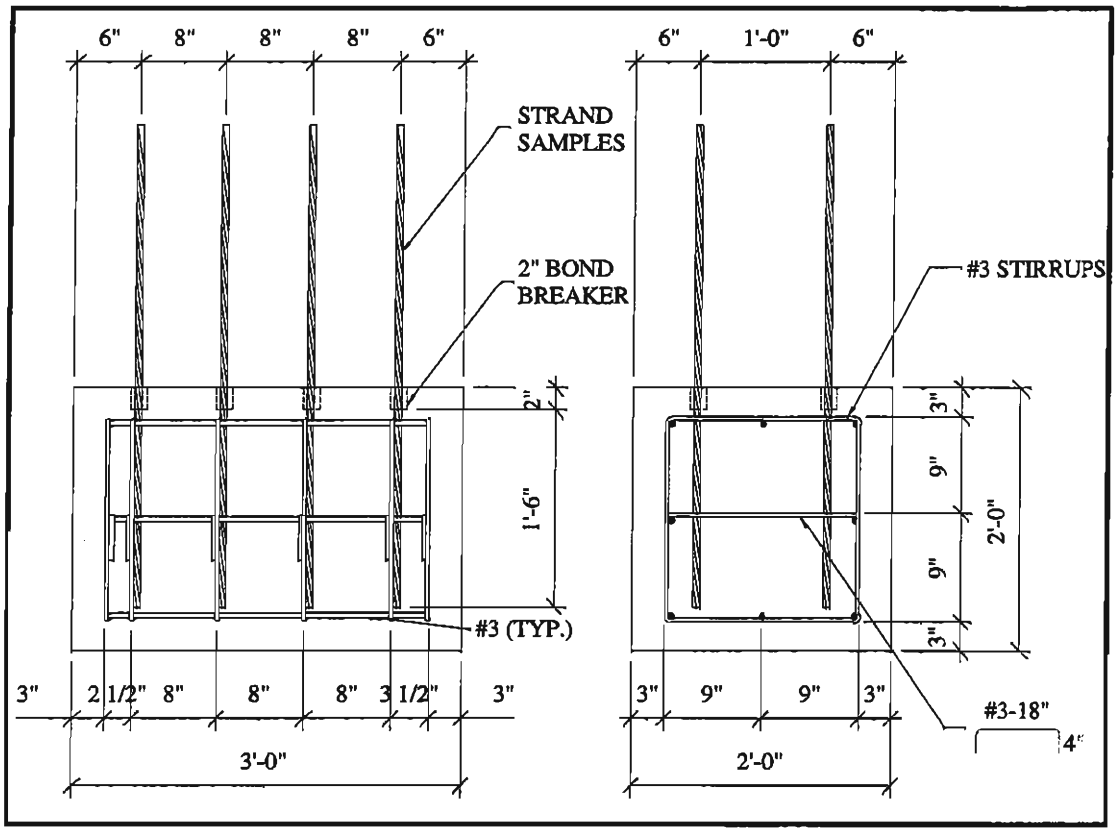

Figure 3.8 - Pullout Test Block Configuration (1 in. = 25.4 mm)

concrete during curing. The maximum temperature recorded is presented in Section 3.4.3.

3.4 SPECIMEN FABRICATION

The girder specimens were fabricated by Rocky Mountain Prestress (RMP) in Denver, Colorado. Personnel from CU, CDOT, and FHWA all aided in the planning and installation of the necessary instrumentation during the fabrication process. The following sections describe the methods used in the fabrication and instrumentation of the girder specimens.

3.4.1 Formwork and Steel Placement

The girder specimens were cast end to end inside an adjustable steel box girder form. Because the specimens were relatively small, it was necessary to fabricate a separate set of wood forms within this form. This formwork, shown in Figure 3.9, was designed and installed by the RMP personnel. After installation of the formwork, aluminum strips with mechanical gage target points previously attached, were screwed to the side forms at the appropriate positions.

Figure 3.9 - Girder Reinforcement and Formwork

After installation of the target points, the mild steel reinforcing cages were installed for each of the girders. Nine pretensioning strands were then threaded through each form and attached to the bulkheads at the end of the steel form using strand chucks. A small pretension was applied to the strands to pull them taut. The strands were slightly rusted when installed and were all from the same reel.

As shown in Figure 3.10, the VWSG's and thermocouples were then fixed to the rebar cage at the appropriate positions. The instruments were attached to the data acquisition device and checked for proper function. The RMP personnel were then allowed to place large blocks of Styrofoam in each form which formed the void in the box section. While this was occurring, 1.83 m (6 ft.) long pieces of strand were cut and tied into the two pullout block forms.

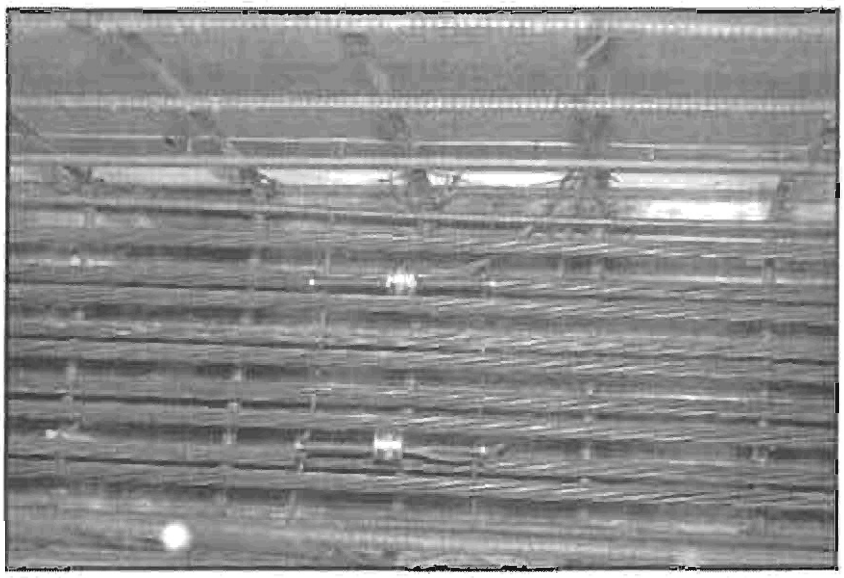

Figure 3.10 - Vibrating Wire Strain Gages Tied in Place

3.4.2 Strand Pretensioning Procedure

On the second day, the nine strands were prestressed according to the usual method used by the contractor. As shown in Figure 3.11, each strand was stressed individually with a hydraulic jack pushing against the end bulkhead. The jacking force and the total extension of the strands from the bulkhead were measured. Each strand was stressed to a value slightly over the jacking force specified in the design to compensate for losses due to anchorage slip.

Figure 3.11 - Strand Pretensioning by RMP Personnel

3.4.3 Concrete Placement

After completion of the prestressing operation, concrete placement began. The girder concrete was batched on-site at the fabricator's batch plant. The fabricator developed the mix design, shown in Table 3.3, to achieve the 56 day design concrete compressive strength of 69 MPa (10 ksi).

Table 3.3 - Girder Concrete Mix Design

Material	Quantity kg/m^3 (lb./yd.^{3})
Type III Cement	474 (800)
Water	156 (263)
Coarse Aggregate (3/8" pea gravel, Cooley)	930 (1570)
Fine Aggregate (Sand, Cooley)	782 (1320)
Silica Fume	14 (30)
Water Reducer (Polyheed 997)	2.96 L/m^3 (100 oz./yd.^{3})
Water Reducer (Rheo 1000)	5.91 L/m^3 (120-200 oz./yd.^{3})

Concrete was transported from the on-site batch plant to the girders in 4 cu. yd. buckets. The girders were poured successively, with each girder being poured from a fresh batch of concrete. The concrete remaining in each bucket was used to fabricate the material test specimens. The concrete slump was measured by RMP and was approximately 114 mm (4.5 in.).

After the first girder was poured, the water content in the remaining batches was increased to improve workability. This change did not appear to significantly affect the concrete strength among the three girders. Upon completion of concrete pouring, the girders were covered by a tarp and cured overnight. Steam was passed through pipes surrounding the existing adjustable box form for approximately 8 hours to accelerate the hydration of the concrete. The maximum temperatures measured during the curing process by the thermocouples in each girder are shown in Table 3.4. Detailed time-history plots are provided in Appendix C.

Table 3.4 - Heat of Hydration Data

Girder	Maximum Recorded Temperature Degrees Celsius (Fahrenheit)	Time to Reach Maximum Temperature Hours after Casting
1	80 (176)	17.5
2	80 (176)	16.0
3	79 (174)	13.5

3.4.4 Material Test Specimens

Materials specimens were cast from all three batches of concrete for future testing. As all the concrete was presumably identical, no effort was made to differentiate between the separate batches.

The following specimens were cast:

- 75 - 102 mm x 203 mm (4 in. x 8 in.) cylinders for compression and creep tests
- 42 - 152 mm x 305 mm (6 in. x 12 in.) cylinders for split cylinder tests
- 42 - Modulus of rupture beams
- 6 - Shrinkage prisms
- 2 - Pullout blocks for pullout tests

With the exception of the pullout blocks, half of each set of specimens were steam cured with the girders while the other half were moist cured. The steam cured specimens were cured in the Structures Laboratory at CU at room temperature after steam curing was completed. These specimens are referred to as air cured specimens in this report. All handling and curing of the specimens was per ASTM standards where applicable.

Figure 3.12 - Flame Cutting of Strands

3.4.5 Stress Transfer Procedure

Following overnight curing of the girder concrete, preparation for strand detensioning began. The contractor removed the forms to allow the CU staff access to the girders. The strain gage target points were cleaned and end slip devices were attached to the strands at the end of each girder. Bolts were affixed to each girder and fishing line was stretched tight between them for camber measurement.

Approximately 42 hours after girder casting, initial readings were taken and the prestress was released. This process was delayed because of the additional time needed to prepare the embedded target points for mechanical gage measurements. The pretension was released by cutting each strand with an oxy-acetylene torch. The strands close to the bulkheads were cut first, with the strands at both ends cut simultaneously. Following the same procedure, the strands between the first and the second and the second and the third girders were cut. The girders were not restrained

Table 3.5 - Topping Slab Concrete Mix Design

Material	Quantity kg/m^3 (lb./yd.^{3})
Type III Cement	418 (705)
Water	163 (275)
Coarse Aggregate (3/4" pea gravel, Cooley)	1103 (1860)
Fine Aggregate (Sand, Cooley)	694 (1170)
Water Reducer (Polyheed 997)	2.48 L/m^3 (84 oz./yd.^{3})
Water Reducer (Pozzolith 322N)	0.83 L/m^3 (28 oz./yd.^{3})

from movement, and they were observed to move several inches each time a strand was cut. This movement was the most significant during the first set of cuts, and was much less pronounced when cutting the strands in-between the girders.

3.4.6 Topping Slab Placement

Seven days after the girder concrete was poured, the topping slabs were cast for each girder. The procedure was the same as the procedure used to pour the girders. The topping slab concrete was batched on-site at the fabricator's batch plant. The fabricator developed their own mix design, shown in Table 3.5, to achieve the 28 day design concrete compressive strength of 40 MPa (5.8 ksi).

The topping slabs were successively cast, a curing compound was applied to the slab surface, and the girders were covered and allowed to air cure. Thirty 102 mm x 203 mm (4 in. x 8 in.) cylinders were cast from the concrete and transported back to CU where half were moist cured and half were air cured.

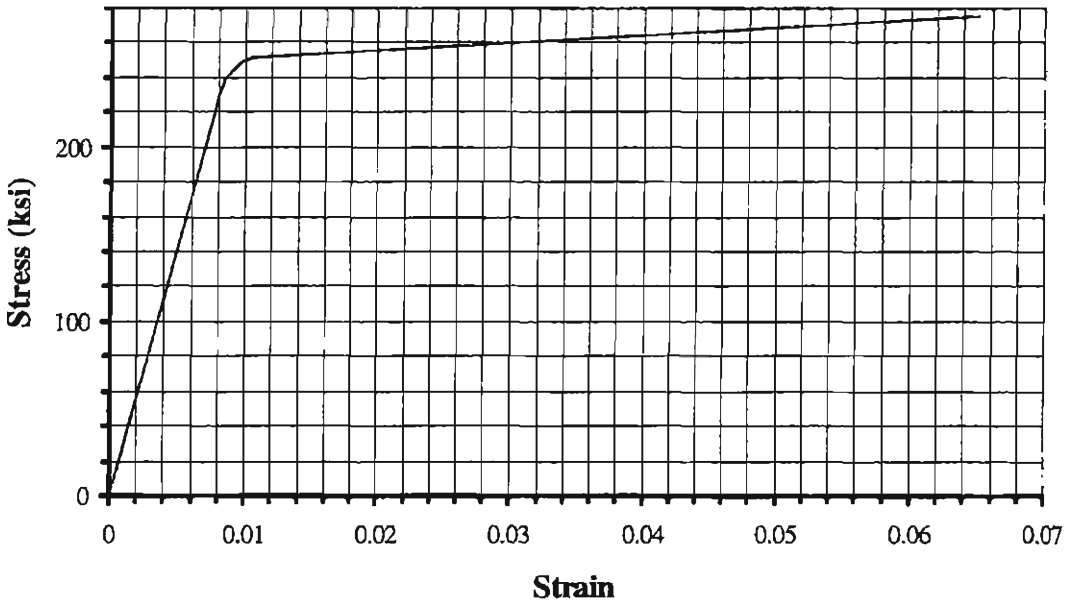

Figure 3.13 - Stress-Strain Relationship for Strand (1 ksi = 6.89 MPa)

3.5 MATERIAL PROPERTIES

3.5.1 Prestressing Strands

The prestressing strands used in the test specimens were manufactured by Insteel Wire Products. All strand was 15.2 mm (0.6 in.) diameter, Grade 270, low-relaxation prestressing strand meeting the requirements of ASTM A-416-94. The stress-strain curve for the strand was supplied by the manufacturer and is reproduced in Figure 3.13. The elastic modulus of the strand was 198 GPa (28,700 ksi). Chemical tests were conducted on samples of strand to determine the amount of surface phosphate. Results of the chemical tests are shown in Appendix E.

3.5.2 Non-Prestressing Steel

All non-prestressing steel consisted of standard Grade 60 rebar.

3.5.3 Girder Concrete

Materials tests were conducted per ASTM standards on moist and air cured specimens of the girder concrete. Tests to identify compressive strength, modulus of elasticity, modulus of rupture, shrinkage behavior, and split cylinder strength were conducted at the CU Structures Laboratory. Tests to identify shrinkage and creep behavior were also performed by Commercial Testing Laboratories (CTL/Thompson) of Denver, Colorado.

Table 3.6 - Compressive Strength and Elastic Modulus of Girder Concrete

Age Test Date	**Curing**	**Compressive Strength MPa (ksi)**		**Elastic Modulus MPa (ksi)**	
		Mean	*Standard Deviation*	*Mean*	*Standard Deviation*
2 Days	*Air*	53.7 (7.8)	0.2 (0.03)	32414 (4700)	293 (42)
8/15/96	*Moist*	NA	NA	NA	NA
7 Days	*Air*	61.6 (8.9)	1.5 (0.22)	29697 (4306)	NA
8/20/96	*Moist*	61.4 (8.9)	2.3 (0.34)	32254 (4677)	NA
15 Days	*Air*	64 (9.3)	1.6 (0.24)	32366 (4693)	NA
8/28/96	*Moist*	68.1 (9.9)	1.7 (0.25)	35631 (5166)	1563 (227)
28 Days	*Air*	61.4 (8.9)	NA	31484 (4565)	NA
9/10/96	*Moist*	71.1 (10.3)	NA	36716 (5324)	NA
50 Days	*Air*	67.3 (9.8)	NA	31321 (4542)	NA
10/2/96	*Moist*	72.2 (10.5)	2.0 (0.29)	NA	NA
65 Days	*Air*	66.8 (9.7)	1.3 (0.18)	30335 (4399)	NA
10/17/96	*Moist*	77.4 (11.2)	1.4 (0.21)	38661 (5606)	NA
79 Days	*Air*	63.8 (9.2)	13.5 (1.96)	29389 (4261)	NA
10/31/96	*Moist*	83.5 (12.1)	0.5 (0.07)	36138 (5240)	NA
90 Days	*Air*	69.4 (10.1)	1.2 (0.17)	NA	NA
11/11/96	*Moist*	76.1 (11.0)	2.9 (0.42)	NA	NA

Compressive strength and modulus of elasticity tests were performed on 102 mm x 203 mm (4 in. x 8 in.) cylinder specimens. A summary of the results of these tests is shown in Table 3.6. The concrete strength is plotted against age in Figure 3.14. Also shown are curve fits to the data. Detailed compressive stress-strain plots for the concrete cylinders are provided in Appendix A.

The moist cured cylinders of girder concrete achieved the required design compressive strength at 28 days, and reached a strength of 76 MPa (11 ksi) at 90 days. As expected, the air cured specimens yielded consistently lower strengths than the moist cured specimens.

Modulus of rupture testing was performed on standard beam specimens. Brazilian split-cylinder testing was performed on 152 mm x 305 mm (6 in. x 12 in.) cylinders. A summary of the results of these tests is shown in Table 3.7.

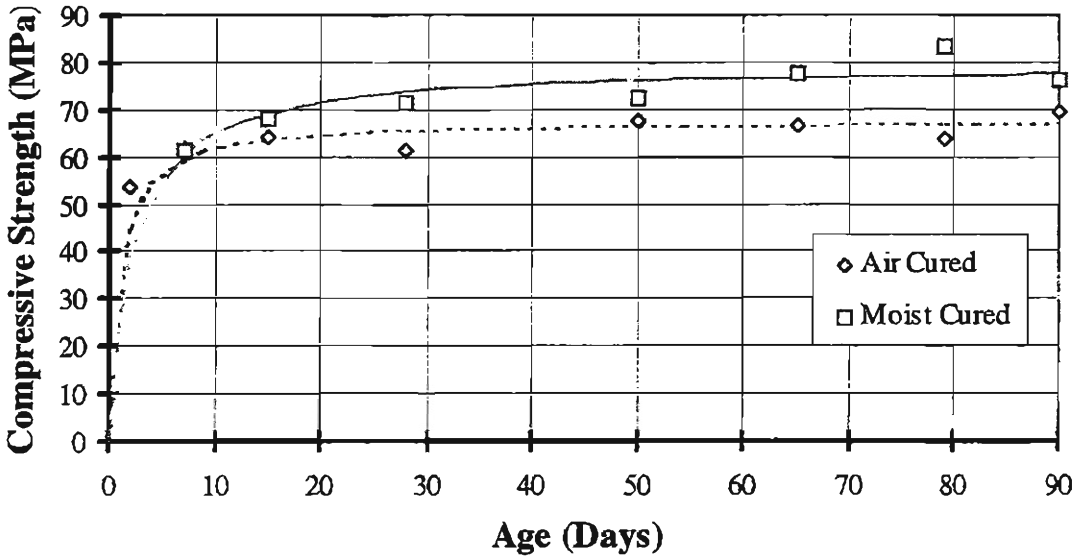

Figure 3.14 - Girder Concrete Compressive Strength

Figure 3.15 and Figure 3.16 show the graphs of the modulus of rupture and elastic modulus data versus $\sqrt{f'_c}$, with f'_c in psi. Linear fits to these data were performed and are shown with the equations representing these lines. Also shown are the equations given by the ACI 318 [2] for estimating the modulus of rupture and the modulus of elasticity. Additionally, an equation recommended for high strength concrete by researchers at Cornell University, is presented [17].

The expression for the modulus of rupture of normal weight concrete is given in Section 9.5.2.3 of the ACI Code [2] as

$$f_r = 7.5\sqrt{f'_c}$$

whereas the expression for the modulus of elasticity for normal weight concrete, given in Section 8.5.1 of the ACI Code [2], is

$$E_c = 57{,}000\sqrt{f'_c}$$

In both of these expressions, f'_c and the resulting values are in psi. For normal weight concrete with a compressive strength between 30 MPa (3,000 psi) and 83 MPa (12,000 psi), the equation recommended for the modulus of elasticity by the researchers at Cornell University [17] is

$$E_c = \left(40{,}000\sqrt{f'_c} + 1{,}000{,}000\right)\left(\frac{w_c}{145}\right)^{1.5}$$

in which w_c is the unit weight of the hardened concrete in pcf and all other terms are as defined previously.

Table 3.7 - Modulus of Rupture and Split Cylinder Strength of Girder Concrete

Age Test Date	Curing	Modulus of Rupture MPa (ksi)		Split-Cylinder Strength MPa (ksi)	
		Mean	*Standard Deviation*	*Mean*	*Standard Deviation*
3 Days	*Air*	4.1 (0.6)	0.21 (0.03)	4 (0.58)	NA
8/16/96	*Moist*	6.9 (1.0)	NA	3.9 (0.57)	0.22 (0.032)
7 Days	*Air*	6.9 (1.0)	0.41 (0.06)	4.2 (0.61)	NA
8/20/96	*Moist*	6.9 (1.0)	NA	4.3 (0.62)	0.3 (0.044)
15 Days	*Air*	6.9 (1.0)	NA	4.3 (0.62)	NA
8/28/96	*Moist*	7.6 (1.1)	0.07 (0.01)	4.7 (0.68)	0 (0)
28 Days	*Air*	7.6 (1.1)	0.48 (0.07)	4.5 (0.65)	NA
9/10/96	*Moist*	8.3 (1.2)	0.76 (0.11)	5 (0.73)	NA
50 Days	*Air*	NA	NA	4.7 (0.68)	0.1 (0.015)
10/2/96	*Moist*	NA	NA	NA	NA
65 Days	*Air*	7.6 (1.1)	NA	4.6 (0.66)	NA
10/17/96	*Moist*	8.3 (1.2)	NA	5 (0.73)	0 (0)
79 Days	*Air*	7.6 (1.1)	0.76 (0.11)	4.9 (0.71)	NA
10/31/96	*Moist*	8.3 (1.2)	0.21 (0.03)	NA	NA

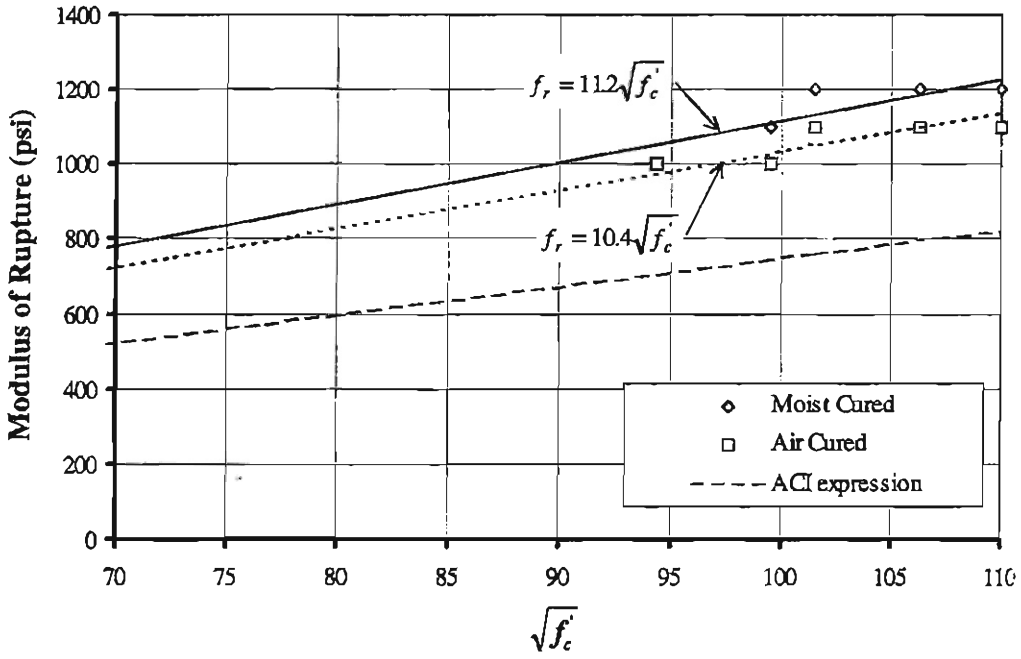

Figure 3.15 - Modulus of Rupture Data and ACI Expression (f'_c in psi; 1 psi = $6.89x10^3$ Pa)

As can be seen from the graphs, the ACI formula for modulus of rupture is somewhat conservative for our data while the formula for modulus of elasticity is somewhat high. However, the equation from Cornell University fits the modulus of elasticity data on the moist cured specimens well.

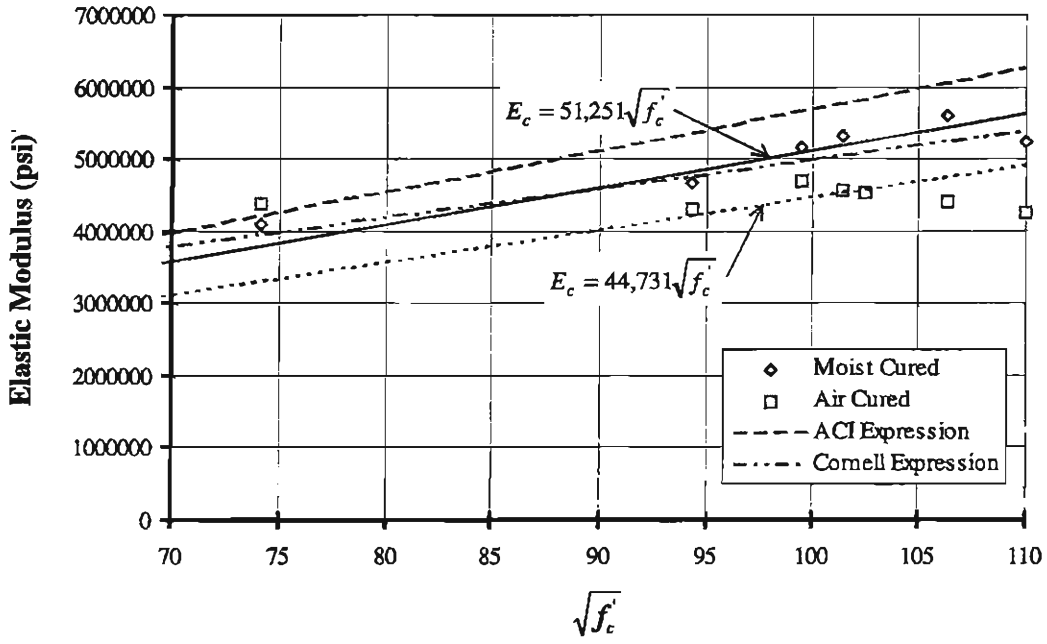

Figure 3.16 - Modulus of Elasticity Data and ACI and Cornell Expression (f'_c in psi) (1 psi = 6.89x10^3 Pa)

Shrinkage measurements were taken at both CU and CTL/Thompson. CU tested four air cured specimens and two lime-water cured specimens. The four air cured specimens were steam cured with the girders, cured in lime-saturated water for the following two days, and air cured at room temperature thereafter. The two lime-water cured specimens were cured in lime-saturated water for the first 28 days after casting and were air cured at room temperature thereafter. Measurements for lime-water cured specimens began the day after girder casting. Measurements for the air

cured specimens began three days after girder casting, upon removal from the lime-saturated water. A graph of the average results is shown in Figure 3.17. These

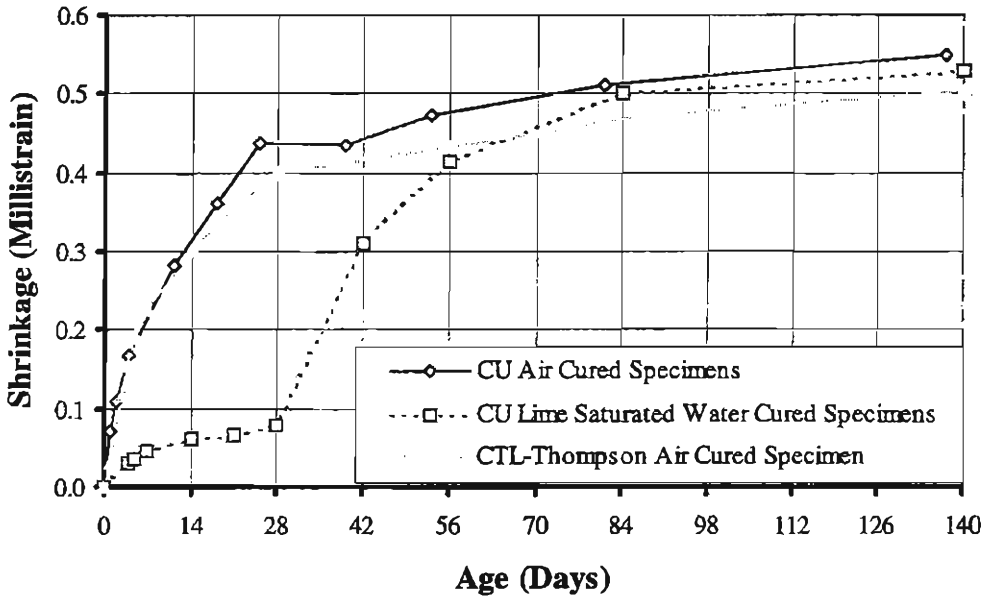

Figure 3.17 - Average Shrinkage Strain for Girder Concrete

shrinkage results are typical for this type of concrete [17]. The moist cured specimens shrank very little during the 28 days they were immersed in lime-saturated water. However, after they were removed from the lime-saturated water, they exhibited shrinkage nearly identical to that of the air cured specimens.

Creep tests were performed on 102 mm x 203 mm (4 in. x 8 in.) cylinders by CTL/Thompson. Owing to measurement problems with the specimens initially cast with the girders, these specimens were cast several weeks after the girders were cast using the same mix design as the girder concrete. The specimens were steam cured in the same way as the girders and subsequently air cured in the laboratory at a temperature of 23°C (73°F) and a relative humidity of 50%. Loading began after two

days of curing. The test results (reproduced from Appendix B) are plotted in Figure 3.18. Shrinkage measurements were taken together with the creep tests. The shrinkage specimens were cured under the same condition as the creep specimens. As shown in Figure 3.17, the shrinkage obtained by CTL/Thompson was very close to that exhibited by the air cured specimens at CU, with the former being slightly lower.

Creep was also calculated using the following empirical expression.

$$\delta_t = \frac{t^{0.60}}{10 + t^{0.60}} \delta_u \qquad (3\text{-}1)$$

in which δ_t is the unit creep strain at time t, t is the time in days after loading, and δ_u is the ultimate creep strain [17]. For 69 MPa (10 ksi) concrete, based on research at Cornell University, an ultimate unit creep strain equal to 41×10^{-6} per MPa (0.28×10^{-6} per psi) is suggested [17]. With the aforementioned value, the results obtained with Eq. (3-1) are plotted in Figure 3.18.

As can be seen from the graph, the creep exhibited by the laboratory specimens is significantly higher than the calculated values.

3.5.4 Topping Slab Concrete

Materials tests were conducted per ASTM standards on moist and air cured specimens of the topping slab concrete to identify the compressive strength and modulus of elasticity. A summary of these results is shown in Table 3.8. A graph of compressive strength versus age is shown in Figure 3.19. Also shown are curve fits to the data.

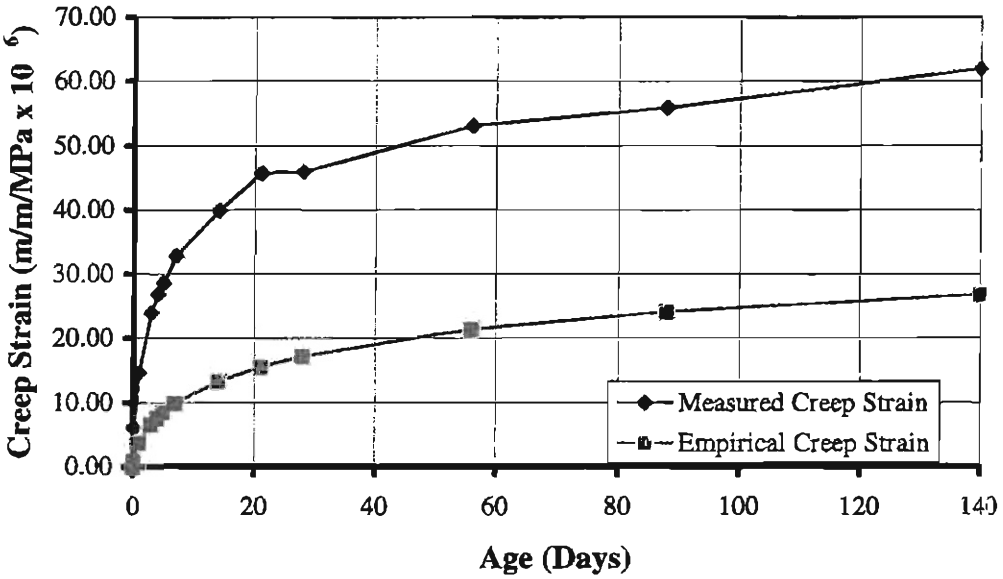

Figure 3.18 - Unit Creep Strain for Girder Concrete

Table 3.8 - Compressive Strength and Modulus of Elasticity of Topping Concrete

Age Test Date	Curing	Compressive Strength MPa (ksi)		Elastic Modulus MPa (ksi)	
		Mean	*Standard Deviation*	*Mean*	*Standard Deviation*
7 Days	*Air*	48.3 (7.0)	0 (0)	NA	NA
8/27/96	*Moist*	48.3 (7.0)	0 (0)	NA	NA
14 Days	*Air*	53.1 (7.7)	NA	NA	NA
9/3/96	*Moist*	50.3 (7.3)	0 (0)	NA	NA
28 Days	*Air*	NA	NA	NA	NA
9/17/96	*Moist*	NA	NA	NA	NA
43 Days	*Air*	53.9 (7.8)	2.1 (0.3)	31146 (4516)	3024 (438)
10/2/96	*Moist*	50.7 (7.4)	1.7 (0.2)	NA	NA
58 Days	*Air*	53.8 (7.8)	3 (0.4)	31288 (4537)	824 (119)
10/17/96	*Moist*	56.7 (8.2)	1.3 (0.2)	32778 (4753)	1505 (218)
72 Days	*Air*	54.4 (7.9)	4.6 (0.7)	30967 (4490)	1027 (149)
10/31/96	*Moist*	57.5 (8.3)	5.2 (0.8)	39722 (5760)	5069 (735)

The topping slab concrete exceeded the required design compressive strength by a significant amount, reaching a strength of 57.5 MPa (8.3 ksi) in 72 days. The results for the moist and air cured specimens are quite close, however, the moist cured specimens tend to have higher compressive strengths. The elastic modulus of the concrete is, on average, about 10% lower than the value given by the ACI formula.

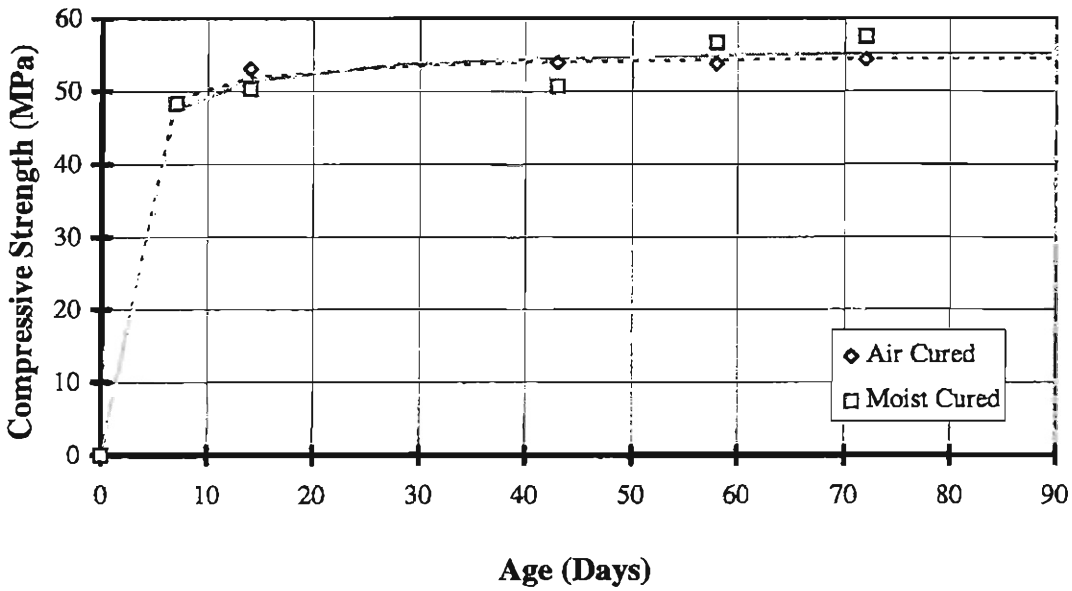

Figure 3.19 - Topping Concrete Compressive Strength

4. TEST RESULTS

4.1 PULLOUT TEST RESULTS

Pullout tests were conducted two days after the casting of the two pullout blocks. The concrete compressive strength at this time was 39.2 MPa (5,690 psi). Load was applied to each strand until strand slip was detected. The load at which this occurred was recorded. Loading was then continued until the strand could no longer sustain further load increases. The load at which this occurred and the total distance the strand was pulled out of the block were then recorded.

All eight strands were tested in the first pullout block. The results were very consistent within this group, and thus, only one strand was tested in the second block. A summary of the test results is presented in Table 4.1.

Table 4.1 - Pullout Test Results

Strand Number	Load at First Slip kN (kips)	Maximum Load kN (kips)	Ram Extension at Maximum Load mm (in.)
1	128.1 (28.8)	209.5 (47.1)	35.1 (1.38)
2	123.7 (27.8)	189.0 (42.5)	38.1 (1.50)
3	145.4 (32.7)	192.2 (43.2)	62.0 (2.44)
4	133.9 (30.1)	189.0 (42.5)	50.8 (2.00)
5	110.8 (24.9)	218.4 (49.1)	50.8 (2.00)
6	130.8 (29.4)	224.2 (50.4)	50.8 (2.00)
7	101.9 (22.9)	241.5 (54.3)	54.1 (2.13)
8	122.3 (27.5)	224.2 (50.4)	63.5 (2.50)
9	206.4 (46.4)	247.3 (55.6)	36.6 (1.44)
Average	*133.7 (30.1)*	*215.0 (48.3)*	*49.1 (1.93)*

The maximum loads attained in each of these tests are all well above the benchmark capacity of 160 kN (36 kips) suggested for 12.7 mm (0.5 in.) diameter strands by Logan [13]. A benchmark for 15.2 mm (0.6 in.) diameter strands has not yet been established. Thus, the performance of this strand relative to other 15.2 mm (0.6 in.) diameter strand is unclear at this time.

4.2 STRAND SLIP AT TRANSFER

Strand slip was measured for each of the nine strands at the end of each girder. The distance between a fixed reference point on each strand and the end of the girder was measured immediately before and after prestress release. The difference between these two measurements gives the apparent strand slip. The elastic shortening which occurred over the strand between the end of the girder and the reference point was calculated and subtracted from the apparent strand slip to give the actual strand slip.

Girder movement during prestress release caused minor concrete spalling near the ends of the girders. As a result of this, the slip for a number of strands could not

Table 4.2 - Average Strand Slip Measurements Immediately after Transfer

Girder End		Average End Slip Measured mm (in.)
1-E	live end	1.44 (0.057)
1-W		1.61 (0.063)
2-E		1.48 (0.058)
2-W		1.73 (0.068)
3-E		1.46 (0.057)
3-W	live end	1.27 (0.050)
Average		1.49 (0.059)

be measured. Additionally, during girder transportation, further concrete spalling and damage to the C-channels occurred. This damage made strand slip measurements at later ages impossible. The averages of the strand slips measured for each girder end immediately after release are presented in Table 4.2. The values in the table are the actual strand slips with the elastic shortening of the strand taken out form the raw data.

The end slips measured for these members are consistent with those measured in previous studies using high strength concrete and 15.2 mm (0.6 in.) diameter strands [9].

4.3 CAMBER MEASUREMENTS

The results of the camber measurements taken at midspan for each of the girders are presented in Table 4.3. A time step procedure was also used to estimate the camber for the girders [17]. Use of this method requires knowledge of the girder section properties, concrete creep and shrinkage behavior, steel relaxation behavior, and the variation of the concrete elastic modulus with time. With the exception of steel relaxation, all of these properties were measured in the testing program. Steel relaxation was estimated using the following empirical equation for low relaxation strand [17].

$$\frac{f_s}{f_{si}} = 1 - \frac{\log t}{45}\left(\frac{f_{si}}{f_{sy}} - 0.55\right) \qquad (4\text{-}1)$$

in which f_s is the steel stress at time t, f_{sy} is the effective yield stress, f_{si} is the initial prestress, t is the time in hours after stressing, and log t is to the base 10.

Table 4.3. - Measured Girder Camber

Time of Measurement (Concrete Age)	**Camber mm (in.)**		
	Girder 1	*Girder 2*	*Girder 3*
Immediately After Release (2 Days)	22.2 (0.88)	22.2 (0.88)	20.6 (0.81)
Before Topping (7 Days)	31.8 (1.25)	30.2 (1.19)	28.6 (1.13)
After Topping (7 Days)	27.0 (1.06)	30.2 (1.19)	30.2 (1.19)
12 Days After Release (14 Days)	31.8 (1.25)	30.2 (1.19)	30.2 (1.19)
26 Days After Release (28 Days)	31.8 (1.25)	NA	30.2 (1.19)

Table 4.4 - Section Properties Used in Time Step Calculations (1 in. = 25.4 mm)

Section Properties	
Before Topping	
I_x (in.^{4})	7443
A_c (in.^{2})	206.3
After Topping	
I_x (in.^{4})	12206
A_c (in.^{2})	247.5

The values used in the time step computations are summarized in Table 4.4 and Table 4.5. As shown in Table 4.4, the girder section properties were changed to reflect the addition of the topping slab at 7 days. The reduction in camber due to the weight of the topping slab was also calculated and subtracted from the values obtained at 7 days without the topping slab. The results of these calculations and the average measured camber at midspan are shown in Table 4.7. As can be seen, the

calculated camber using these values was significantly higher than the measured camber.

Table 4.5 - Time Dependent Variables Used in Time Step Procedure
(1 psi = 6.89x10^3 Pa; 1 ksi = 6.89 MPa)

Time	Creep		Shrinkage		Steel Relaxation		Modulus of Elasticity
Days	(in./in.)/psi x 10^6		in./in.				ksi
	δ_t	$\Delta\delta_t$	$\varepsilon_{sh,t}x10^{-6}$	$\Delta\varepsilon_{sh,t}x10^{-6}$	f_s/f_{si}	$\Delta(1-f_s/f_{si})$	
-2	-	-	0	-	1.000	-	0
0 (Release)	0	-	73	73	0.987	0.013	4300
7	0.226	0.226	249	176	0.983	0.005	4677
14	0.275	0.049	318	69	0.981	0.002	5166
28	0.316	0.041	402	84	0.979	0.002	5324
90	0.388	0.072	473	71	0.975	0.004	5700

Table 4.6 - Variation of Unit Creep Strain using Empirical Equation

Time	Creep	
Days	δ_t x 10^{-6}	$\Delta\delta_t$ x 10^{-6}
-2	-	-
0 (Release)	0	-
7	0.07	0.07
14	0.09	0.02
28	0.12	0.03
90	0.17	0.05

Creep is the prime contributor to increases in camber and it is suspected that the measured creep values were too high. Part of this could be due to the different curing temperatures of the creep specimens and the girders. Thus, the time step procedure was carried out again using creep values generated from the empirical equation, Eq. (3-1), presented in Section 3.5.3. The values of unit creep strain

Table 4.7 - Measured and Calculated Camber using Measured and Empirical Creep Equation

Time	Calculated Midspan Camber using Measured Creep	Calculated Midspan Camber using Creep Equation	Measured Midspan Camber
Days After Release	**mm (in.)**	**mm (in.)**	**mm (in.)**
0	26.0 (1.02)	26.0 (1.02)	21.7 (0.86)
7 (Before Topping)	49.3 (1.94)	32.7 (1.29)	30.2 (1.19)
7 (After Topping)	46.7 (1.84)	30.1 (1.19)	29.1 (1.15)
14	51.4 (2.02)	32.4 (1.28)	30.7 (1.21)
28	55.1 (2.17)	34.9 (1.38)	31.0 (1.22)
90	61.6 (2.43)	39.6 (1.56)	NA

calculated using this equation are presented in Table 4.6. These results are much closer to the measured values.

4.4 CONCRETE STRAINS AFTER TRANSFER

Concrete strains after transfer were calculated using the measurements taken with the Whittemore gage discussed previously. The initial distances between the embedded points in the girders were measured immediately before prestress release. These readings were then subtracted from subsequent measurements to yield the total change in distance between the points over the time period elapsed since the initial readings. Knowing this change in distance, the change in strain was calculated by dividing each value by the initial measured distance between the points. This change in strain was assumed to occur midway between the two points in question and at the level of the center of gravity of the strand group.

In this manner, the change in strain was calculated at discrete points along both sides of the three girders. For each girder, the strains for the corresponding

points on both sides were averaged to obtain one set of readings along the girder length. On the following pages, the resulting strains are plotted for the three girders. Each page contains two plots, one plot showing strains for the west half (W) of a girder and one showing strains for the east half (E) of a girder. For each girder, strains at the following times are shown:

- After Release
- Seven days after girder casting, immediately before topping slab casting (7 Day-ND)
- Seven days after girder casting, immediately after topping slab casting (7-Day-WD)
- 28 Days after girder casting
- Just before development length testing

The information in parentheses indicates the nomenclature used in the legend for each plot.

4.5 TRANSFER LENGTH

4.5.1 Determination of Transfer Length

Transfer length was determined using the 95% average maximum strain plateau method [21]. The strain data collected was examined and the region in which the strains appeared to level out, or plateau, was identified. The strain values in this region were then averaged to determine the magnitude of the average maximum strain. This value was then reduced by 5% to obtain the magnitude of the 95% average maximum strain plateau. Both the 100% and 95% average maximum strain plateaus are shown as horizontal lines in Figure 4.13 through Figure 4.24.

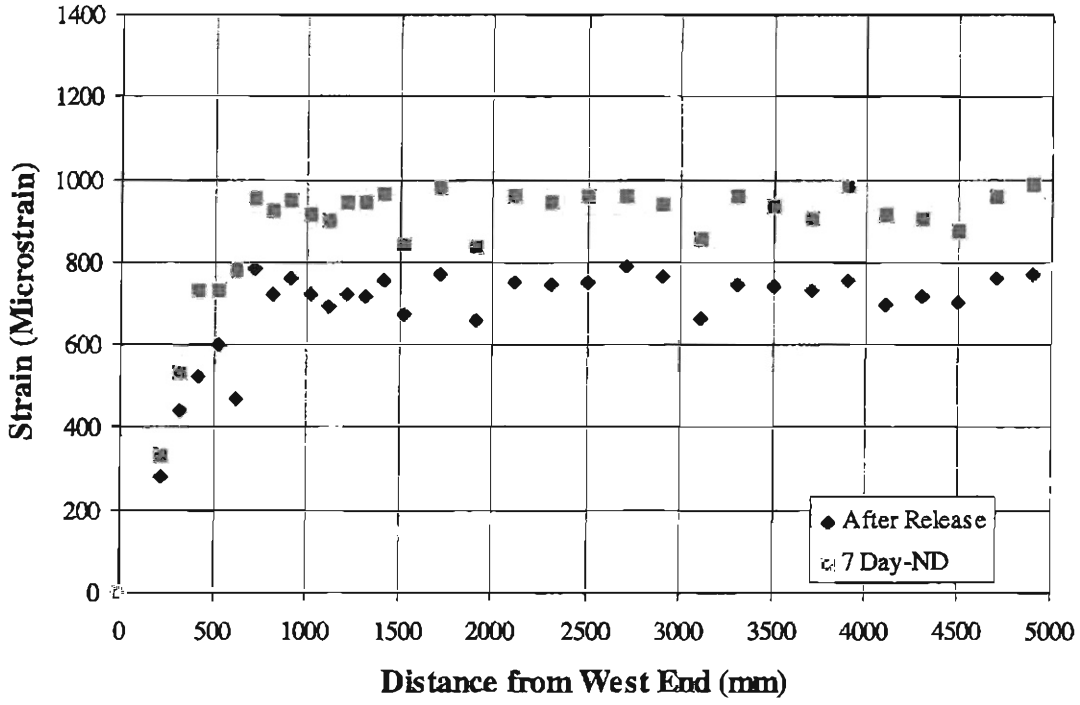

Figure 4.1 - West End Strain Readings for Girder 1 After Release and at 7 Days (Before Topping)

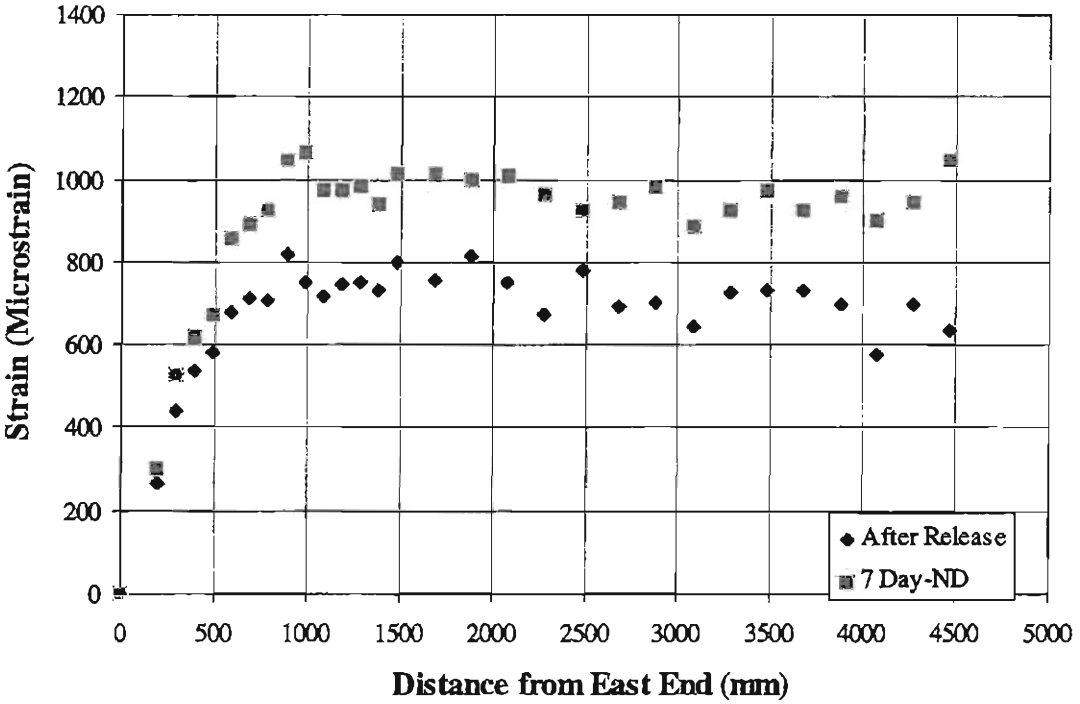

Figure 4.2 - East End Strain Readings for Girder 1 After Release and at 7 Days (Before Topping)

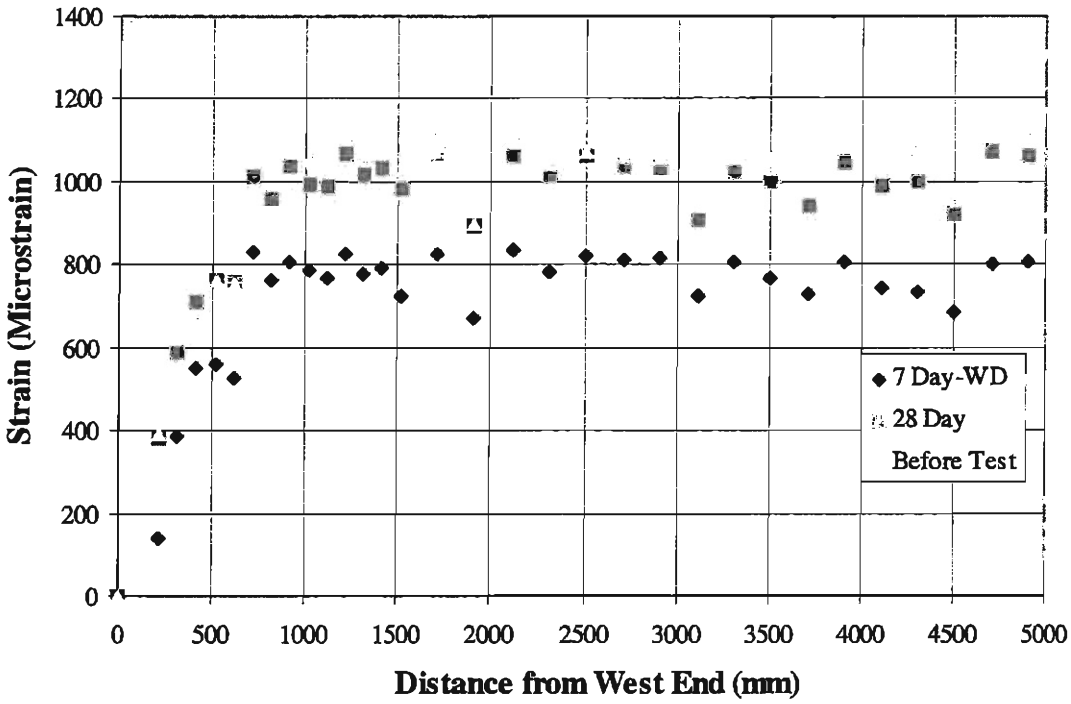

Figure 4.3 - West End Strain Readings for Girder 1 at 7 Days (After Topping), 28 Days, and 59 Days

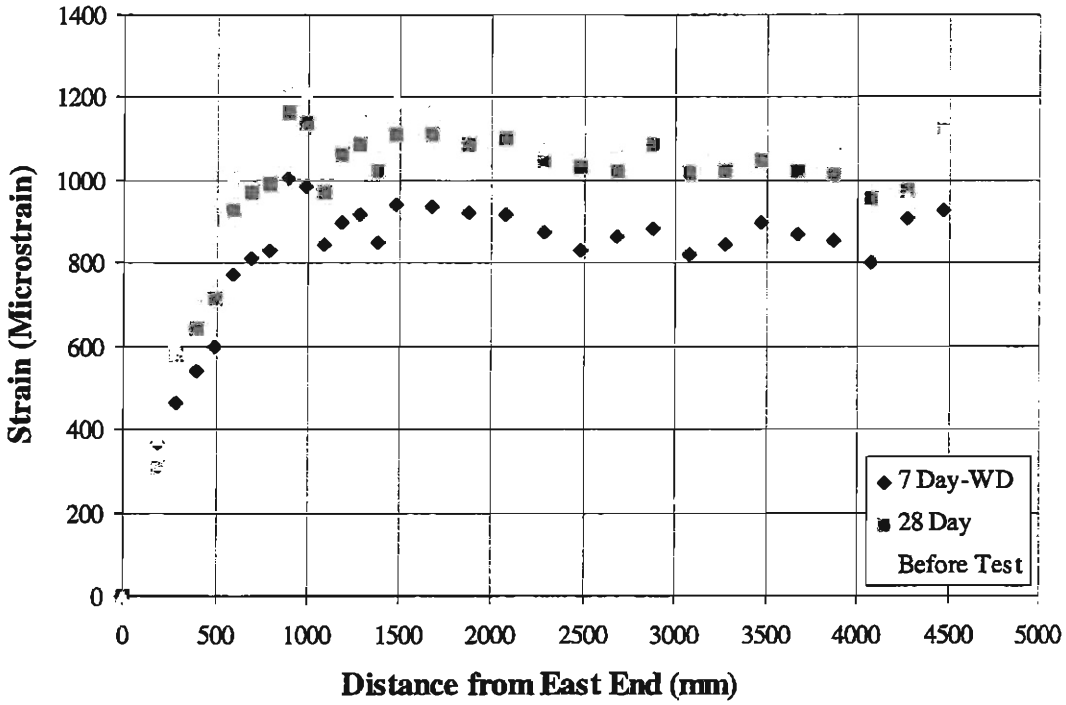

Figure 4.4 - East End Strain Readings for Girder 1 at 7 Days (After Topping), 28 Days, and 50 Days

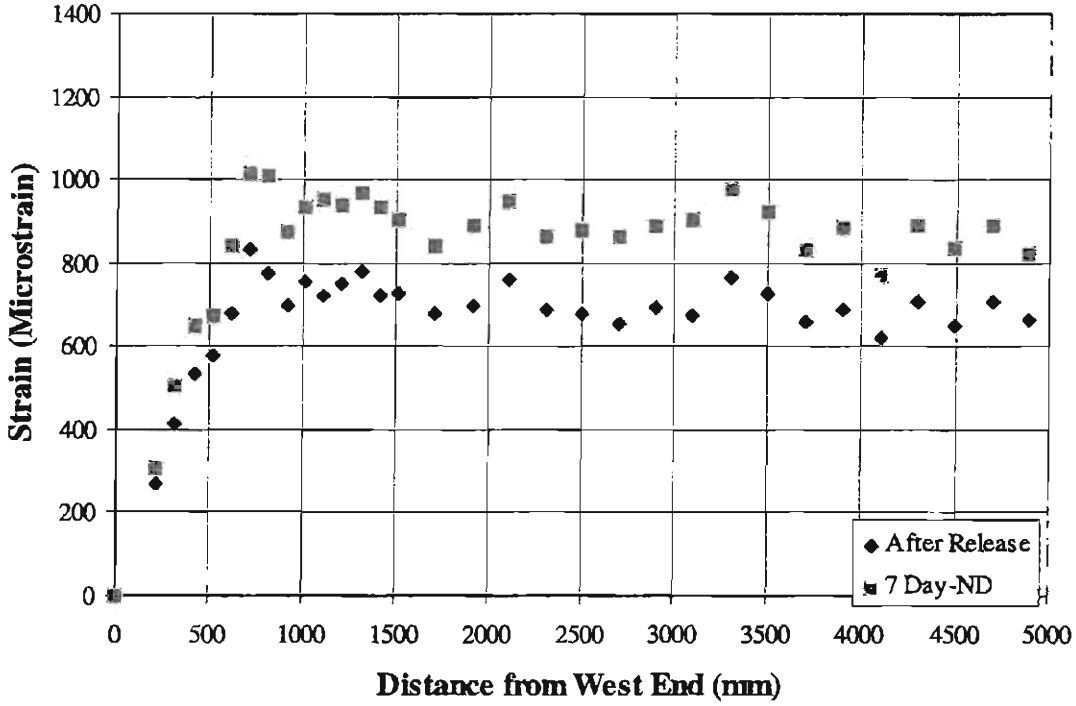

Figure 4.5 - West End Strain Readings for Girder 2 After Release and at 7 Days (Before Topping)

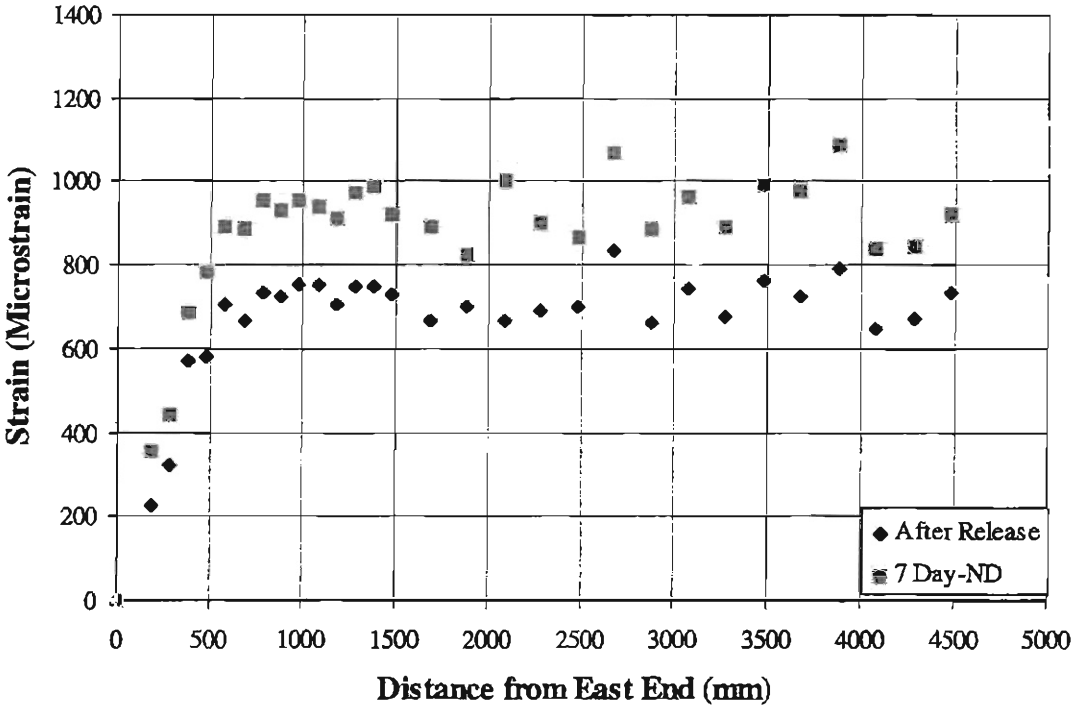

Figure 4.6 - West End Strain Readings for Girder 2 After Release and at 7 Days (Before Topping)

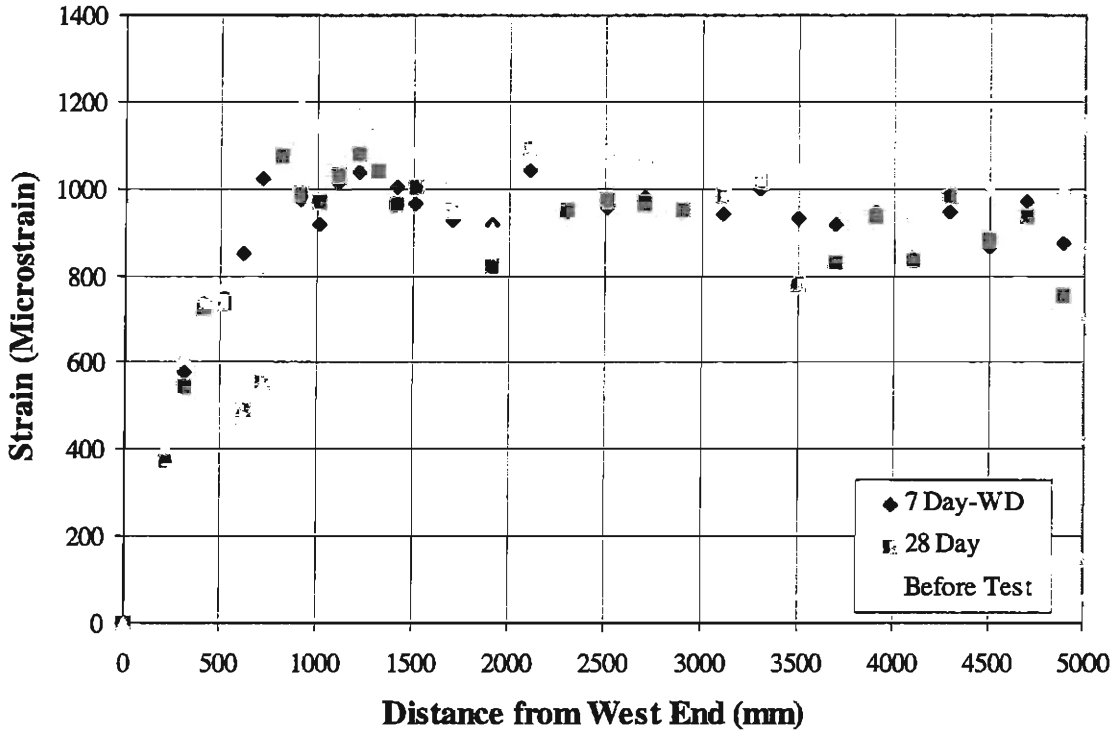

Figure 4.7 - West End Strain Readings for Girder 2 at 7 Days (After Topping), 28 Days, and 69 Days

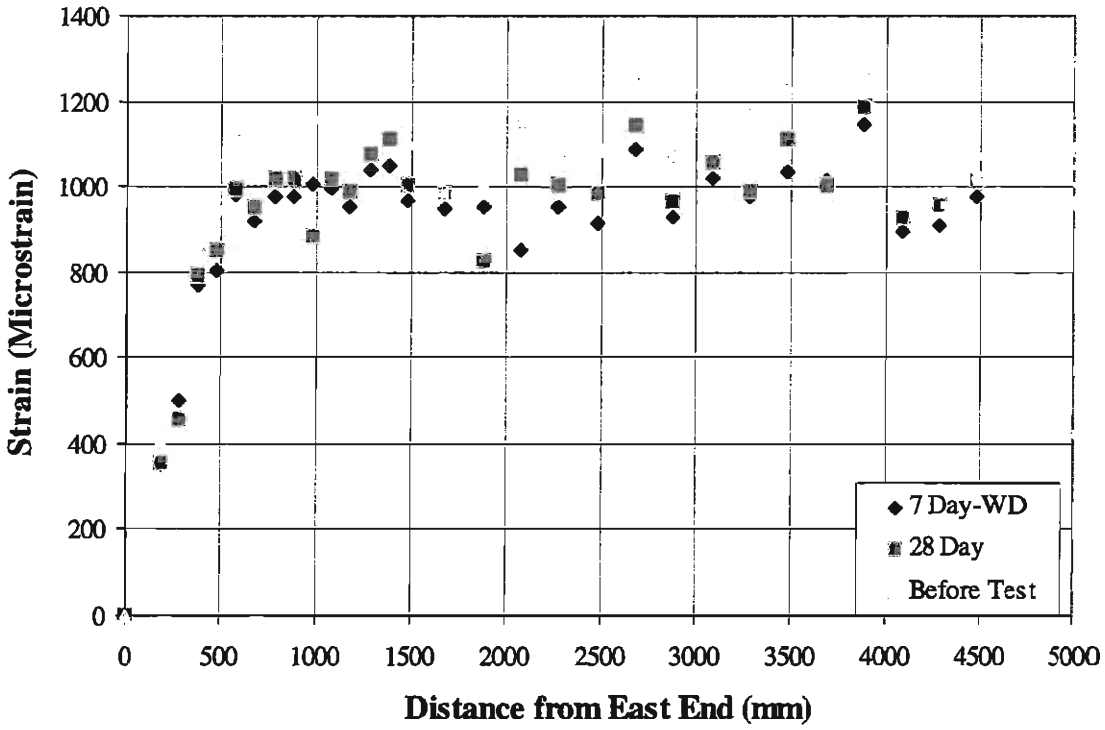

Figure 4.8 - East End Strain Readings for Girder 2 at 7 Days (After Topping), 28 Days, and 76 Days

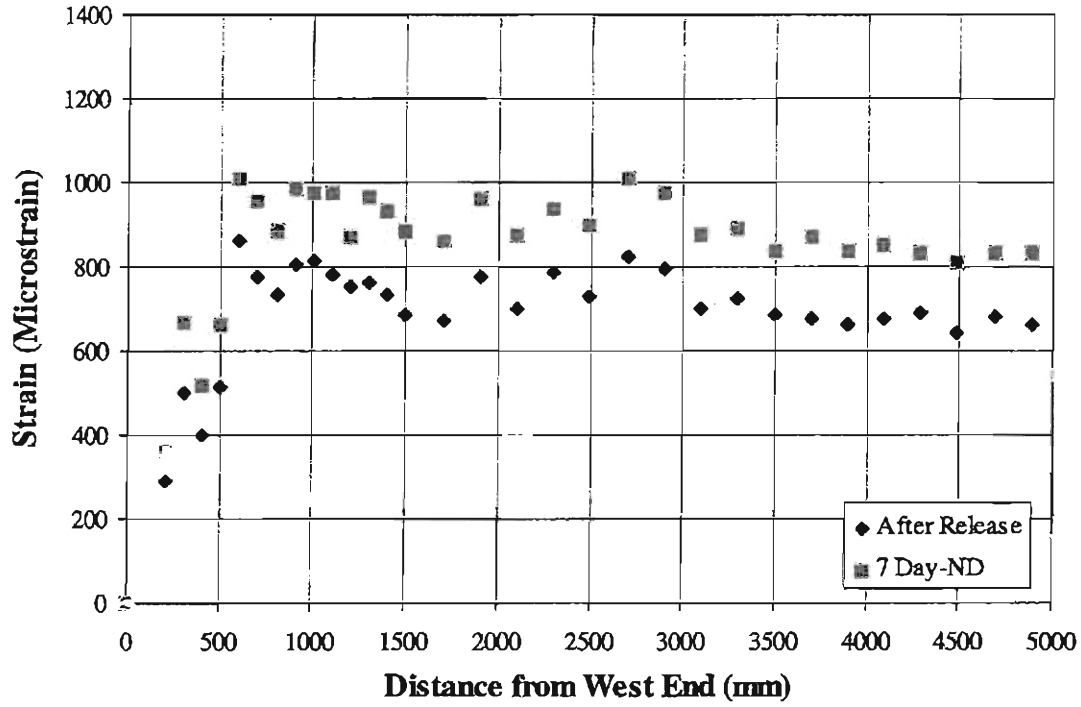

Figure 4.9 - West End Strain Readings for Girder 3 After Release and at 7 Days (Before Topping)

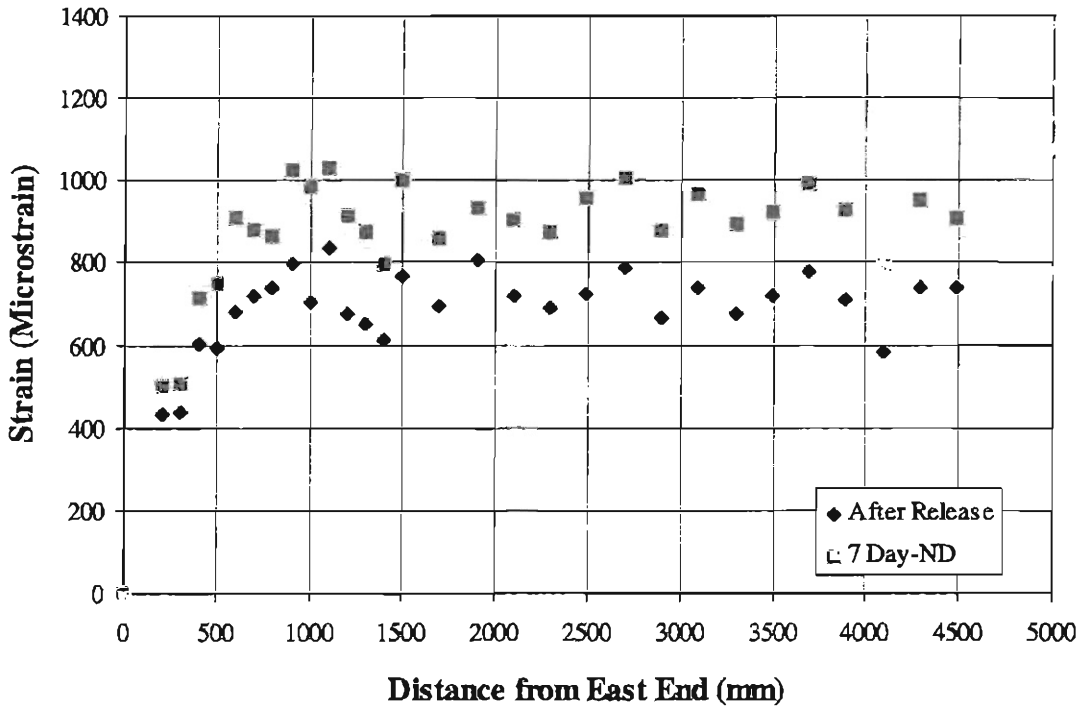

Figure 4.10 - East End Strain Readings for Girder 3 After Release and at 7 Days (Before Topping)

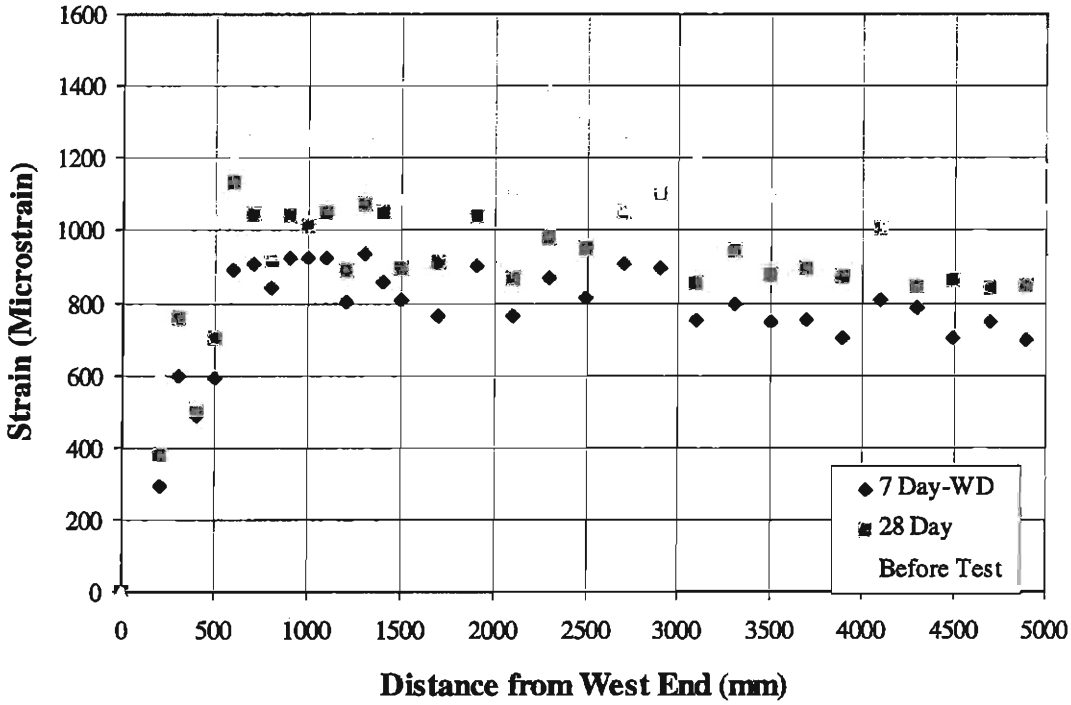

Figure 4.11 - West End Strain Readings for Girder 3 at 7 Days (After Topping), 28 Days, and 90 Days

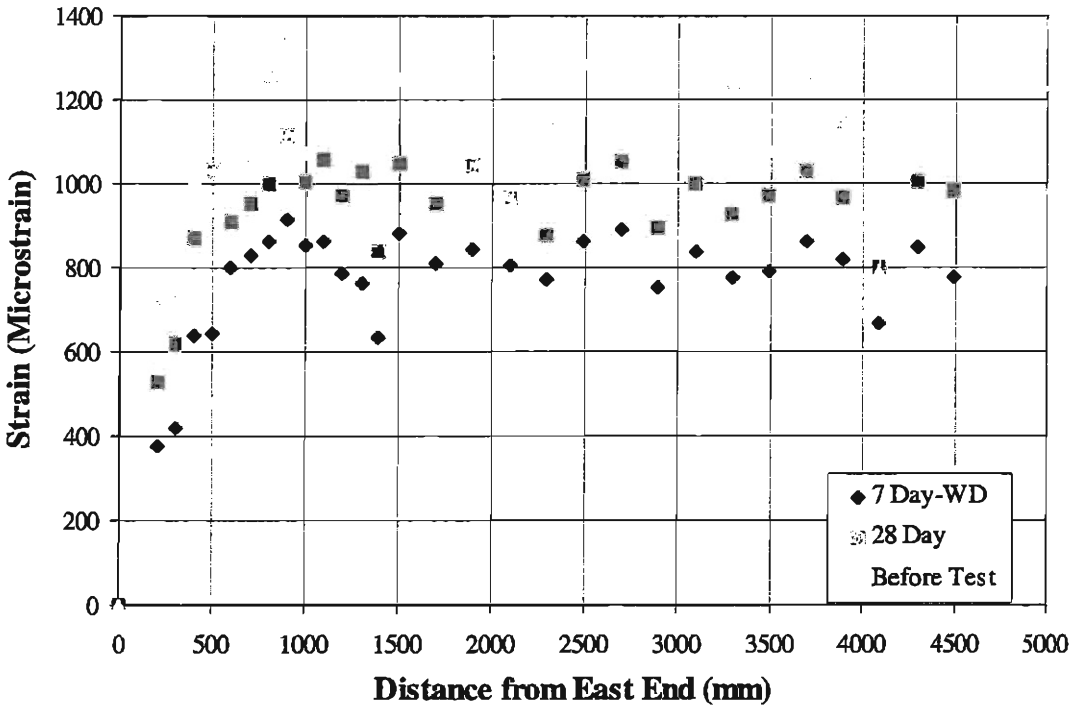

Figure 4.12 - West End Strain Readings for Girder 3 at 7 Days (After Topping), 28 Days, and 90 Days

Table 4.8 - Transfer Length Results

Girder End	L_t by 95% Average Maximum Strain Plateau Method	
	Immediately After Release mm (in.)	*28 Days after Girder Casting mm (in.)*
1-E	615 (24.2)	720 (28.3)
1-W	620 (24.4)	670 (26.4)
2-E	560 (22.0)	560 (22.0)
2-W	605 (23.8)	650 (25.6)
3-E	605 (23.8)	650 (25.6)
3-W	555 (21.9)	550 (21.7)
Average	*593 (23.4)*	*633 (24.9)*

On the same plots, the measured strain data points were plotted with lines connecting the points. The intersection of the line representing the 95% average maximum strain plateau and a line passing through the measured data points is then used to estimate the value of the transfer length. Although several intersections may occur on each plot, the distance to the intersection nearest the girder end is taken as the transfer length.

The transfer length was determined at each girder end immediately after release and at 28 days after girder casting using this method. The strain values, the calculated plateau values, and the transfer length found for each of these cases are shown in Figure 4.13 through Figure 4.24. The transfer lengths determined for each girder end are summarized in Table 4.8.

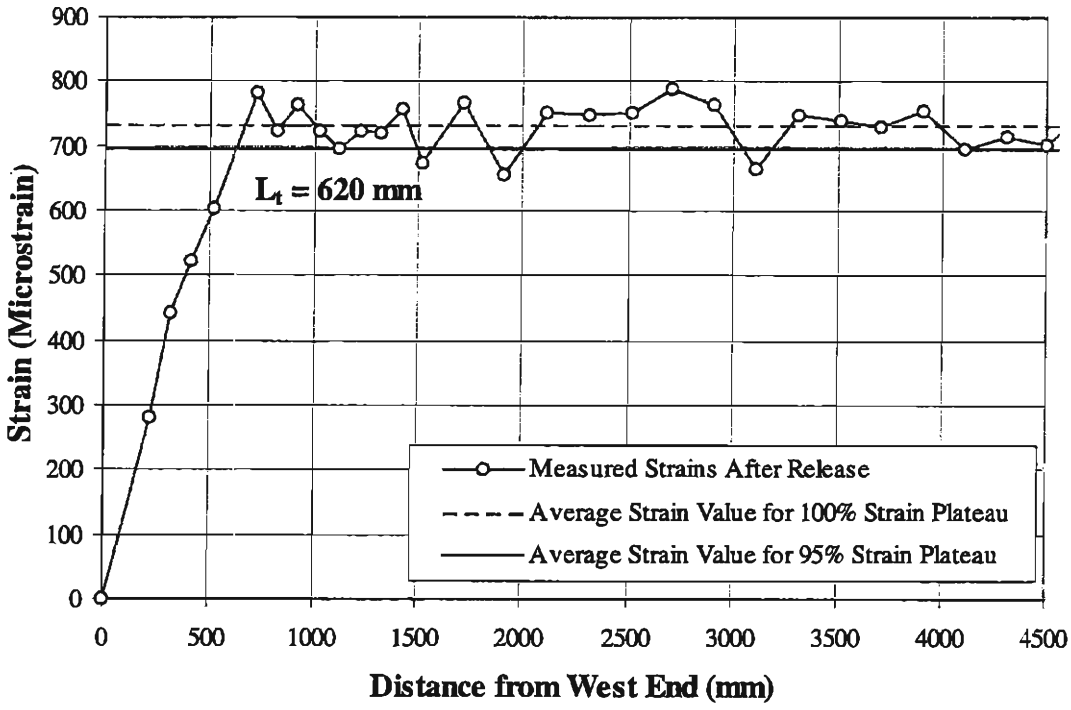

Figure 4.13 - Transfer Length After Release by 95% Average Maximum Strain Plateau Method (1-W)

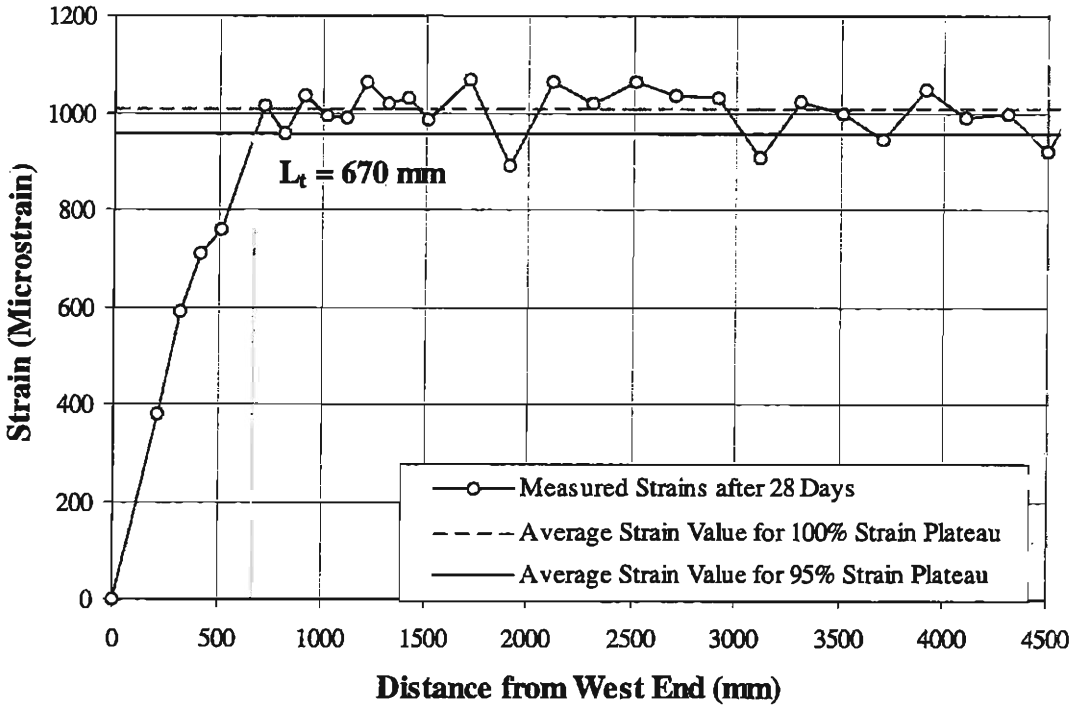

Figure 4.14 - Transfer Length after 28 Days by 95% Average Maximum Strain Plateau Method (1-W)

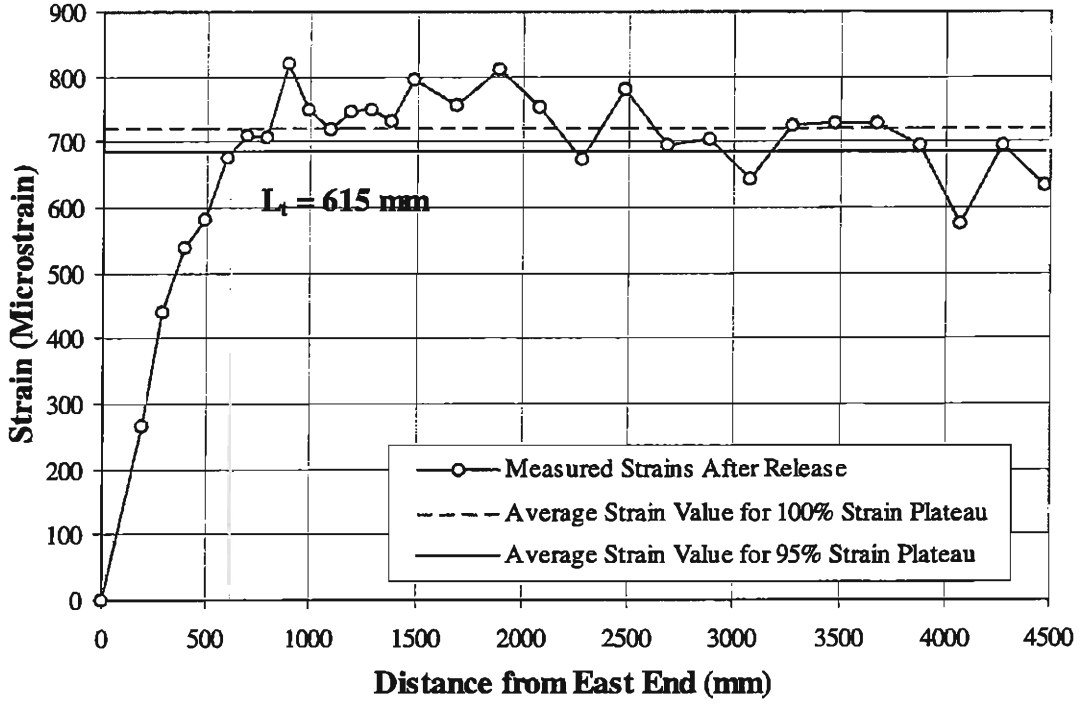

Figure 4.15 - Transfer Length After Release by 95% Average Maximum Strain Plateau Method (1-E)

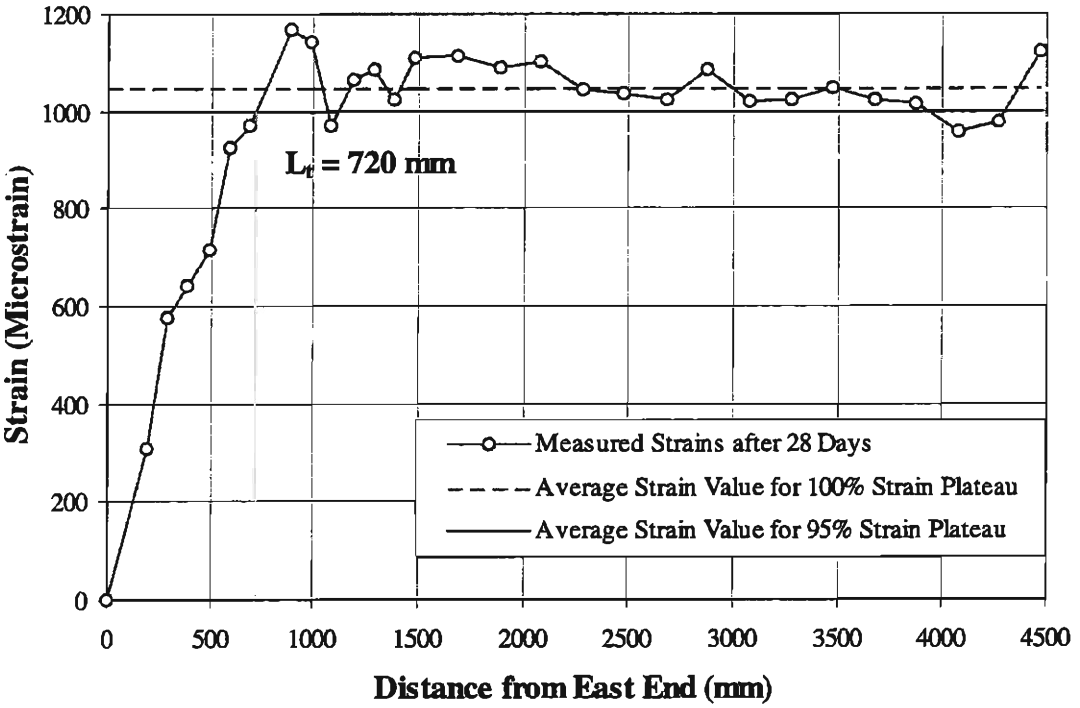

Figure 4.16 - 28 Day Transfer Length after 28 Days by 95% Average Maximum Strain Plateau Method (1-E)

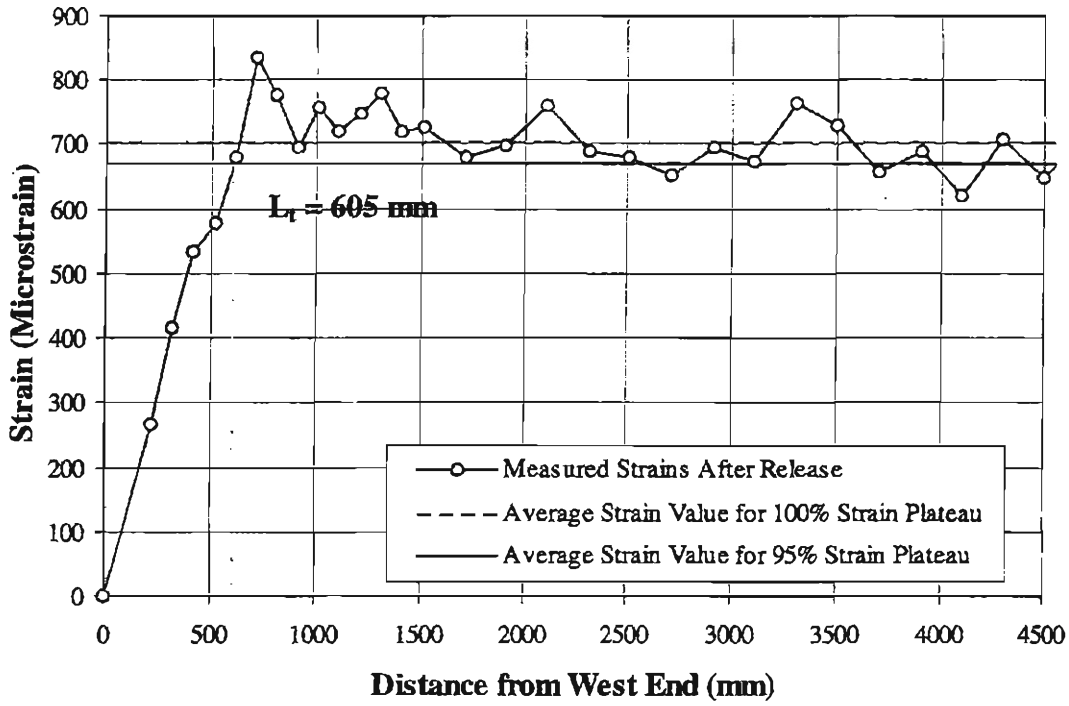

Figure 4.17 - After Release Transfer Length After Release by 95% Average Maximum Strain Plateau Method (2-W)

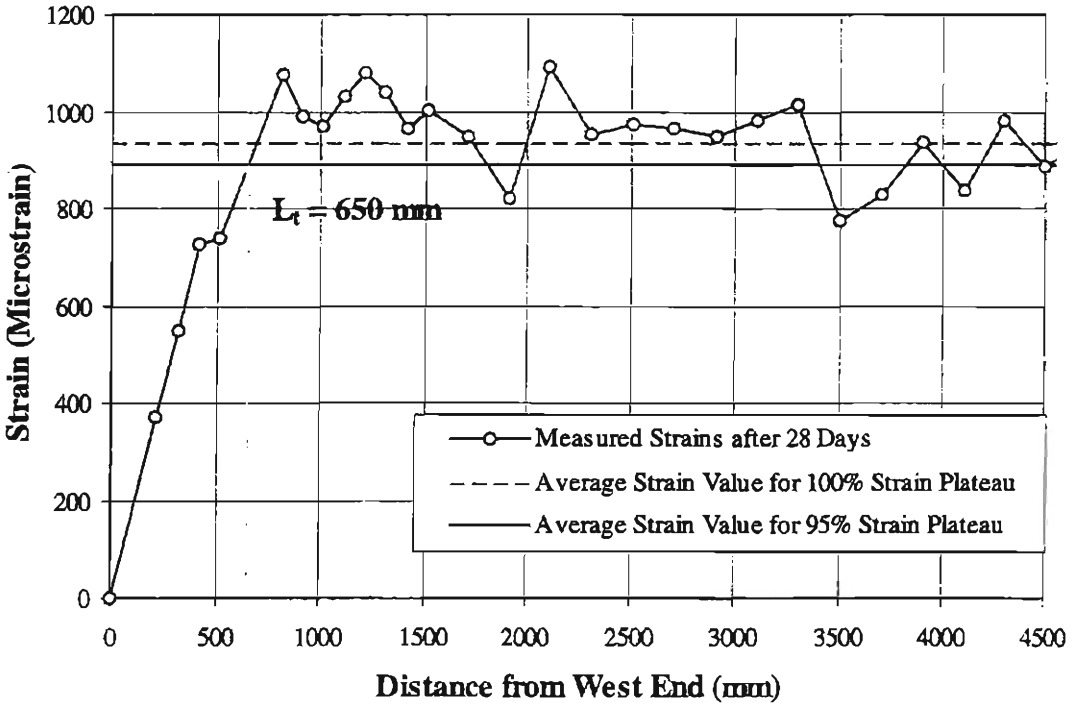

Figure 4.18 - Transfer Length after 28 Days by 95% Average Maximum Strain Plateau Method (2-W)

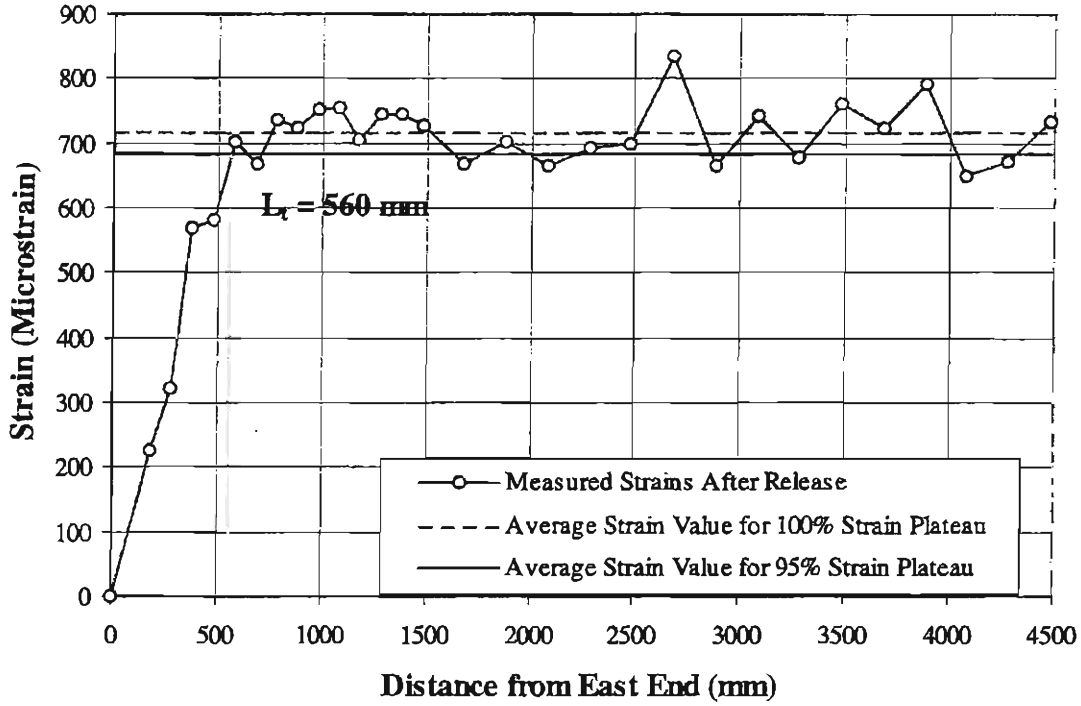

Figure 4.19 - Transfer Length After Release by 95% Average Maximum Strain Plateau Method (2-E)

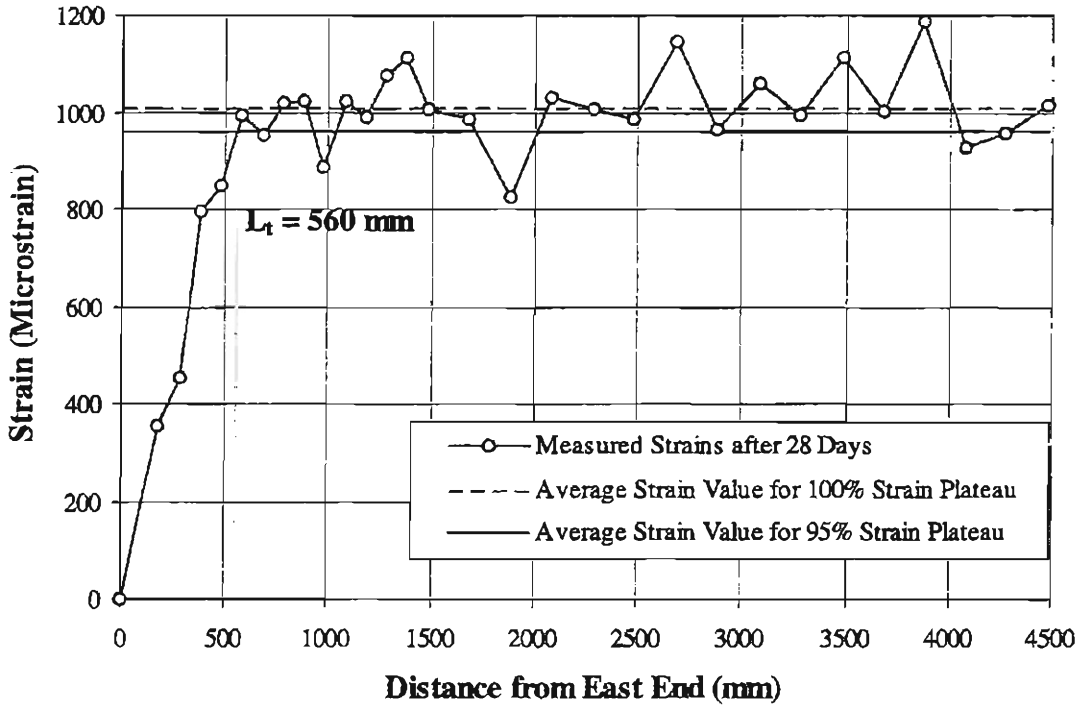

Figure 4.20 - Transfer Length after 28 Days by 95% Average Maximum Strain Plateau Method (2-E)

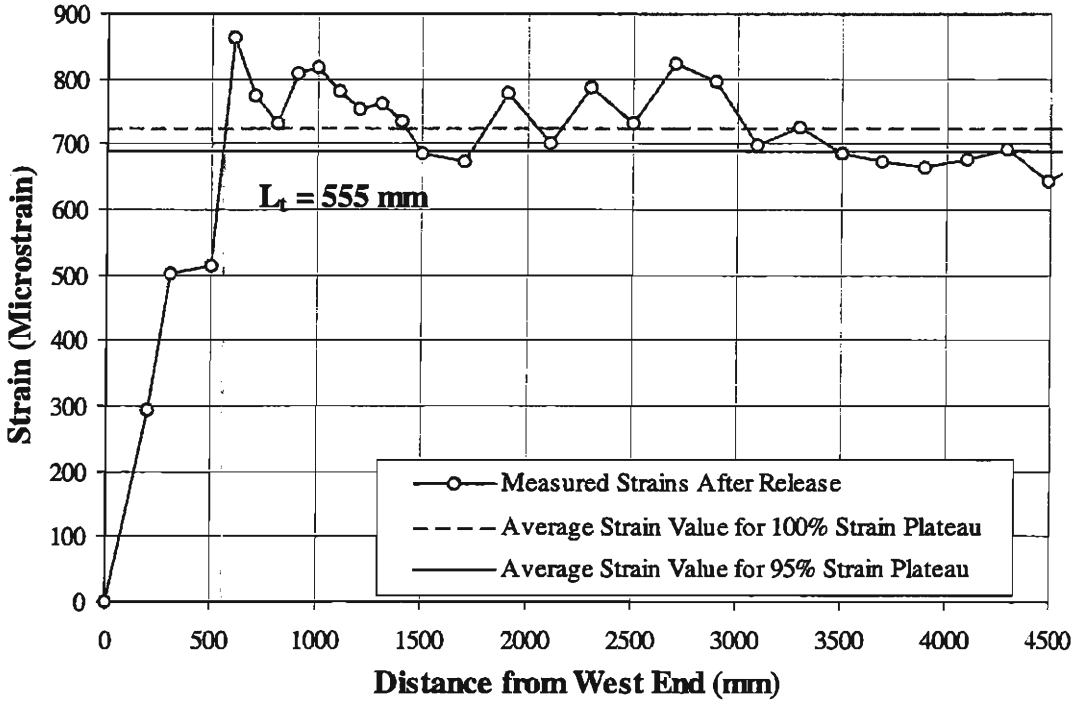

Figure 4.21 - Transfer Length After Release by 95% Average Maximum Strain Plateau Method (3-W)

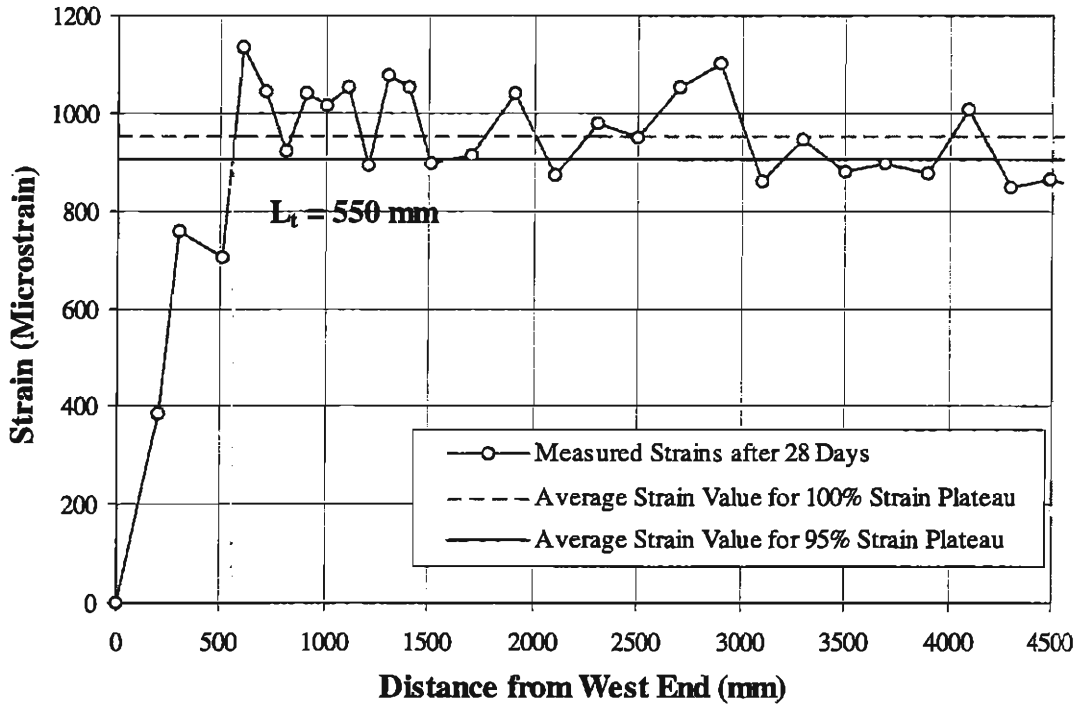

Figure 4.22 - Transfer Length after 28 Days by 95% Average Maximum Strain Plateau Method (3-W)

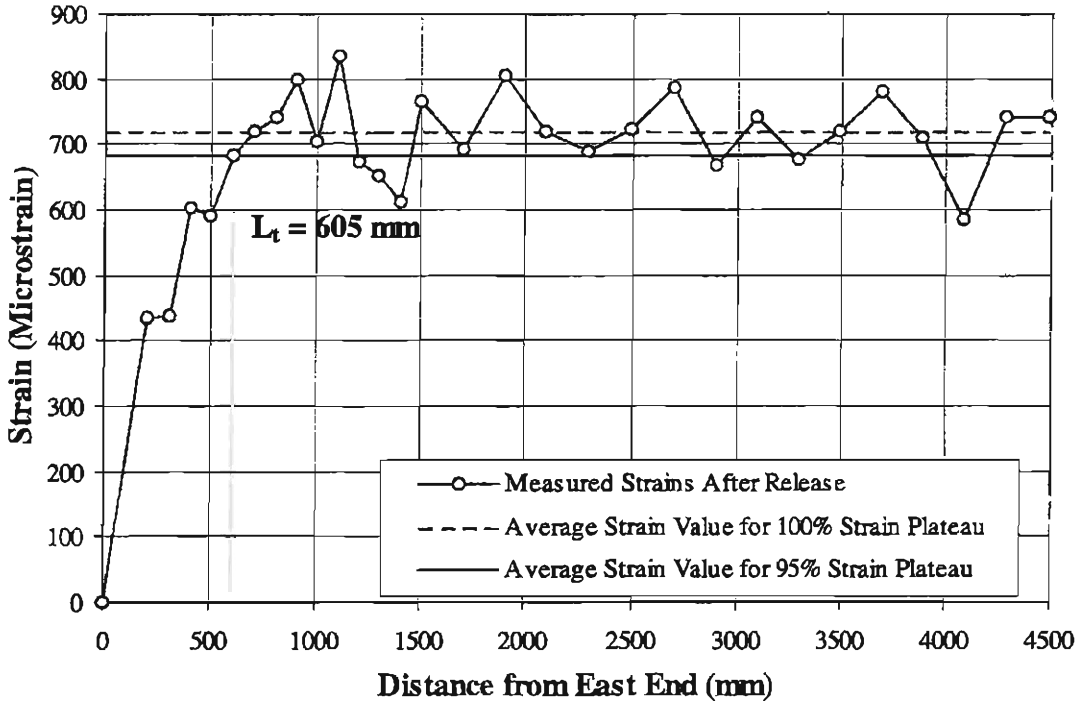

Figure 4.23 - Transfer Length After Release by 95% Average Maximum Strain Plateau Method (3-E)

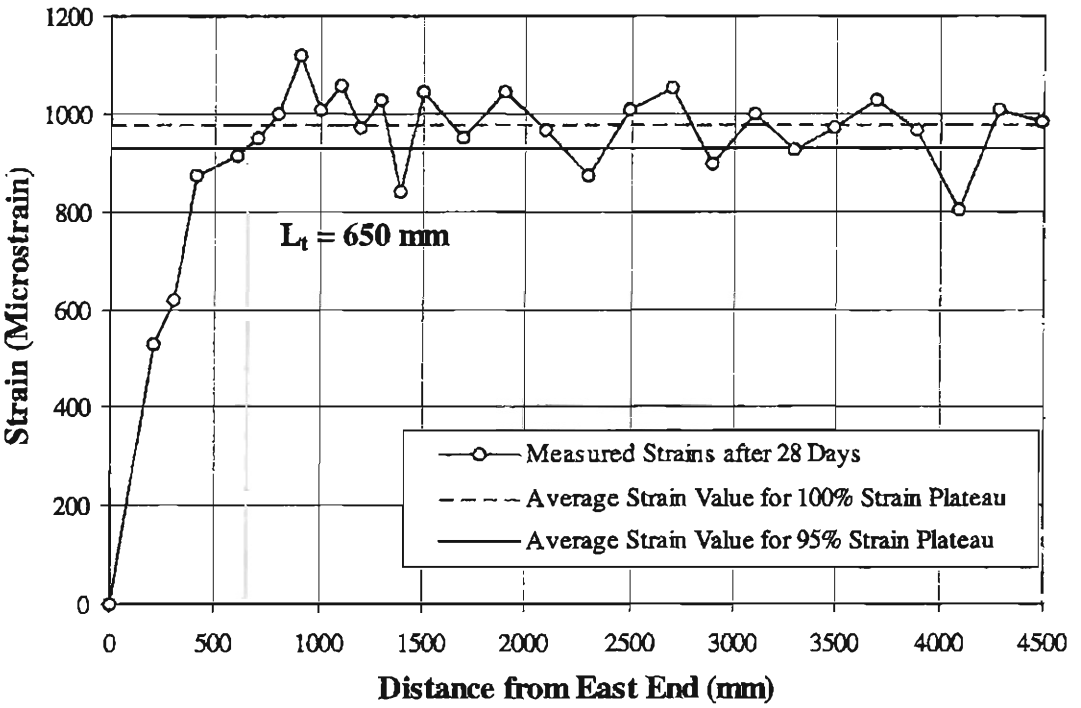

Figure 4.24 - Transfer Length after 28 Days by 95% Average Maximum Strain Plateau Method (3-E)

4.6 PRESTRESS LOSSES

Using the strain measurements discussed previously, prestress losses were calculated at different times for each of the girders. The strain values throughout the plateau regions for each time were subtracted from the corresponding initial readings to obtain strain changes along the girder length. The changes in strain due to the application of the topping slab were calculated from the measurements taken immediately before and after the topping slab was cast. The strain values for the later times were adjusted to account for these changes. The differences in strain obtained at each time were then averaged and multiplied by the strand modulus of elasticity to obtain the cumulative prestress loss up to the time in question. The calculated prestress losses are shown in Table 4.9.

Table 4.9 - Measured Prestress Losses

Days After Release	**Prestress Losses MPa (ksi)**		
	Girder		
	1	*2*	*3*
0	143 (20.7)	139 (20.2)	141 (20.5)
7	186 (26.9)	179 (26.0)	176 (25.5)
14	204 (29.6)	181 (26.2)	186 (27.0)
28	231 (33.5)	190 (27.6)	206 (29.9)
50	238 (34.5)	NA	NA
59	244 (35.4)	NA	NA
69	NA	214 (31.0)	NA
76	NA	239 (34.6)	NA
83	NA	NA	246 (35.7)
90	NA	NA	265 (38.4)

This method of calculation accounts for all prestress losses except those due to steel relaxation. Steel relaxation causes a decrease in steel stress and a corresponding elastic rebound of the surrounding concrete. The concrete strain is further decreased due to the decrease in the moment applied by the strands. Thus, the surface strains measured not only do not include the steel relaxation but they also include strain due to elastic rebound. These effects cause the total prestress losses calculated to be lower than they actually are. The magnitude of the elastic rebound depends on the section properties and the material properties of the strand and the concrete. For an eccentrically prestressed member, the total measurement error in prestress losses can be calculated by the following equation.

$$\text{Error in Prestress Losses} = \Delta f_{s,rel}\left(1+\frac{E_s A_s}{E_c}\left(\frac{1}{A_c}+\frac{e^2}{I_c}\right)\right) \qquad (4\text{-}2)$$

in which $\Delta f_{s,rel}$ is the steel relaxation loss, A_c is the cross sectional area of concrete, I_c is the moment of inertia of the section, e is the prestress eccentricity, and E_c and E_s are the moduli of elasticity of the concrete and the strand, respectively. For the test girders, with the average material property values, Eq. (4-2) yields an error in prestress losses of approximately 1.13 times the steel relaxation, $\Delta f_{s,rel}$.

The prestress losses calculated using the mechanical gage measurements were adjusted by adding 1.13 times the steel relaxation calculated with Eq. (4-1). The adjusted prestress losses for the three girders were then averaged at each time to yield the adjusted prestress losses shown in Table 4.10. The average of the unadjusted prestress losses calculated using the mechanical gage measurements are also shown in Table 4.10.

Table 4.10 - Average Measured and Calculated Prestress Losses

Days After Release	Unadjusted Average Prestress Losses MPa (ksi)	Estimated Steel Relaxation Loss, $\Delta f_{s,rel}$ MPa (ksi)	Adjusted Average Prestress Losses MPa (ksi)	Calculated Prestress Losses using Measured Creep Data MPa (ksi)	Calculated Prestress Losses using Empirical Creep Equation MPa (ksi)
0	141 (20.5)	17.7 (2.57)	161 (23.4)	157 (22.7)	157 (22.7)
7	180 (26.1)	24.5 (3.56)	208 (30.1)	334 (48.4)	239 (34.6)
14	190 (27.6)	27.1 (3.93)	221 (32.1)	377 (54.7)	269 (39.0)
28	209 (30.3)	29.9 (4.34)	243 (35.2)	419 (60.7)	303 (44.0)
90	265 (38.4)	35.0 (5.08)	305 (44.2)	476 (69.0)	350 (50.8)

Prestress losses were also calculated using the time step procedure discussed in Section 4.3. The results of these calculations, using the measured creep strain and the creep strain generated from the empirical expression, are presented in Table 4.10. It is apparent that the prestress losses calculated using the empirical creep equation are much closer to the adjusted prestress losses than those calculated using the measured creep data. This supports the speculation that the measured creep data is not representative of the girder concrete.

4.7 DEVELOPMENT LENGTH TESTS

In this section, the results of the six development length tests are presented. The strand slip values measured during the tests are presented in Appendix D.

4.7.1 Test 1-E

Development length testing began 50 days after girder casting, with the first test conducted on end "E" of girder 1. In this test, the load was applied at 2159 mm (85 in.) from the end of the member. By this time, the girder concrete had attained a

compressive strength of 76 MPa (11 ksi), while the topping concrete had attained a compressive strength of 55 MPa (7.9 ksi). These values are obtained from the curve for the moist cured specimens in Figure 3.14.

In all the tests, the load was initially increased in increments of approximately 890 kN (20 kips). After initial cracking, the load increment was reduced to approximately 445 kN (10 kips). Cracking was first observed at a load of approximately 400 kN (90 kips), which corresponds to a maximum moment of 681 kN-m (502 kip-ft.). A flexural compression failure occurred at the load of approximately 525 kN (118 kips), which corresponds to a maximum moment of 893 kN-m (659 kip-ft.). The maximum shear at failure was 431 kN (97 kips).

No strand slip was observed to occur during this test. Deflection was measured beneath the load point throughout the test and is plotted in Figure 4.25.

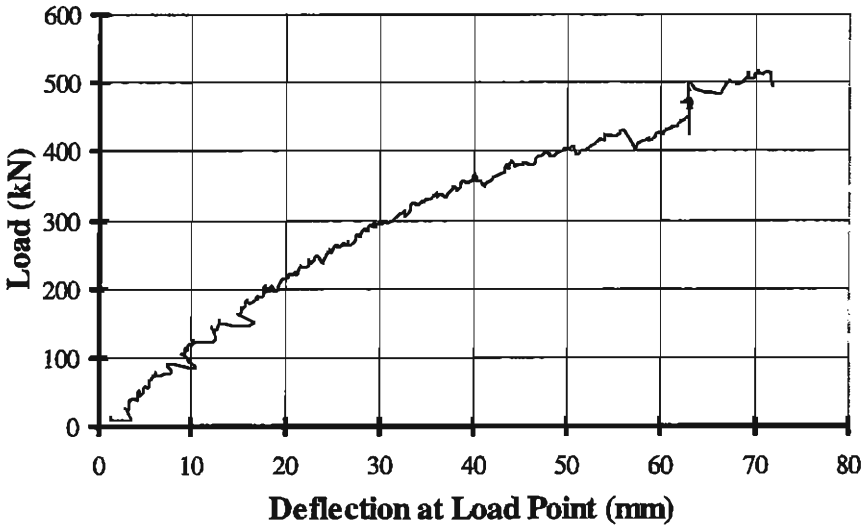

Figure 4.25 - Load versus Deflection for Test 1-E

Flexural cracks were even and well distributed as shown in Figure 4.27. Delamination of the topping slab, shown as the horizontal cracks near the top of the member in Figure 4.27, occurred in all of the tests due to the shear forces developed at the interface between the topping slab and the girder. This was expected behavior and the vertical bars which crossed the interface were provided in the design to maintain composite action between the topping slab and the girder.

Strains were measured along the girder surface before and during the test using the Whittemore gage mentioned previously. Measurements were taken immediately before testing, and then repeated upon reaching selected load magnitudes. These measurements were then used to generate a plot which shows, approximately, the variation of strand stress with time.

In calculating the stress values for this plot, the strand strain before release was assumed to be equal to 0.0711, which corresponds to the jacking stress, after anchorage losses, of 1407 MPa (204 ksi). To calculate strain changes in the strands, it was necessary to assume that the change in strain measured between the embedded surface points was reflective of the average change in strain in the nine strands over the same distances. This assumption is approximately correct as long as no slip occurs between the strand and the concrete. The change in strain due to prestress release, calculated from the mechanical gage measurements, was subtracted from the initial strand strain to yield the after release strand strain along the length of the girder.

However, because slip occurs in the transfer region immediately after release, the change in concrete strain cannot be assumed equal to the change in strand strain in

the transfer region. Thus, a linear interpolation was performed assuming that the strand strain varied linearly over the transfer distance determined using the 95% average maximum strain plateau method. In keeping with the simple transfer length theory, the strand strain was assumed to vary from zero at the free end of the strand to the previously determined after release strand strain at the end of the transfer region. The resulting strains were then multiplied by the strand modulus of elasticity to obtain the after release variation in average strand stress with distance in the transfer zone as shown in Figure 4.26. The elastic modulus of the strand was determined from the stress-strain curve in Figure 3.13.

The changes in strand strain which occurred in the time period between release and the day of the test were then subtracted from the after release strain values

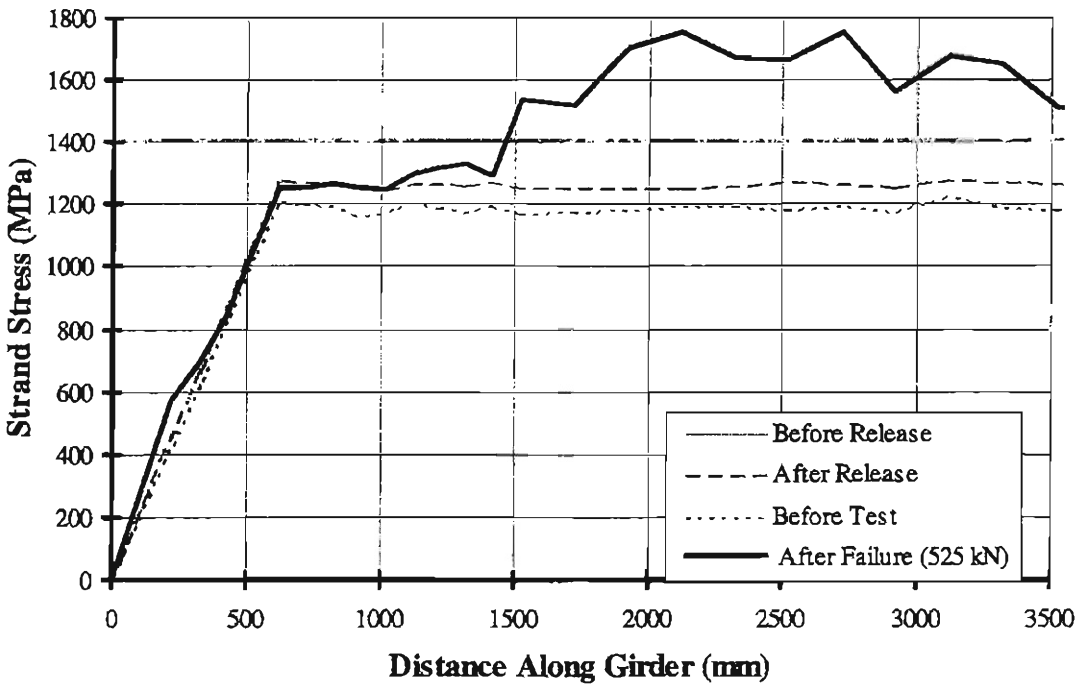

Figure 4.26 - Approximate Strand Stress at Different Times for Girder 1-E

to yield the strand strain before the test. These values were subsequently used to calculate the average strand stress, which is plotted in Figure 4.26. Strain measurements were also taken immediately after flexural failure. These values were also converted to strand strain and then to steel stress using the stress-strain plot in Figure 3.13. These values are plotted as the heavy solid line in Figure 4.26.

The strain values used to develop this plot do not account for steel relaxation or strand slip during testing, and thus, the steel stress values cannot be considered entirely accurate. However, the resulting plot is still quite useful as it shows, qualitatively, the variation of strand stress with time. The increases in strand stress due to the applied loading can be clearly seen. It is apparent that these increases did not reach the transfer region and that the embedment length tested was apparently greater than the development length. It is also clear that an increase in strand stress had occurred in the transfer region. This appears to result from shear cracks which had propagated through or near the strand anchorage region.

4.7.2 Test 1-W

Development length testing was performed on end "W" of girder 1 fifty-nine

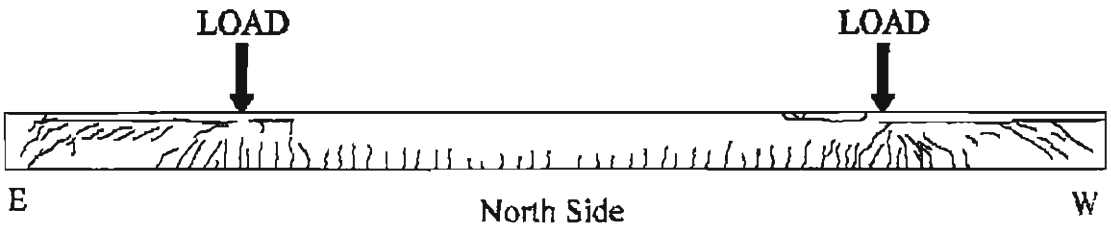

Figure 4.27 - Girder 1 After Testing

days after girder casting. In this test, the load was applied at 2057 mm (81 in.) from the end of the member. By this time, the girder concrete had a compressive strength of 77 MPa (11 ksi), while the topping slab concrete had obtained a compressive strength of 55 MPa (8.0 ksi).

The test procedure was the same as that used in the first test. Cracking was first observed at a load of approximately 356 kN (80 kips), which corresponds to a maximum moment of 584 kN-m (431 kip-ft.). A flexural compression failure occurred at a load of approximately 534 kN (120 kips), which corresponds to a maximum moment of 876 kN-m (646 kip-ft.). The maximum shear at failure was 444 kN (100 kips).

No strand slip was observed to occur during this test. The deflection measured beneath the load point during the test is plotted in Figure 4.28. Flexural cracking was even and well distributed as shown in Figure 4.27.

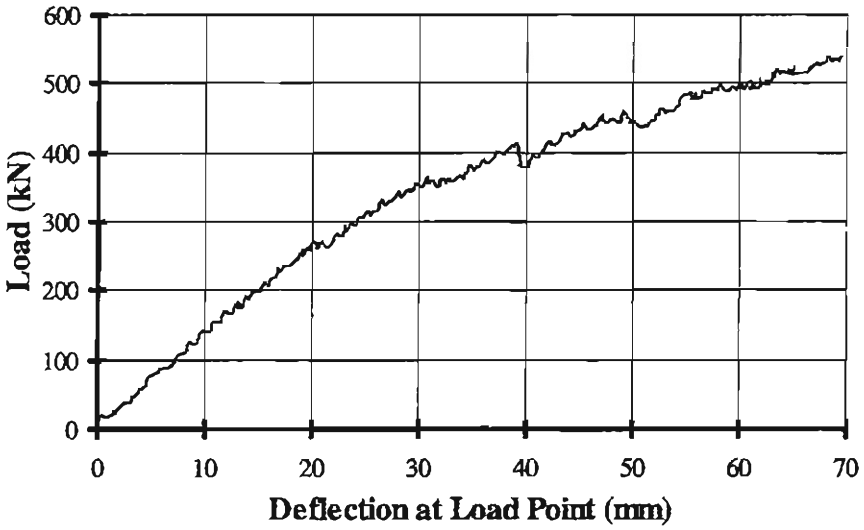

Figure 4.28 - Load versus Deflection for Test 1-W

Figure 4.29 shows the variation of average strand stress with distance along the girder. This plot was developed following the procedure discussed in the previous section. Figure 4.29 clearly shows the increases in strand stress due to the applied loading. It is apparent that these increases did not reach the transfer region and that the embedment length tested was apparently greater than the development length.

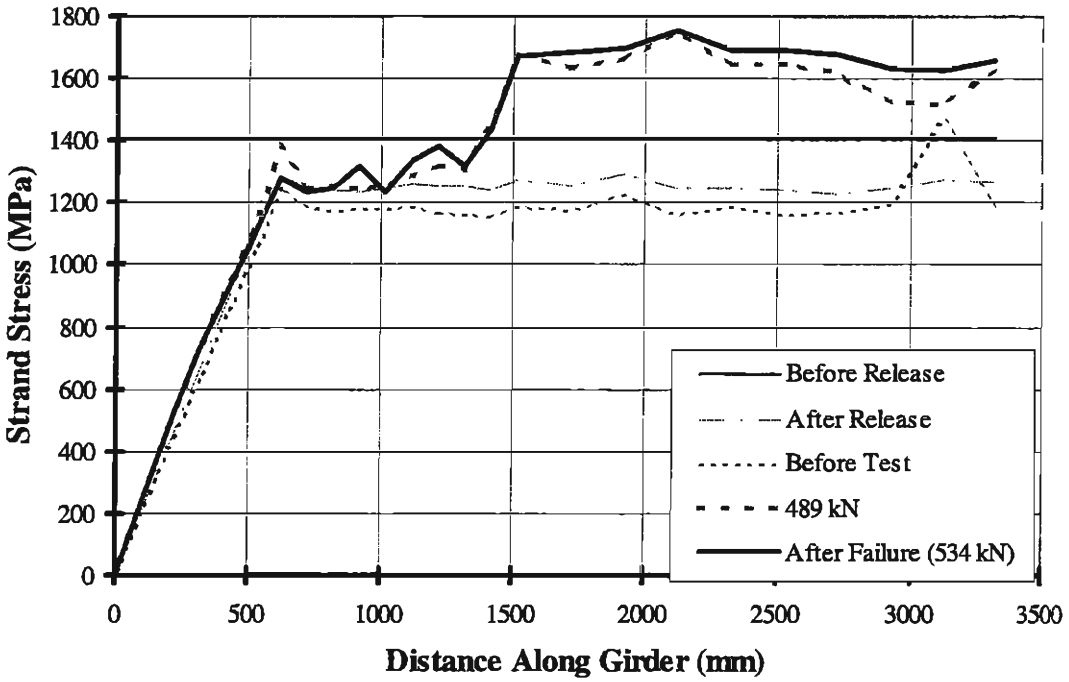

Figure 4.29 - Approximate Strand Stress at Different Times for Girder 1-W

4.7.3 Test 2-W

Development length testing was performed on end "W" of girder 2 sixty-nine days after girder casting. In this test, the load was applied at 1918 mm (76 in.) from the end of the member. By this time, the girder concrete had a compressive strength of 77 MPa (11 ksi), while the topping concrete had a compressive strength of 55 MPa (8.0 ksi).

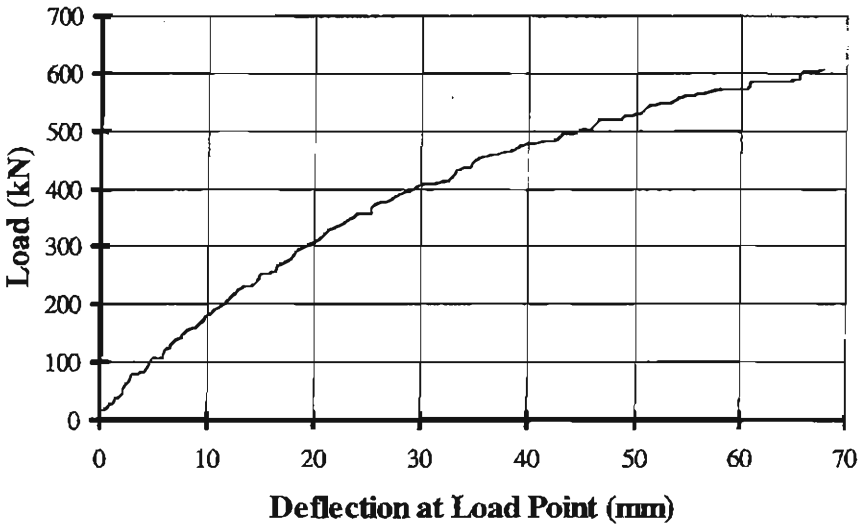

Figure 4.30 - Load versus Deflection for Test 2-W

Cracking was first observed at a load of approximately 356 kN (80 kips), which corresponds to a maximum moment of 557 kN-m (411 kip-ft.). A flexural compression failure occurred at a load of approximately 534 kN (120 kips), which corresponds to a maximum moment of 681 kN-m (502 kip-ft.). The maximum shear at failure was 504 kN (113 kips). The deflection measured beneath the load point during the test is plotted in Figure 4.30. Flexural cracking was even and well distributed as shown in Figure 4.32.

Eight of the nine strands began to slip at a load of approximately 489 kN (110 kips). However, the maximum strand slip measured at failure was only 0.127 mm (0.005 in.). This strand slip did not appear to adversely affect the behavior of the girder and it was concluded that the development length required was shorter than the embedment length used in the tests.

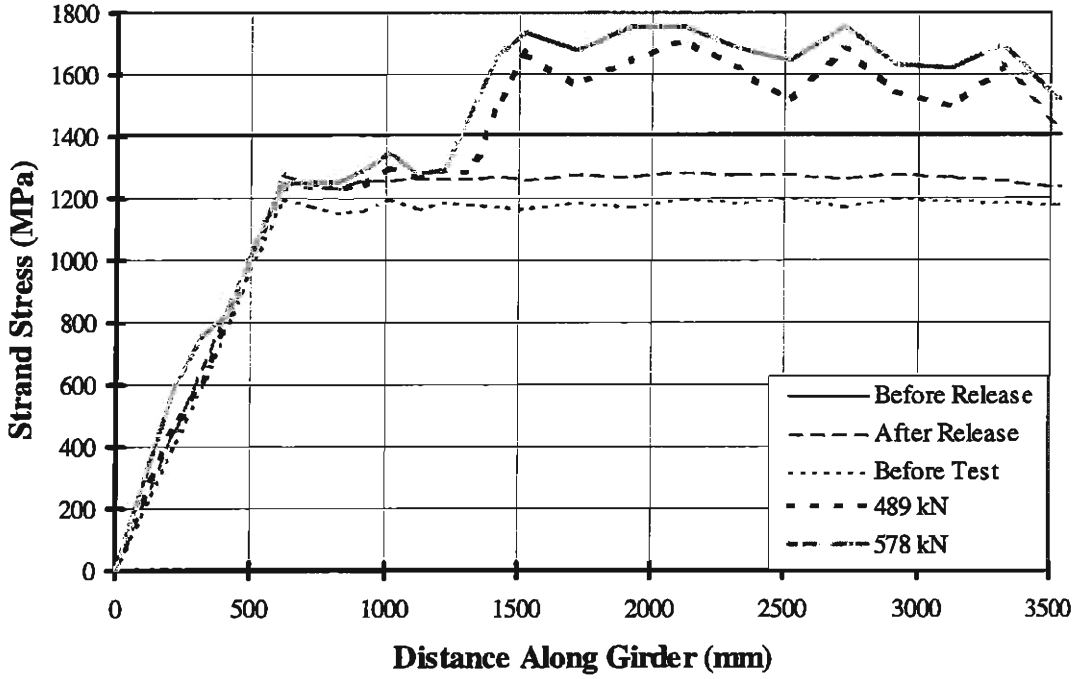

Figure 4.31 - Approximate Strand Stress at Different Times for Girder 2-W

Figure 4.31 shows the variation of average strand stress with distance along the girder. This plot clearly shows the increases in strand stress due to the applied loading. It is apparent that these increases did not reach the transfer region and that the embedment length used was apparently greater than the development length.

In the transfer region, a significant stress increase is seen to occur for loads greater than the first slip load of 489 kN (110 kips). This increase is probably due to the significant shear cracking observed in the transfer region which had propagated

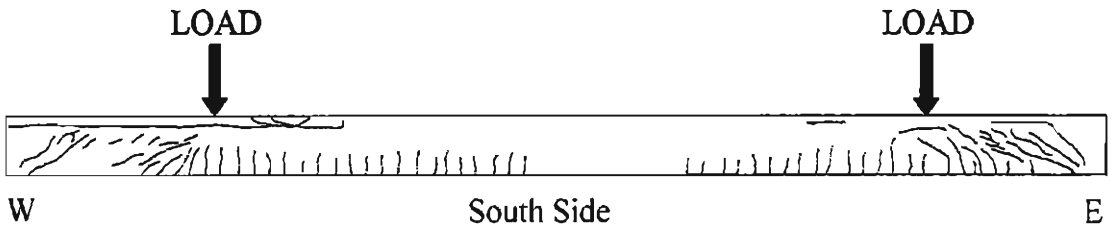

Figure 4.32 - Girder 2 After Testing

through the strand anchorage region. The increase in strand stress might have led to the small strand slips measured (see Appendix D).

4.7.4 Test 2-E

Development length testing was performed on end "E" of girder 2 seventy-six days after girder casting. In this test, the load was applied at 1651 mm (65 in.) from the end of the member. By this time, the girder concrete had a compressive strength of 77 MPa (11 ksi), while the topping concrete had a compressive strength of 55 MPa (8.0 ksi).

Cracking was first observed at a load of approximately 400 kN (90 kips), which corresponds to a maximum moment of 555 kN-m (409 kip-ft). A flexural compression failure occurred at a load of approximately 601 kN (135 kips), which corresponds to a maximum moment of 831 kN-m (613 kip-ft.). This failure occurred at a lower moment than expected, apparently due to a poorly compacted section of

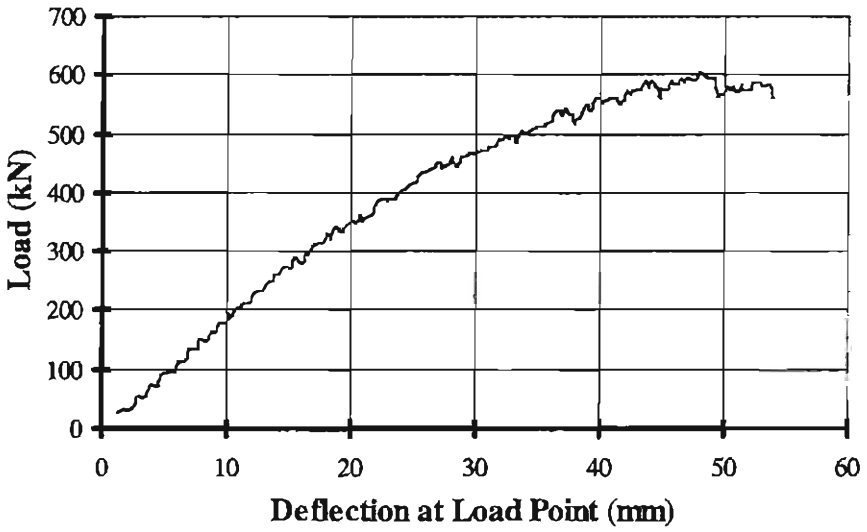

Figure 4.33 - Load versus Deflection for Test 2-E

topping slab near the load point. The maximum shear at failure was 521 kN (117 kips). The deflection measured beneath the load point during the test is plotted in Figure 4.33. Flexural cracking was even and well distributed as shown in Figure 4.32.

Seven of the nine strands began to slip at a load of approximately 445 kN (100 kips). However, the maximum strand slip measured at failure was only 0.178 mm (0.007 in.). This strand slip did not appear to adversely affect the behavior of the girder and it was concluded that the development length required was probably shorter than the embedment length used.

Figure 4.34 shows the variation of average strand stress with distance along the girder. This plot clearly shows the increases in strand stress due to the applied loading. It is apparent that these increases were close to, but did not reach the transfer

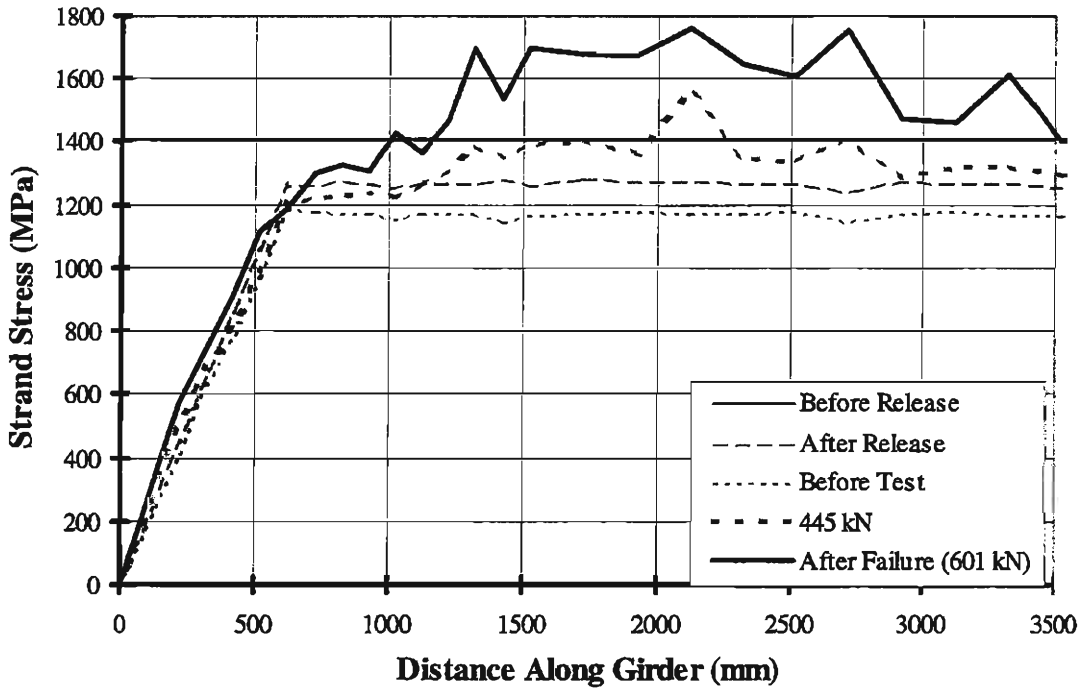

Figure 4.34 - Approximate Strand Stress at Different Times for Girder 2-E

region and that the embedment length used was apparently greater than the development length.

In the transfer region, a significant stress increase is seen to occur for loads greater than the first slip load of 445 kN (100 kips). This increase is probably due to the significant shear cracking observed in the transfer region which had propagated through the strand anchorage region. The increase in strand stress might have led to the small strand slips measured (see Appendix D).

4.7.5 Test 3-E

Development length testing was performed on end "E" of girder 3 eighty-three days after girder casting. In this test, the load was applied at 1524 mm (60 in.) from the end of the member. By this time, the girder concrete had a compressive strength of 77 MPa (11 ksi), while the topping concrete had a compressive strength of 55 MPa (8.0 ksi).

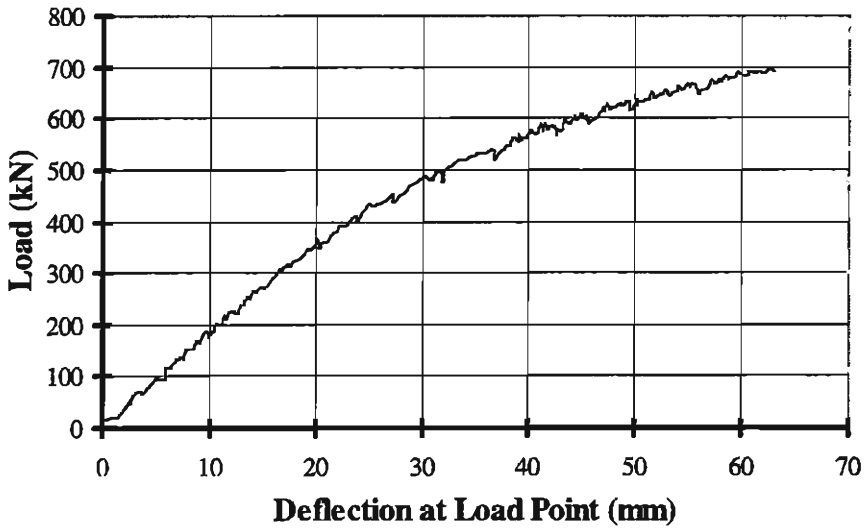

Figure 4.35 - Load versus Deflection for Test 3-E

Cracking was first observed at a load of approximately 445 kN (100 kips), which corresponds to a maximum moment of 577 kN-m (425 kip-ft). All nine strands began to slip at a load of approximately 534 kN (120 kips). This slip increased rapidly as load was increased, ultimately reaching a maximum slip of 2.29 mm (0.09 in.), as shown in Appendix D. A sudden and violent shear failure occurred at a load of approximately 672 kN (151 kips), which corresponds to a maximum moment of 831 kN-m (613 kip-ft.). The strand slip led to the sudden shear failure. The maximum shear at failure was 587 kN (132 kips).

The deflection measured beneath the load point during the test is plotted in Figure 4.35. Flexural cracking was even and well distributed as shown in Figure 4.37.

Figure 4.36 shows the variation of average strand stress with distance along

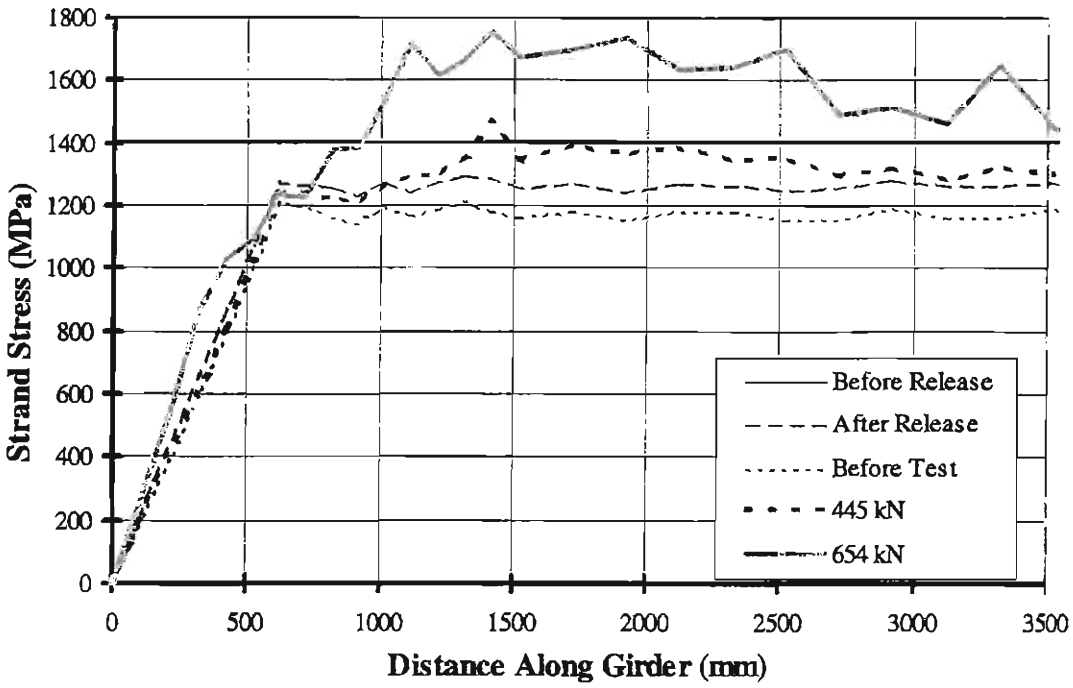

Figure 4.36 - Approximate Strand Stress at Different Times for Girder 3-E

the girder. This plot clearly shows the increases in strand stress due to the applied loading. It is apparent from this figure that the flexural bond stress increase had reached the end of the transfer region at failure. This behavior indicates that the embedment length used was probably the minimum development length required.

In the transfer region, a significant increase in strand stress is seen to occur for loads greater than the first slip load of 534 kN (120 kips), due to the significant shear cracking which had propagated through the strand anchorage zone. However, due to the strain incompatibility resulting from the large strand slip, the accuracy of the strand stress plot is questionable.

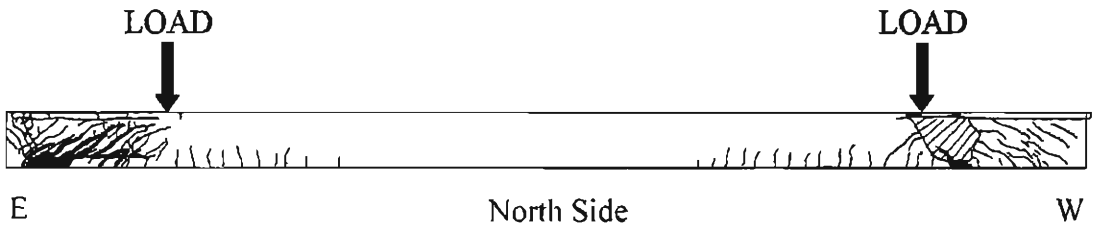

Figure 4.37 - Girder 3 After Testing

4.7.6 Test 3-W

Development length testing was performed on end "W" of girder 3 ninety days after girder casting. In this test, the load was applied at 1497 mm (59 in.) from the end of the member. By this time, the girder concrete had a compressive strength of 77 MPa (11 ksi), while the topping concrete had a compressive strength of 55 MPa (8.0 ksi).

Cracking was first observed at a load of approximately 445 kN (100 kips), which corresponds to a maximum moment of 559 kN-m (419 kip-ft). All nine strands

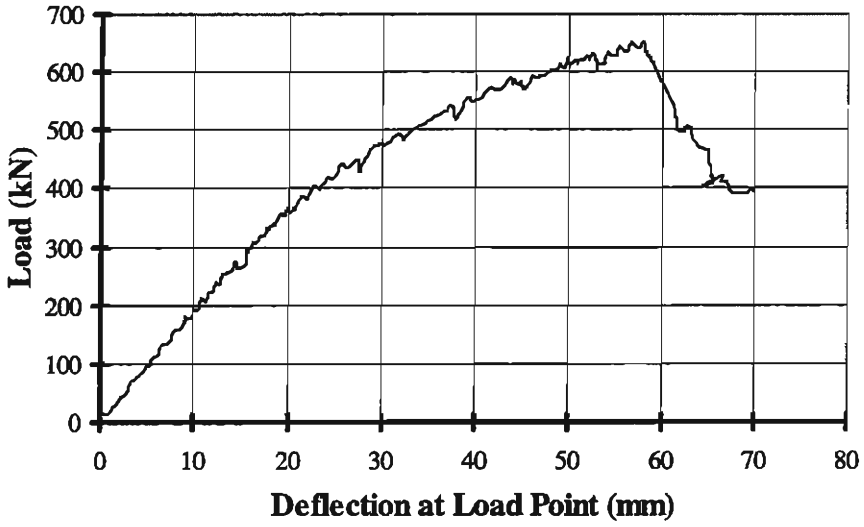

Figure 4.38 - Load versus Deflection for Test 3-W

began to slip at a load of approximately 445 kN (100 kips). This slip increased rapidly as load was increased, ultimately reaching a maximum slip of 2.03 mm (0.08 in.). At a load of approximately 645 kN (145 kips), corresponding to a maximum moment of 831 kN-m (613 kip-ft.), a flexural compressive failure occurred. When this failure occurred, several very large shear cracks opened near the load point. The strand slip was the apparent cause of this failure.

The maximum shear at failure was 552 kN (124 kips). The load is plotted against the deflection measured beneath the load point in Figure 4.38. Flexural cracking was even and well distributed as shown in Figure 4.37.

Figure 4.39 shows the variation of the average strand stress with distance along the girder. This plot clearly shows the increases in strand stress due to the applied loading. It is apparent from this figure that the flexural bond stress increase had propagated close to the end of the transfer region at a load of 623 kN (140 kips).

In the transfer region, a significant increase in strand stress is seen to occur for loads greater than the first slip load of 445 kN (100 kips), due to the significant shear cracking which had propagated through the strand anchorage zone. However, due to the strain incompatibility resulting from the large strand slip, as mentioned previously, the accuracy of the strand stress plot is questionable.

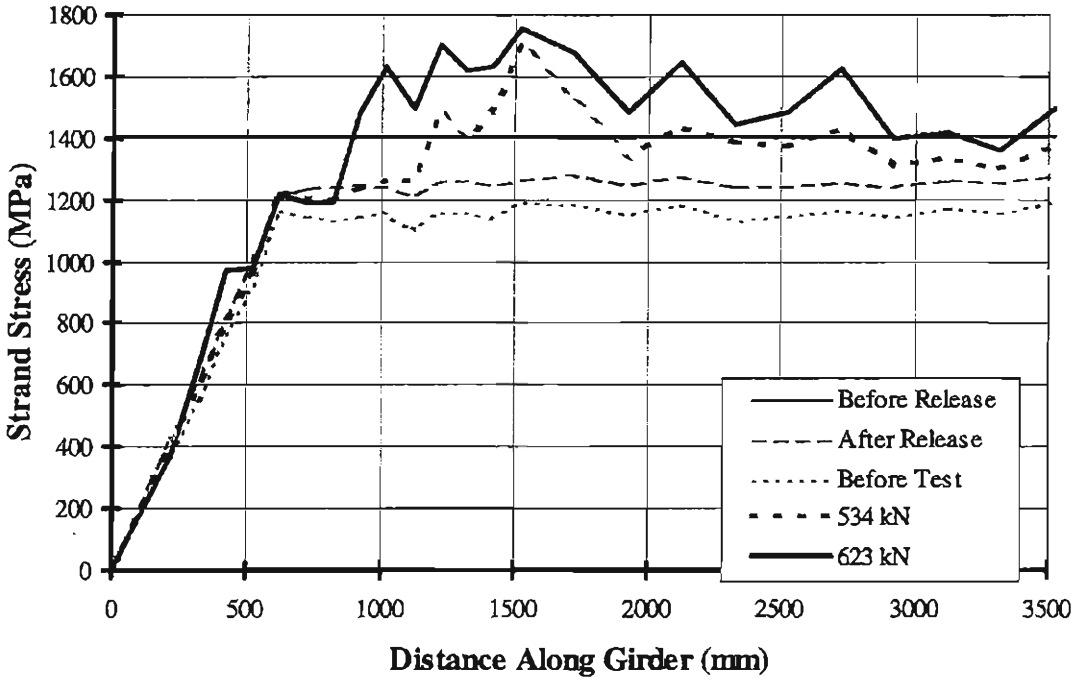

Figure 4.39 - Approximate Strand Stress at Different Times for Girder 3-W

4.7.7 Summary of Results

Both ends of girder 3 were tested at an embedment length of approximately 1524 mm (60 in.) and exhibited significant strand slip at failure. Additionally, the strand stress plots for the last two tests show that the flexural bond stress reached the transfer region at failure. These factors indicate that the development length for the girders is approximately 1524 mm (60 in.). However, it is important to note that

strand slip was first observed in test 2-E at an embedment length of 1918 mm (76 in.). Nonetheless, no bond-slip failure was observed to occur in test 2-E.

In all of the tests, increases in strand stress occurred in the transfer region. This was apparently due to shear cracking in the transfer region which had propagated through the strand anchorage zone. It is, however, unclear how these increases might have affected the behavior of the girders.

Results pertaining to each of the tests are summarized in Table 4.11.

Table 4.11 - Summary of Development Length Test Results

	Test Designation					
	1-E	**1-W**	**2-W**	**2-E**	**3-E**	**3-W**
Test Date	10/2/96	10/11/96	10/21/96	10/28/96	11/4/96	11/11/96
Concrete Age (Days)	50	59	69	76	83	90
Girder Compressive Strength MPa (ksi)	76.0 (11.0)	76.5 (11.1)	76.9 (11.2)	77.1 (11.2)	77.3 (11.2)	77.5 (11.2)
Topping Slab Compressive Strength MPa (ksi)	54.7 (7.9)	54.9 (8.0)	55.1 (8.0)	55.2 (8.0)	55.3 (8.0)	55.3 (8.0)
Embedment Length mm (in.)	2159 (85)	2057 (81)	1918 (76)	1651 (65)	1524 (60)	1497 (59)
Failure Load kN (kips)	525 (118)	534 (120)	601 (135)	601 (135)	672 (151)	645 (145)
Failure Moment[(1)] kN-m (kip-ft.)	925 (682)	907 (669)	967 (714)	857 (632)	895 (660)	848 (626)
Maximum Shear[(1)] kN (kips)	431 (97)	444 (100)	504 (113)	521 (117)	587 (132)	568 (128)
Maximum Deflection under Load mm (in.)	71 (2.8)	69 (2.7)	70 (2.8)	53 (2.1)	64 (2.5)	58 (2.3)
Maximum Slip mm (in.)	0	0	0.127 (0.005)	0.178 (0.007)	2.29 (0.09)	2.03 (0.08)
Failure Type	Flexure	Flexure	Flexure/Slip	Flexure/Slip	Slip/Shear	Slip/Flexure-Shear

(1) Includes girder self weight

5. DISCUSSION OF TEST RESULTS

5.1 FLEXURE AND SHEAR STRENGTH

Flexural strength was calculated for each of the girders using the formulas given in Section 9.17.2 of the AASHTO Specifications [1]. Shear strength was calculated for each of the girders using the formulas given in Section 9.20 of the AASHTO Specifications. The material properties measured at the time of each test were used in these calculations. The results of these calculations and the measured values from the tests are shown in Table 5.1. The maximum moment, M_{test}, and the maximum shear, V_{test}, shown in Table 5.1 include the girder self weight.

Table 5.1 - Comparison of Calculated Flexure and Shear Strength to the Maximum Values Obtained in the Tests

Test	M_{test} kN-m (kip-ft.)	$M_{n,AASHTO}$ kN-m (kip-ft.)	$\frac{M_{test}}{M_{n,AASHTO}}$	V_{test} kN (kips)	$V_{n,AASHTO}$ kN (kips)
1-E	925 (682)	872 (643)	1.06	432 (97)	628 (141)
1-W	907 (669)	874 (644)	1.04	444 (100)	639 (144)
2-W	967 (714)	874 (645)	1.11	504 (113)	661 (149)
2-E	857 (632)	874 (645)	0.98	521 (117)	703 (158)
3-E	895 (660)	874 (645)	1.02	589 (132)	729 (164)
3-W	848 (626)	874 (645)	0.97	568 (128)	729 (164)

The failure moments developed in all the tests were close to the nominal moment strength predicted using the AASHTO formula. In two of the six tests, however, the measured failure moment was somewhat less than the value predicted by the AASHTO formula. For test 3-W, the bond failure observed probably led to the lower than predicted failure moment. The failure moment for test 2-E was lower than

predicted probably due to a premature compression failure of a poorly compacted section of topping slab near the load point.

The maximum measured shear in the girder tests never reached the shear capacity calculated with the AASHTO Specifications. However, both ends of girder 3 failed, in whole or in part, by shear. It appears that the strand slip observed in both of these tests led to the premature shear failures.

5.2 TRANSFER LENGTH

5.2.1 Comparisons with Design Formulas

The average measured transfer length for these girders and the transfer length calculated using the AASHTO formula are shown in Table 5.2. Calculation of the transfer length using the AASHTO formula required the calculation of the effective prestress, f_{se}. The AASHTO Specification defines this value as the strand stress after all losses have occurred. Losses typically reach approximately constant values after 2 or 3 years. For the girders in the test program, the last prestress loss measurements were taken ninety days after casting. Thus, in order to calculate a representative value for the effective prestress, a time step procedure [17] was used to estimate long-term prestress losses.

After three years, the total prestress loss was calculated to be 455 MPa (66 ksi). This yields an effective prestress of 952 MPa (138 ksi). Substituting this value into the AASHTO formula for transfer length, with a strand diameter of 15.2 mm (0.6

Table 5.2 - Measured and Calculated Values of Transfer Length for the Girders

Estimated Total Prestress Losses MPa (ksi)	Estimated Effective Prestress, f_{se} MPa (ksi)	$L_{t,test}$ mm (in.)	$L_{t,AASHTO}$ mm (in.)	$\frac{L_{t,AASHTO}}{L_{t,test}}$
455 (66)	952 (138)	593 (23.4)	701 (27.6)	1.18

in.), yields a transfer length of 701 mm (27.6 in.). This value is 18% greater than the average transfer length, $L_{t,test}$, measured right after stress transfer. These results are summarized in Table 5.2.

5.2.2 Sources of Errors

The accuracy of the determination of transfer length depends primarily on the accuracy of the strain data measured. Errors in strain readings can be introduced directly through human errors, resolution of reading devices, and poorly anchored target points. Errors due to these factors are thought be insignificant as every effort was made to reduce these sources of error to the minimum possible.

Errors can also be introduced as a result of temperature changes in the concrete. The most significant temperature changes occurred during girder curing as a result of the heat generated by concrete hydration. For these girders, initial strain readings were not taken until 41 hours after girder casting by which time the temperature in the concrete had dropped to the surrounding ambient temperature. Thus, errors due to these effects are thought to be minor.

5.3 DEVELOPMENT LENGTH

5.3.1 Comparisons with Design Formulas

The AASHTO formula was used to calculate the development length for comparison to the experimental results. The strand stress at failure, f_{ps}, was calculated using AASHTO Eq. (9-17). The effective prestress used was the same as that used in the transfer length calculations (see Table 5.2). Using these values, the AASHTO formula yields a development length of 2332 mm (91.8 in.).

As shown in Figure 2.5, the AASHTO equation is expected to yield values which fall between the embedment length at which slip first occurs and the embedment length at which general bond failure occurs [20]. In the girder tests, slip was first observed at an embedment length of 1930 mm (76 in.). General bond failure was first observed at an embedment length of 1524 mm (60 in.). The development length calculated using the AASHTO formula is 21% greater than the embedment length, $L_{e,slip}$, at which slip first occurred and 53% greater than the embedment length, $L_{e,bond}$, at which general bond failure occurred.

Table 5.3 - Measured and Calculated Values of Development Length for the Girders

Estimated Strand Stress at Failure, f_{ps} MPa (ksi)	**Embedment Length at First Slip, $L_{e,slip}$ mm (in.)**	**Embedment Length at General Bond Failure, $L_{e,bond}$ mm (in.)**	**$L_{d,AASHTO}$ mm (in.)**	**$\frac{L_{d,AASHTO}}{L_{e,slip}}$**	**$\frac{L_{d,AASHTO}}{L_{e,bond}}$**
1689 (245)	1930 (76)	1524 (60)	2332 (91.8)	1.21	1.53

5.4 COMPARISON WITH PREVIOUS STUDIES

Reported values of transfer length from recent studies on 15.2 mm (0.6 in.) diameter strand range from 363 mm (14.3 in.) to 1417 mm (55.8 in.). In agreement with those studies using high strength concrete, the results from this study fall near the lower end of this range [9, 16].

Reported values of development length from recent studies using 15.2 mm (0.6 in.) diameter strand range from 762 mm (30 in) to 3353 mm (132 in.). Once again, in agreement with those studies using high strength concrete, the results from this study fall near the lower end of this range.

Transfer and development lengths were calculated for the girders using the equations, as listed in Table 2.1, proposed by various researchers. The values used in the calculations are shown in Table 5.4. The strand stress values at various times were derived using the methods and values presented in the preceding sections. The material properties and the end slip, δ_{avg}, are the average of the experimental data

Table 5.4 - Values used in Proposed Equations

Variables used (average values):		
f_{so} **in MPa (ksi)**	Strand Stress Immediately Prior to Release	1407 (204)
f_{si} **in MPa (ksi)**	Initial Prestress	1265 (184)
f_{se} **in MPa (ksi)**	Effective Prestress	952 (138)
f_{ps} **in MPa (ksi)**	Strand Stress at Ultimate Flexural Capacity	1689 (245)
ε_{ps}	Strand Strain at Ultimate Flexural Capacity	0.011
λ	$(0.6+40\varepsilon_{ps})$	1.040
d_b **in mm (in.)**	Nominal Strand Diameter	15.2 (0.6)
E_s **in GPa (ksi)**	Strand Modulus of Elasticity	198 (28700)
f'_{ci} **in Pa (psi)**	Concrete Compressive Strength at Release	53779 (7800)
f'_c **in Pa (psi)**	Concrete Compressive Strength at 28 Days	77221 (11200)
δ_{avg} **in mm (in.)**	End Slip of Strand at Transfer	1.50 (0.059)

Table 5.5 - Transfer and Development Lengths from Proposed Equations

Authors	L_t mm (in.)	L_d mm (in.)
Martin and Scott	1219 (48)	NA
Zia and Mostafa	780 (30.7)	2819 (111)
Cousins, et al.	536 (21.1)	2723 (107.2)
Shahawy, et al.	932 (36.7)	NA
Mitchell, et al.	572 (22.5)	1605 (63.2)
Deatherage, et al.	932 (36.7)	3378 (133)
Buckner	932 (36.7)	2629 (103.5)
Slip Theory	422 (16.6)	1402 (55.2)
Measured	594 (23.4)	1524 (60)

obtained in this study as presented in Chapters 3 & 4.

The results calculated with the proposed equations are shown in Table 5.5. Most of the proposed formulas, except the formulas proposed by Mitchell et al. and the slip theory, substantially overestimate the transfer and development length for these members. Overall, the formulas proposed by Mitchell et al. yield results closest to the measured values of transfer and development length. Their equations are based on tests which included members with high strength concrete. They have found that members made of higher strength concrete have shorter transfer and development lengths, and their equations include a concrete strength factor to account for this effect.

6. SUMMARY AND CONCLUSIONS

6.1 SUMMARY

This study investigated the transfer and development length of Grade 270, 15.2 mm (0.6 in.) diameter prestressing strand spaced at 51 mm (2 in.) on center in high performance concrete. Three box girders with composite topping slabs were tested in the program. These girders were 381 mm (15 in.) wide, 553 mm (21.8 in.) high and spanned 10185 mm (401 in.). Concrete compressive strength for the main girder section was approximately 54 MPa (7.8 ksi) at release and 77 MPa (11 ksi) at the time of development length tests. The girders were pretensioned using nine strands with a strand stress just before release of approximately 1407 MPa (204 ksi). The strand was supplied by a single manufacturer.

6.2 CONCLUSIONS

The conclusions of this study are as follows:

1. The average transfer length for the girders was determined to be 593 mm (23.4 in.) at release and 633 mm (25 in.) at 28 days.

2. The development length for the girders was determined to be about 1524 mm (60 in.).

3. The AASHTO/ACI formulas for transfer and development length overestimate the transfer and development lengths for these girders. The formula for transfer length yields a value 1.18 times the average value measured right after stress release. The formula for development length yields a value 1.53 times the measured value.

4. With the exception of the Slip Theory and the formulas recommended by Mitchell et al., the equations for transfer and development length selected from the literature generally overestimate the results from this study. Mitchell et al.'s formula for transfer length underestimates the average measured transfer length by a factor of 0.96, while their formula for development length overestimates the measured value by a factor of 1.05.

5. The average pullout strength for the untensioned strand was 215 kN (48.3 kips).

6. The average strand slip measured at prestress release was 1.49 mm (0.059 in.).

7. The ACI equation for the modulus of rupture of concrete appears to be conservative for the 69 MPa (10 ksi) concrete used in this study, while the equation for the modulus of elasticity tends to yield values higher than the experimental values. For the modulus of elasticity, the equation proposed by researchers at Cornell University provides a good correlation with the experimental data.

8. The camber calculated with the time-step method, based on the measured creep data, appears to be much higher than the measured cambers. A much better correlation between the measured and the calculated cambers is obtained when the

creep strain is calculated with an empirical equation based on the ultimate unit creep strain recommended by researchers at Cornell University for 69 MPa (10 ksi) concrete.

REFERENCES

1. AASHTO, *Standard Specifications for Highway Bridges*, 15th Edition, American Association of State Highway and Transportation Officials, Washington, D.C., 1992.
2. ACI Committee 318, *Building Code Requirements for Reinforced Concrete (ACI 318-89)*, American Concrete Institute, Detroit, MI, 1989.
3. Anderson, Arthur R., and Anderson, Richard G., "An Assurance Criterion for Flexural Bond in Pretensioned Hollow Core Units," *ACI Journal*, Vol. 73, No. 8, Aug. 1976, pp.457-464.
4. Brooks, Mark D., "The Effect of Initial Strand Slip on the Strength and Behavior of Prestressed Concrete Hollow-Core Slabs," *Master Thesis*, Department of Civil, Environmental, and Architectural Engineering, University of Colorado, Boulder, CO, August, 1985.
5. Buckner, Dale C., "An Analysis of Transfer and Development Lengths for Pretensioned Concrete Structures," *Publication No. FHWA-RD-94-049*, Federal Highway Administration, Washington, D.C., Dec. 1994.
6. Cousins, T.E., Johnston, D.W., and Zia, P., "Transfer and Development Length of Epoxy Coated and Uncoated Prestressing," *PCI Journal*, Vol. 36, No. 4, Jul./Aug. 1990, pp. 92-103.
7. Cousins, Thomas E., Badeaux, Michael H., and Moustafa, Saad, "Proposed Test for Determining Bond Characteristics of Prestressing Strand," *PCI Journal*, Vol. 37, No. 1, Jan./ Feb. 1992, pp. 66-73.
8. Deatherage, J.H., Burdette, Edwin G., and Chew, Chong K., "Development Length and Lateral Spacing Requirements of Prestressing Strand for Prestressed Concrete Bridge Girders," *PCI Journal*, Vol. 39, No. 1, Jan./Feb. 1994, pp. 70-82.
9. Gross, Shawn P., and Burns, Ned H., "Transfer and Development Length of 15.2 mm (0.6 in.) Diameter Prestressing Strand in High Performance Concrete: Results of the Hoblitzell-Buckner Beam Tests," *Research Project 9-580*, Center for Transportation Research, University of Texas, Austin, TX, June 1995.
10. Hanson, Norman W., and Kaar, Paul H., "Flexural Bond Tests of Pretensioned Prestressed Beams," *ACI Journal*, Vol. 30, No. 7, Jan. 1959, pp. 783-802.
11. Janney, Jack R., "Nature of Bond in Pre-Tensioned Prestressed Concrete," *ACI Journal*, Vol. 25, No.9, May 1954, pp.717-736.

12. Kaar, Paul H., LaFraugh, Robert W., and Mass, Mark A., "Influence of Concrete Strength on Strand Transfer Length," *PCI Journal*, Vol. 8, No.5, Oct. 1963, pp.47-64.

13. Logan, Donald R., "Acceptance Criteria for Bond Quality of Strand for Pretensioned Prestressed Concrete Applications," *PCI Journal*, Vol. 42, No. 7, Mar./Apr. 1997, pp. 52-90.

14. Logan, Donald R., "Reader Comments on: A Review of Strand Development Length for Pretensioned Concrete Members by C. Dale," *PCI Journal*, Vol. 41, No. 2, Mar./Apr. 1996, pp. 112-127.

15. Martin, Leslie D., and Scott, Norman L., "Development of Prestressing Strand in Pretensioned Members," *ACI Journal*, Vol. 73, No. 8, Aug. 1976, pp. 453-456.

16. Mitchell, D., Cook, W.D., Khan, A.A., and Tham, T., "Influence of High Strength Concrete on Transfer and Development Length of Pretensioning Strand," *PCI Journal*, Vol. 38, No. 3, May/Jun. 1993, pp. 52-65.

17. Nilson, Arthur H., *Design of Prestressed Concrete*, John Wiley & Sons, 1987.

18. Over, R. S., and Au, T., "Prestress Transfer Bond of Pretensioned Strands in Concrete," *ACI Journal*, Vol. 62, No. 11, Nov. 1965, pp. 1451-1460.

19. Shahawy, Mohsen A., Issa, Moussa, and deV Batchelor, Barrington, "Strand Transfer Lengths in Full Scale AASHTO Prestressed Concrete Girders," *PCI Journal*, Vol. 37, No. 3, May/Jun. 1992, pp. 84-96.

20. Tabatabai, Habib, and Dickson, Timothy J., "The History of the Prestressing Strand Development Length Equation," *PCI Journal*, Vol. 38, No. 6, Nov./Dec. 1993, pp. 64-75.

21. Unay, I. O., Russell, B. W., Burns, N. H., and Kreger, M. E., "Measurement of Transfer Length on Prestressing Strands in Prestressed Concrete Specimens," *Research Report 1210-1*, Center for Transportation Research, University of Texas, Austin, TX, 1991.

22. Zia, P., and Mostafa, T., "Development Length of Prestressing Strands," *PCI Journal*, Vol. 22, No. 5, Sep./Oct. 1977, pp. 54-65.

APPENDIX A. CONCRETE STRESS-STRAIN PLOTS

Plots of stress-strain curves for the girder concrete are presented in this appendix.

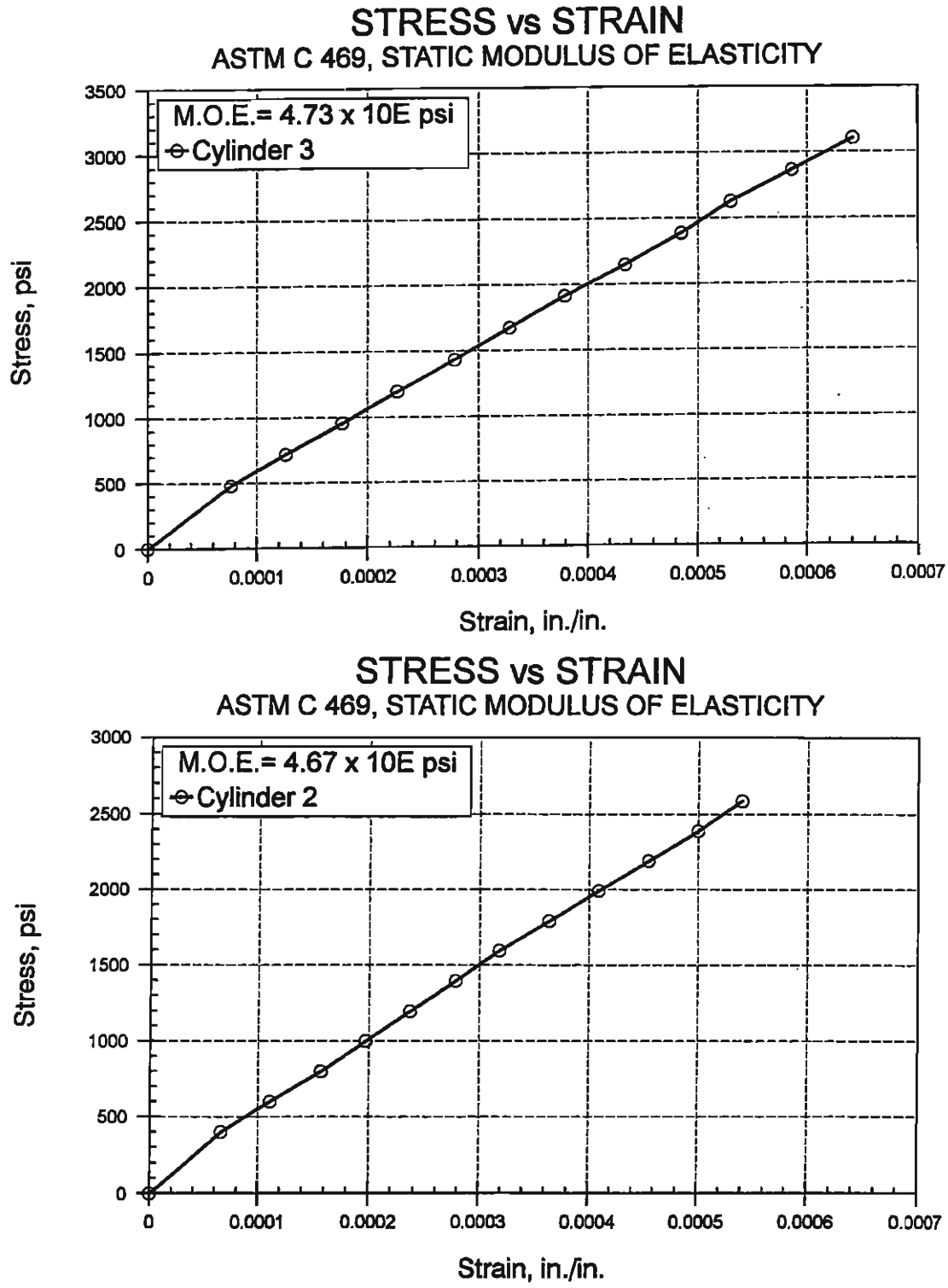

Figure A.1 - Stress-Strain Curves for Air Cured Girder Concrete at 2 Days (CTL/Thompson) (1 psi = 6.89 x 10^3 Pa)

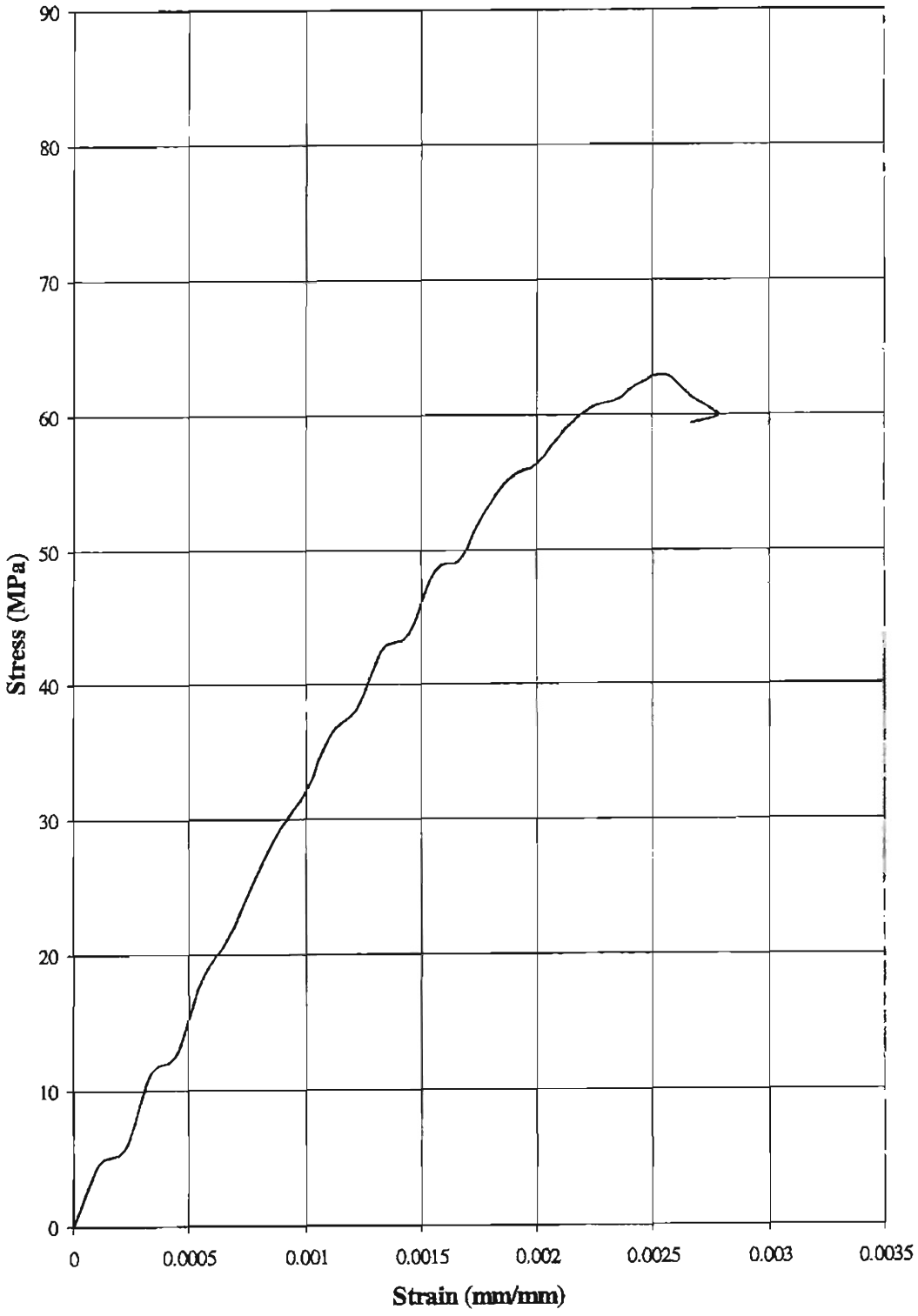

Figure A.2 - Stress-Strain Curve for Moist Cured Girder Concrete at 7 Days

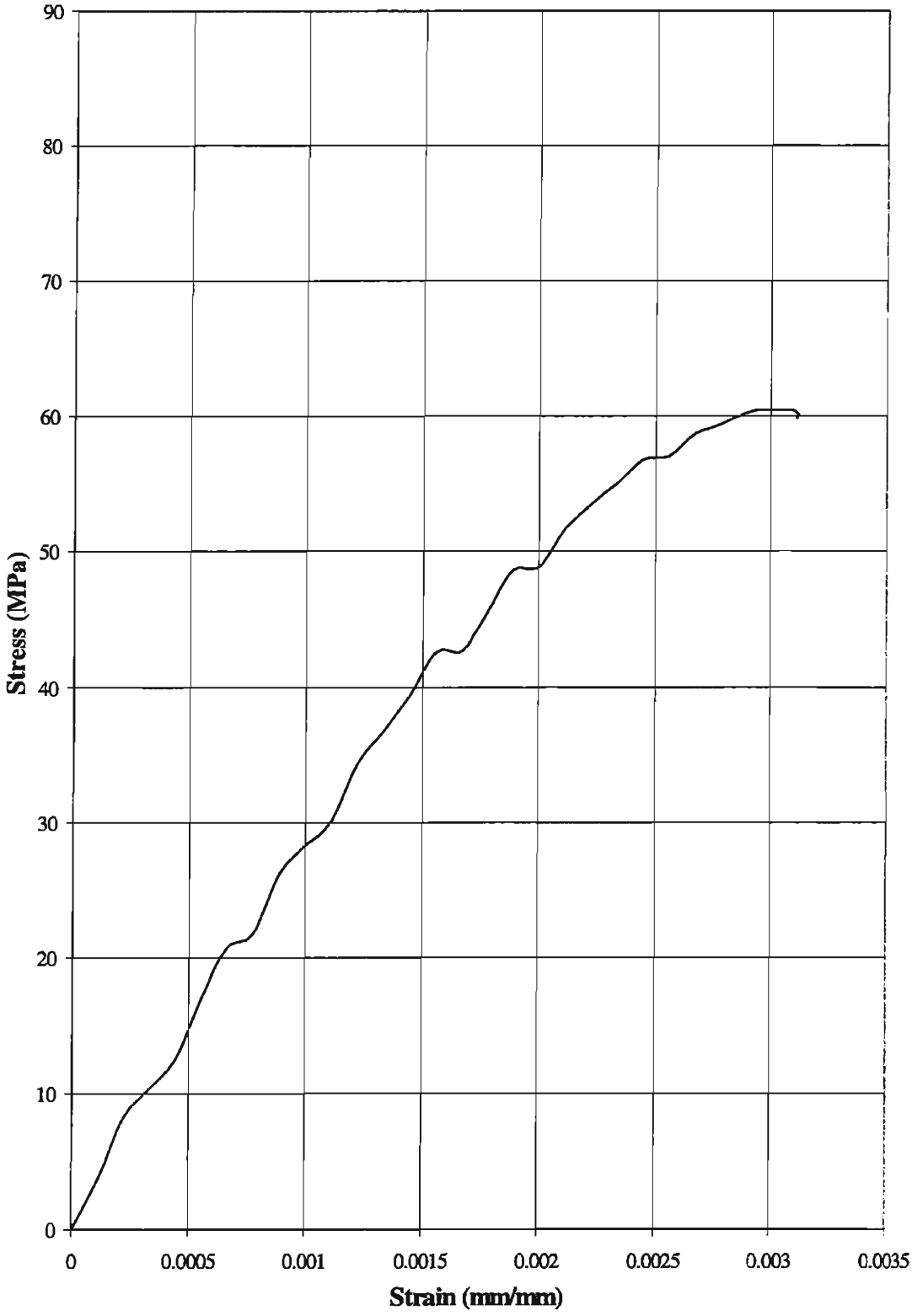

Figure A.3 - Stress-Strain Curve for Air Cured Girder Concrete at 7 Days

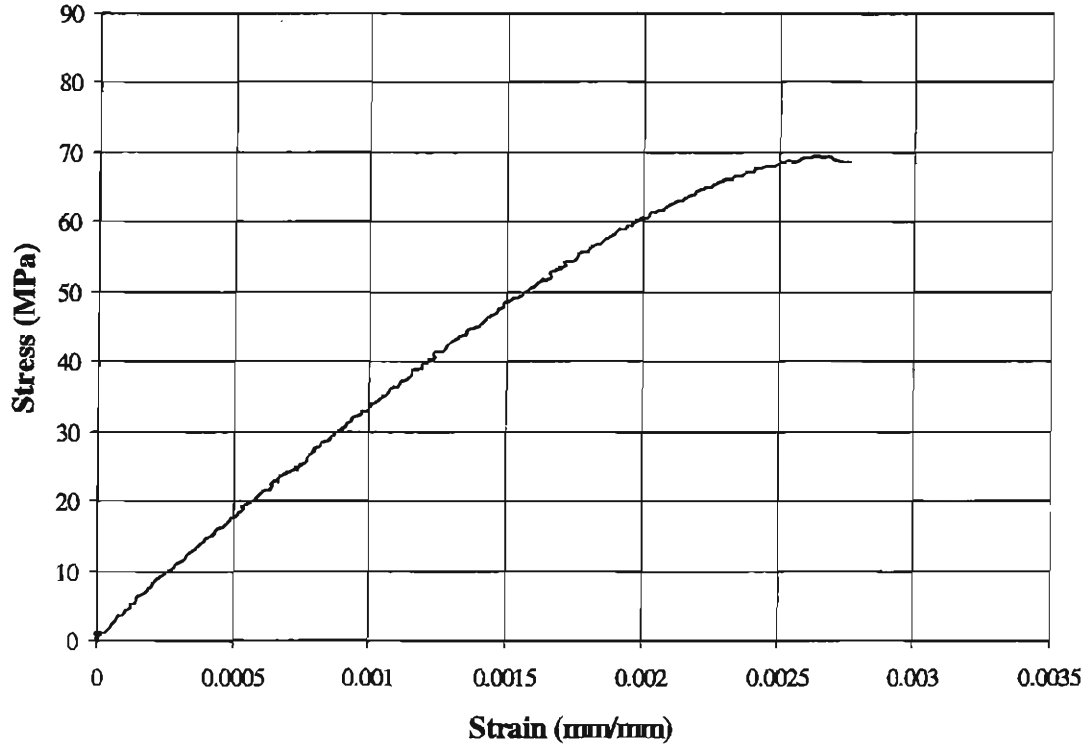

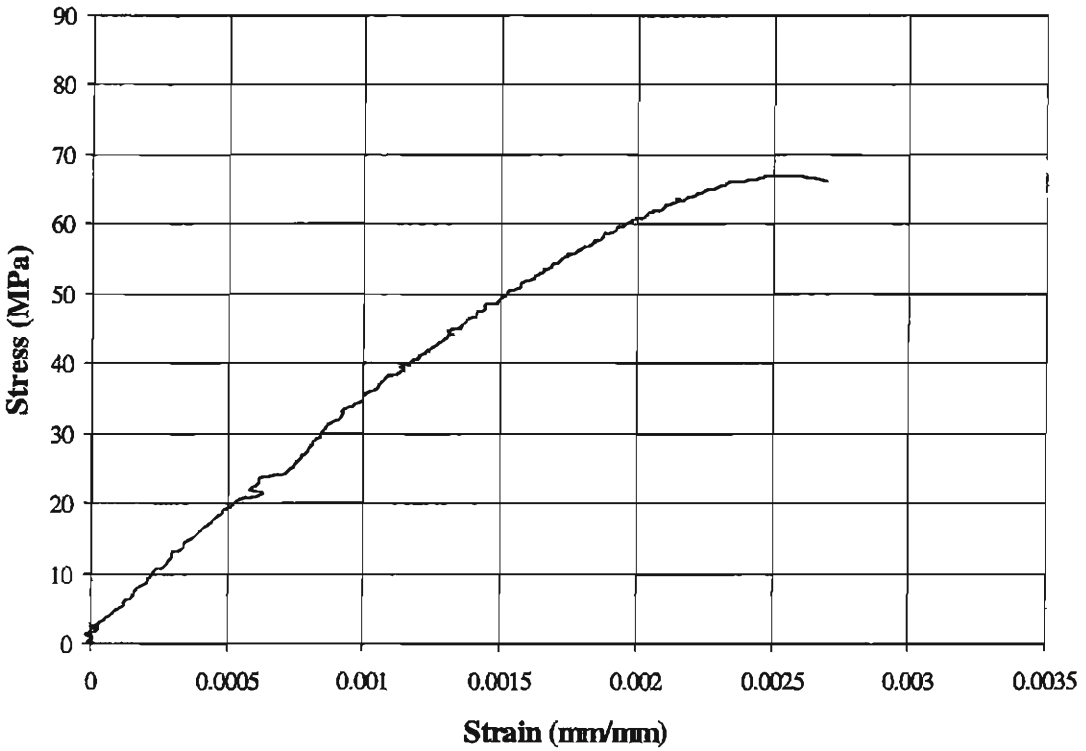

Figure A.4 - Stress-Strain Curves for Moist Cured Girder Concrete at 15 Days

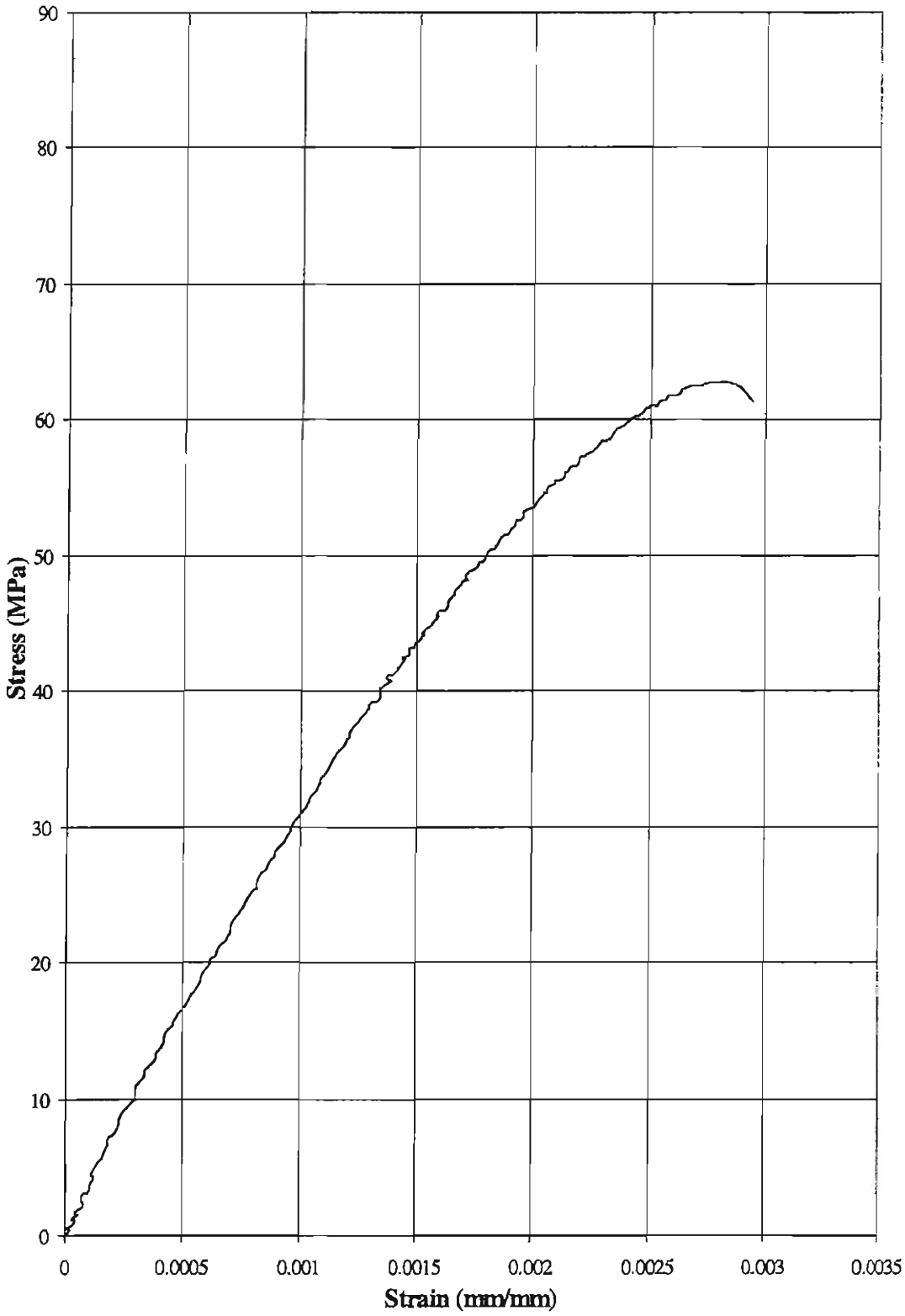

Figure A.5 - Stress-Strain Curve for Air Cured Girder Concrete at 15 Days

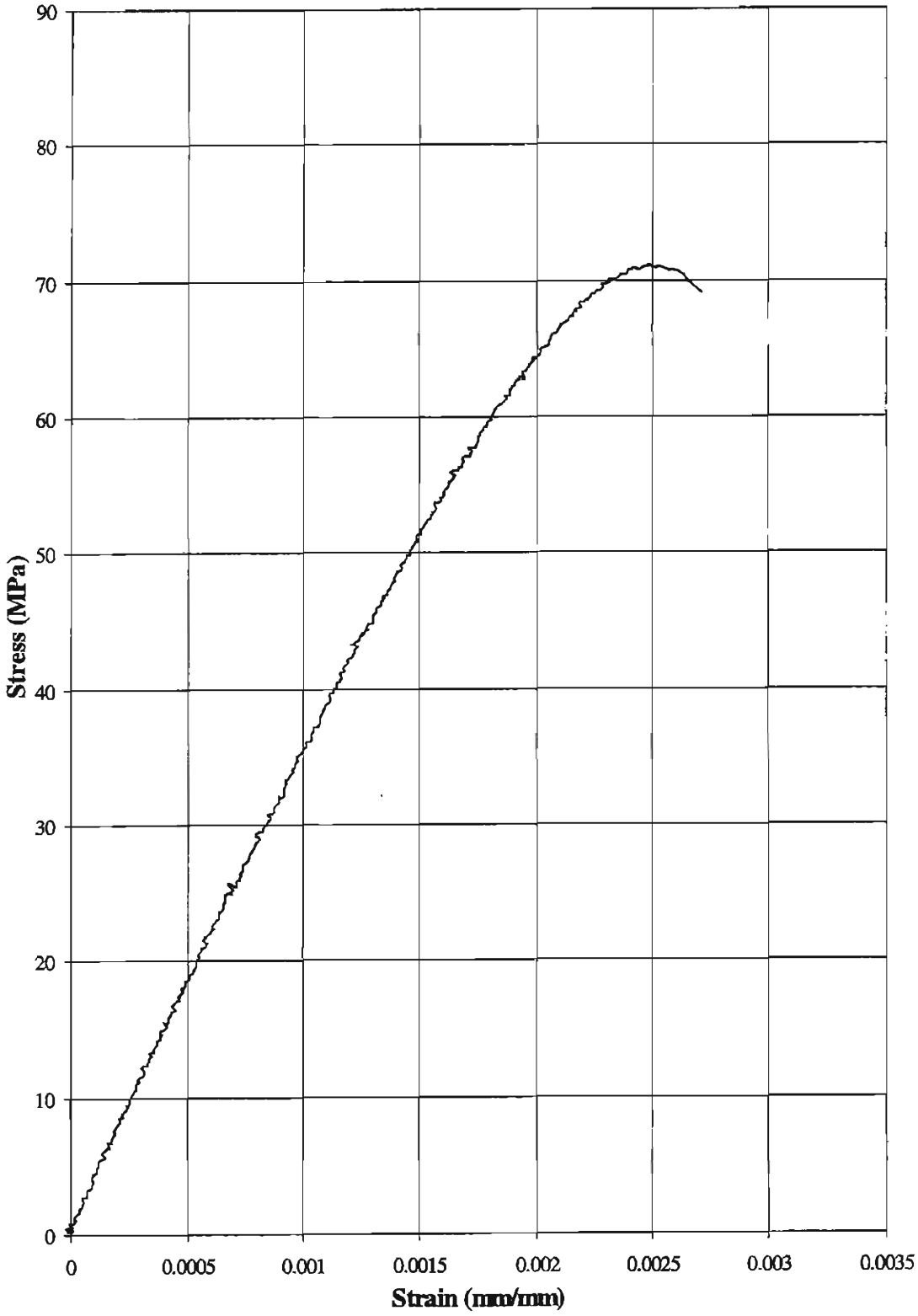

Figure A.6 - Stress-Strain Curve for Moist Cured Girder Concrete at 28 Days

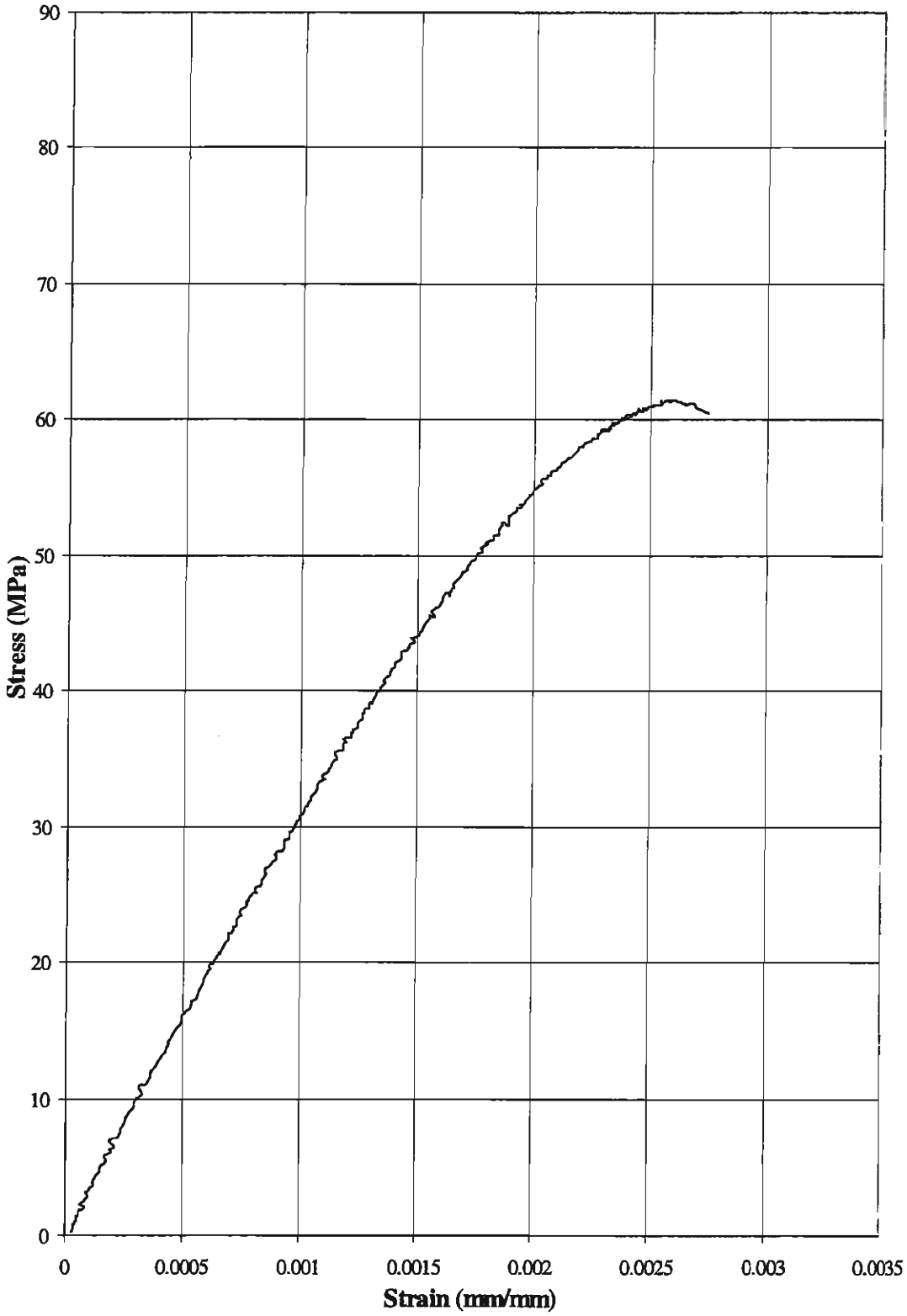

Figure A.7 - Stress-Strain Curve for Air Cured Girder Concrete at 28 Days

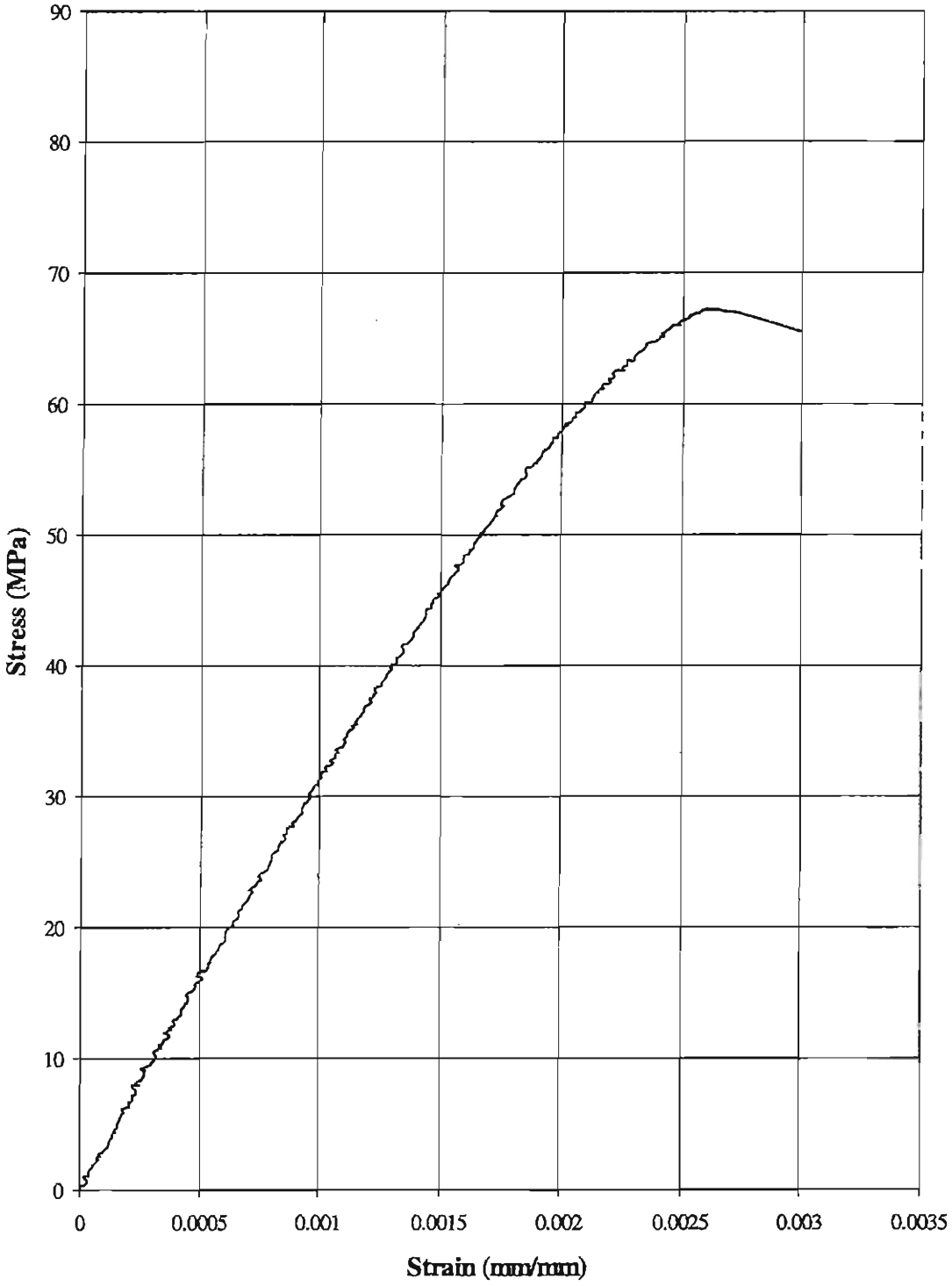

Figure A.8 - Stress-Strain Curve for Air Cured Girder Concrete at 50 Days

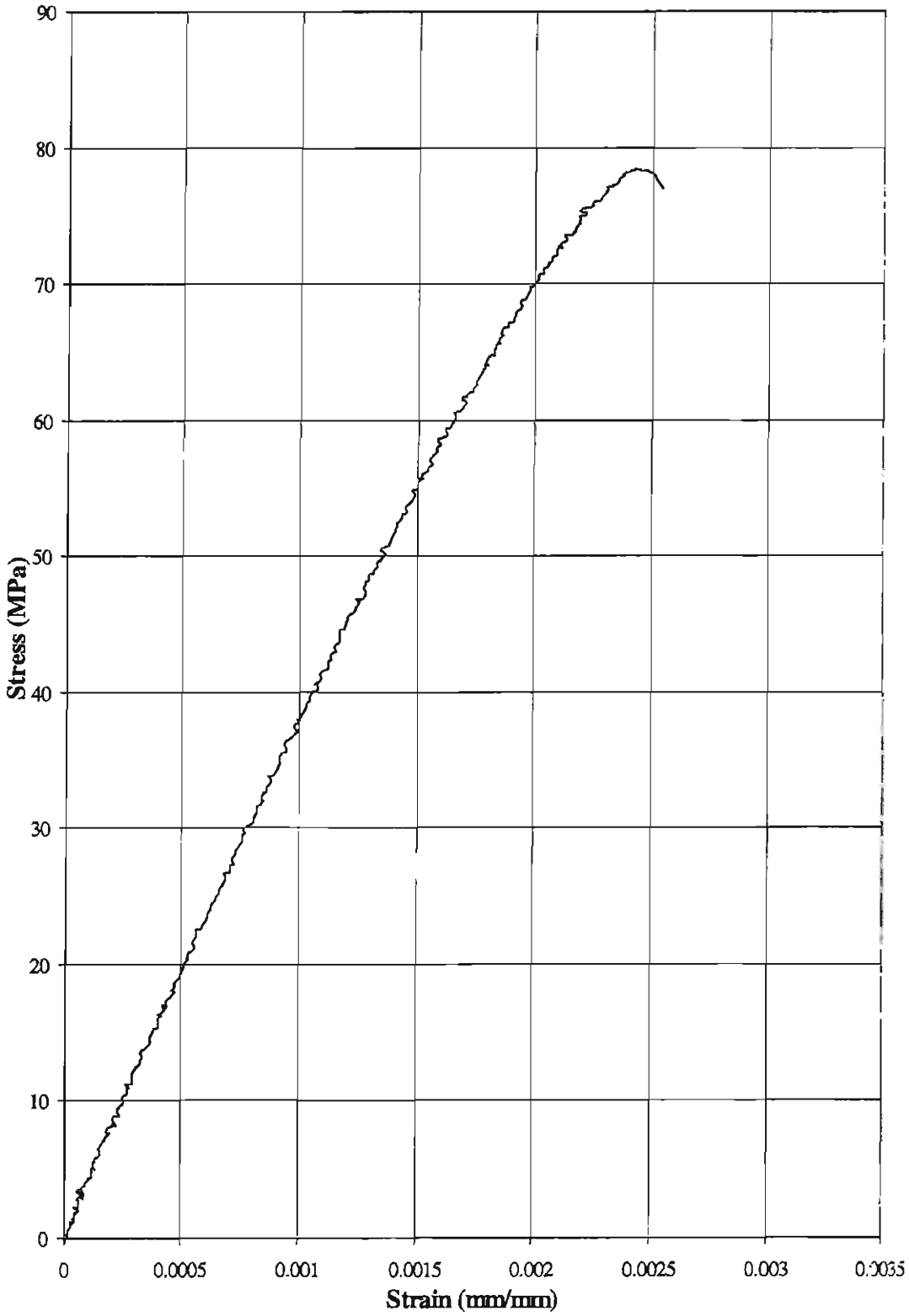

Figure A.9 - Stress-Strain Curve for Moist Cured Girder Concrete at 65 Days

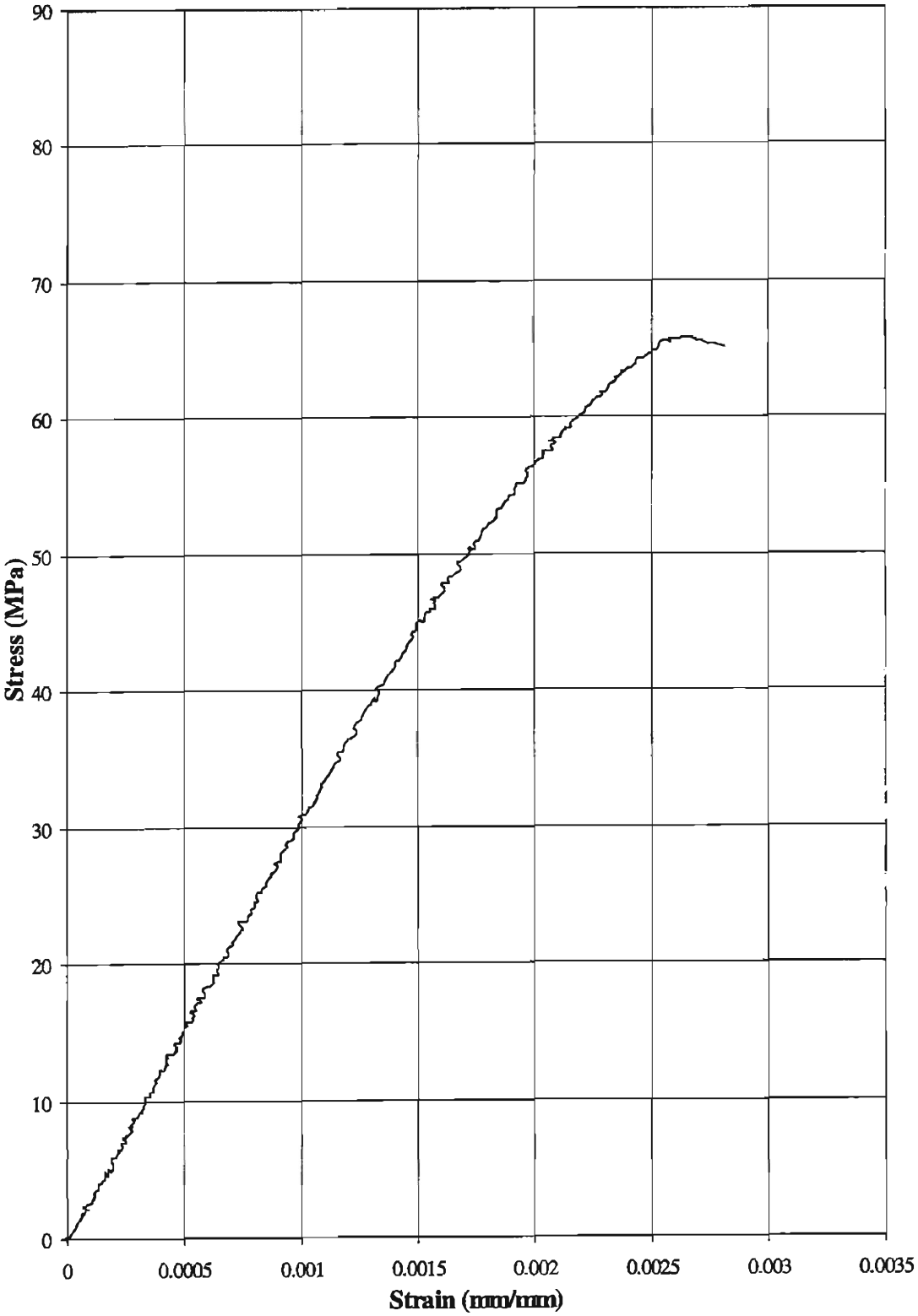

Figure A.10 - Stress-Strain Curve for Air Cured Girder Concrete at 65 Days

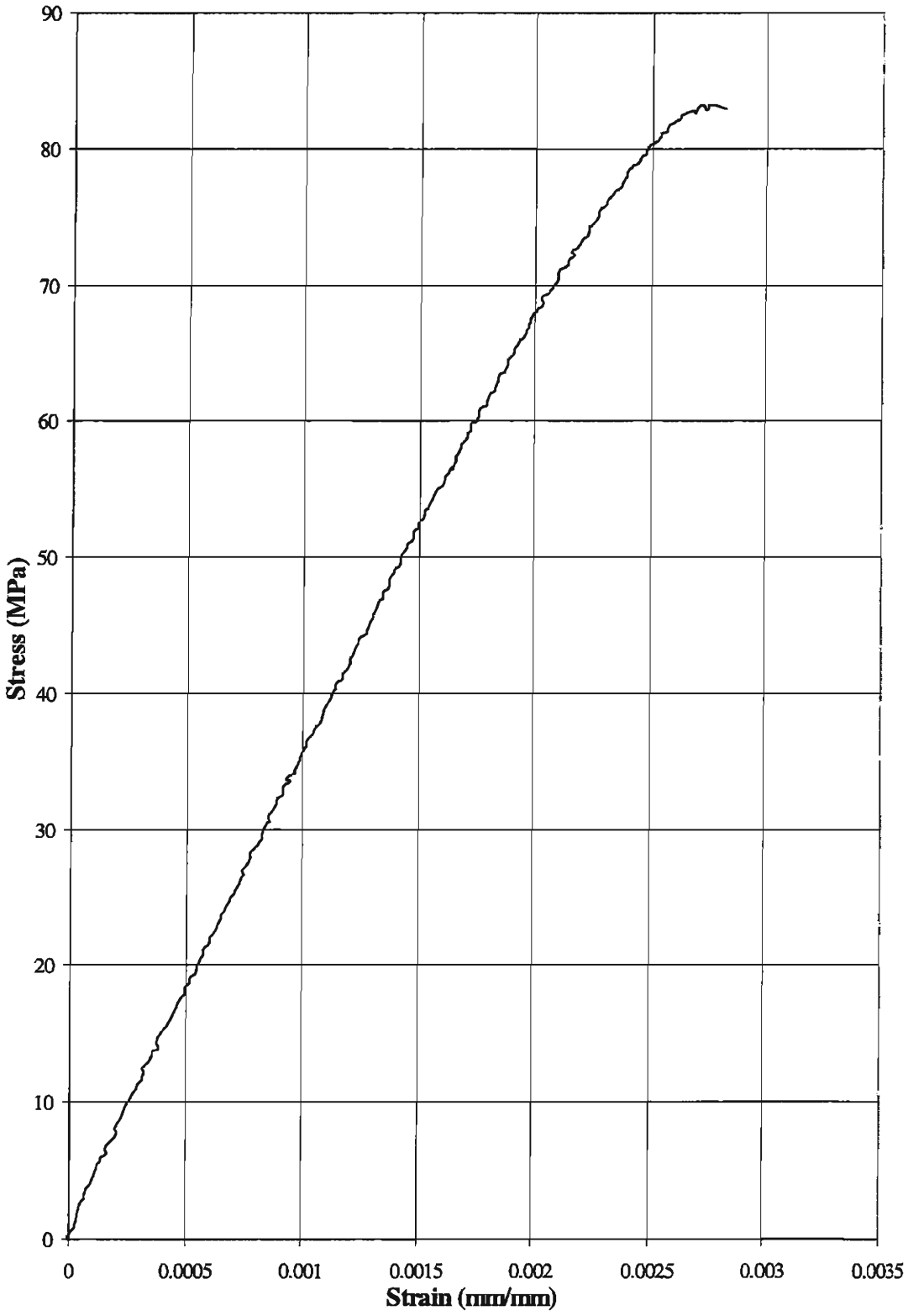

Figure A.11 Stress-Strain Curve for Moist Cured Girder Concrete at 79 Days

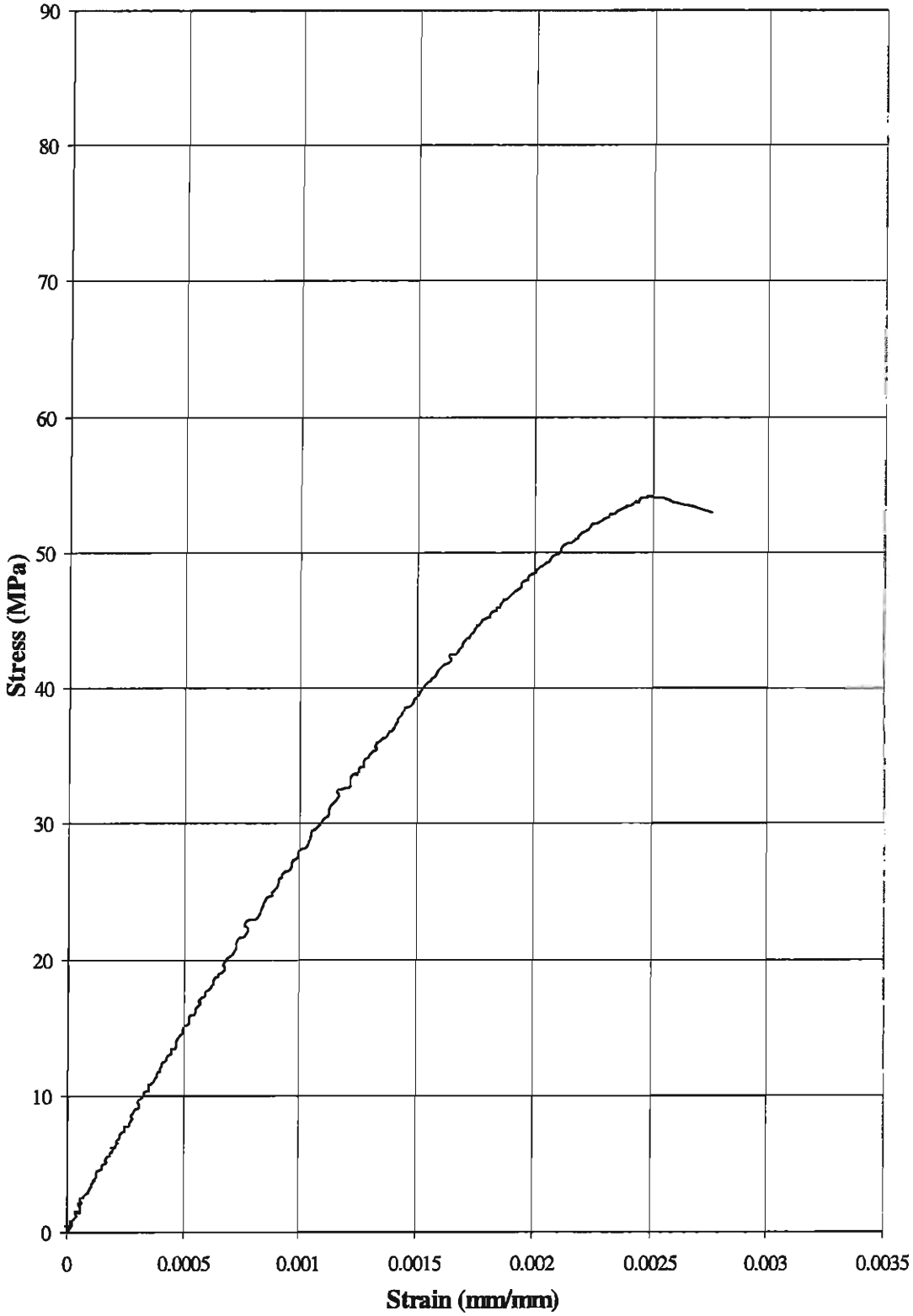

Figure A.12 - Stress-Strain Curve for Air Cured Girder Concrete at 79 Days

APPENDIX B. GIRDER CONCRETE CREEP PLOT

A plot of the creep data obtained by CTL-Thompson for the girder concrete is shown in this appendix.

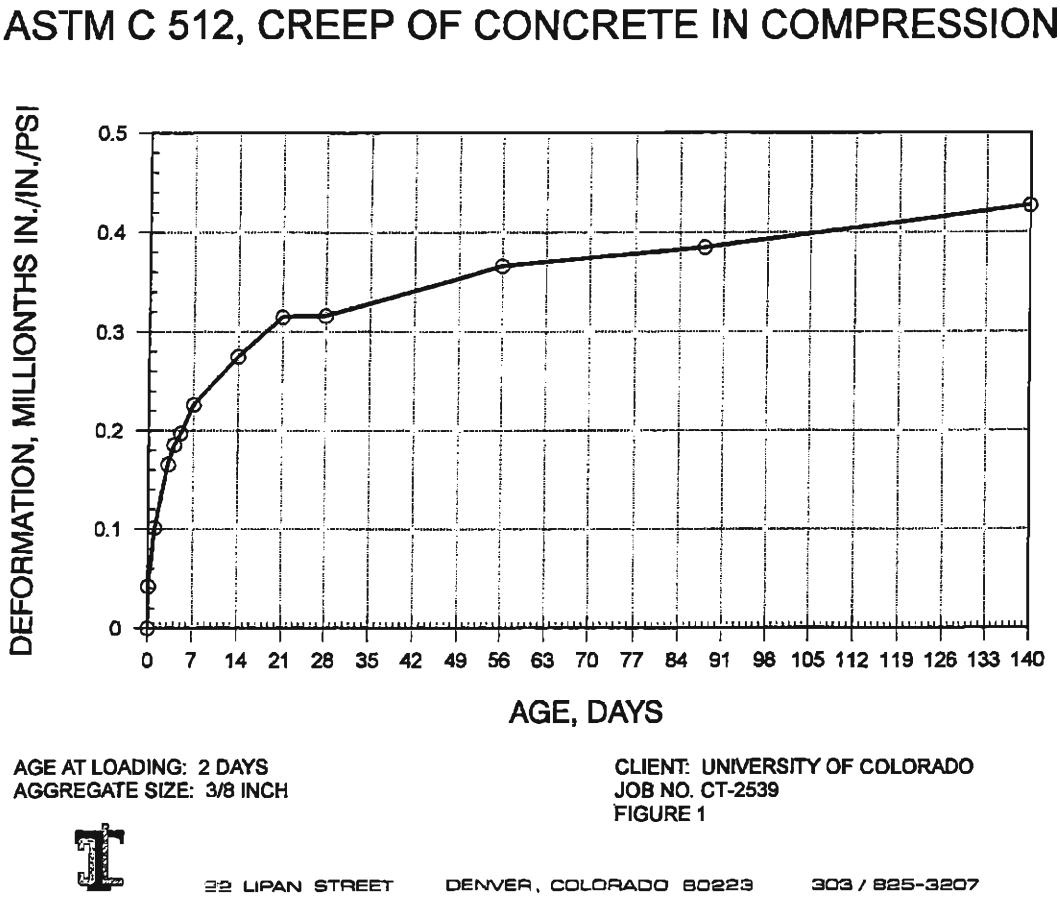

Figure B.1 - Girder Concrete Creep Plot (CTL/Thompson)

(1 psi = 6.89 x 10^3 Pa)

APPENDIX C. GIRDER CURING TEMPERATURE PLOTS

Temperatures measured by the thermocouples in each of the girders over the first 21 hours after casting are shown in the plots in this appendix.

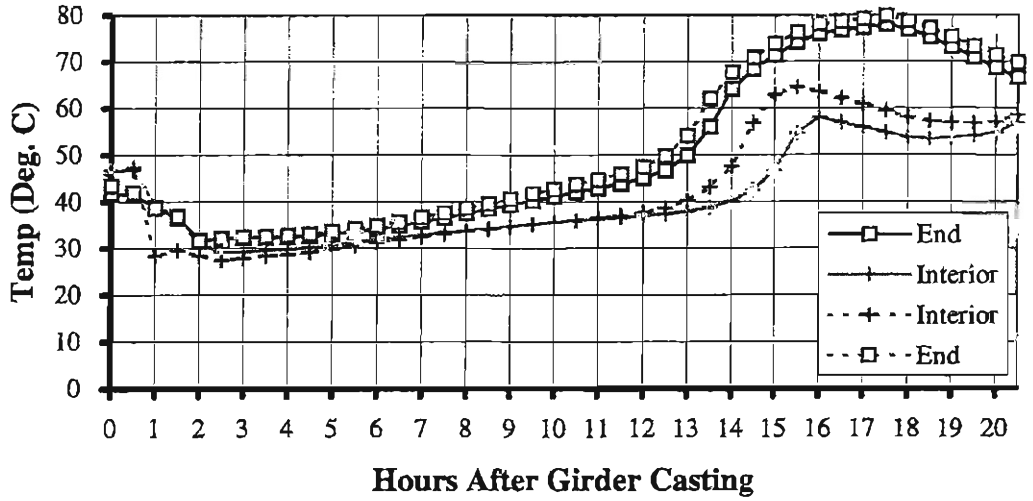

Figure C.1 - Curing Temperatures for Girder 1

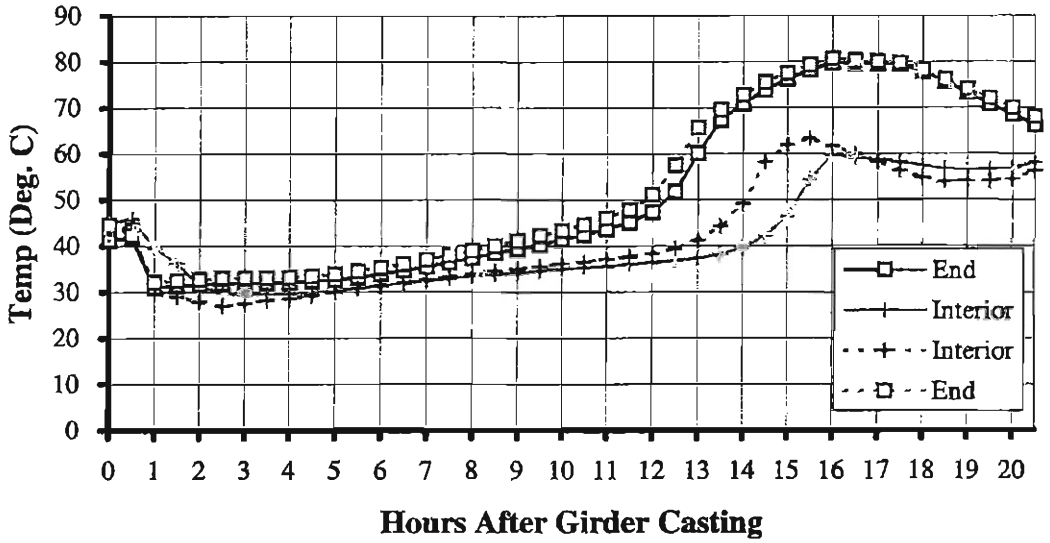

Figure C.2 - Curing Temperatures for Girder 2

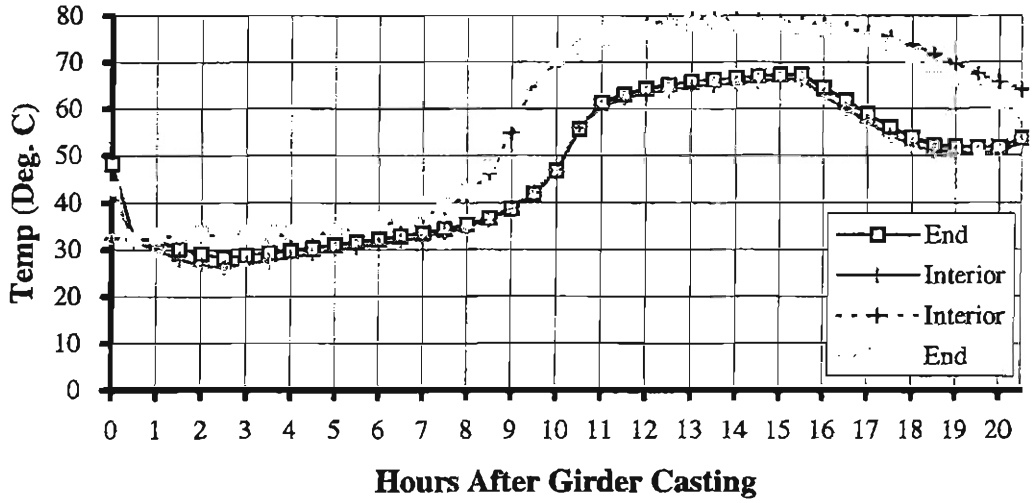

Figure C.3 - Curing Temperatures for Girder 3

APPENDIX D. STRAND SLIP PLOTS

Strand slips measured by the LVDT's during each girder test are shown in this appendix. Only the results from tests in which strand slip occurred are shown.

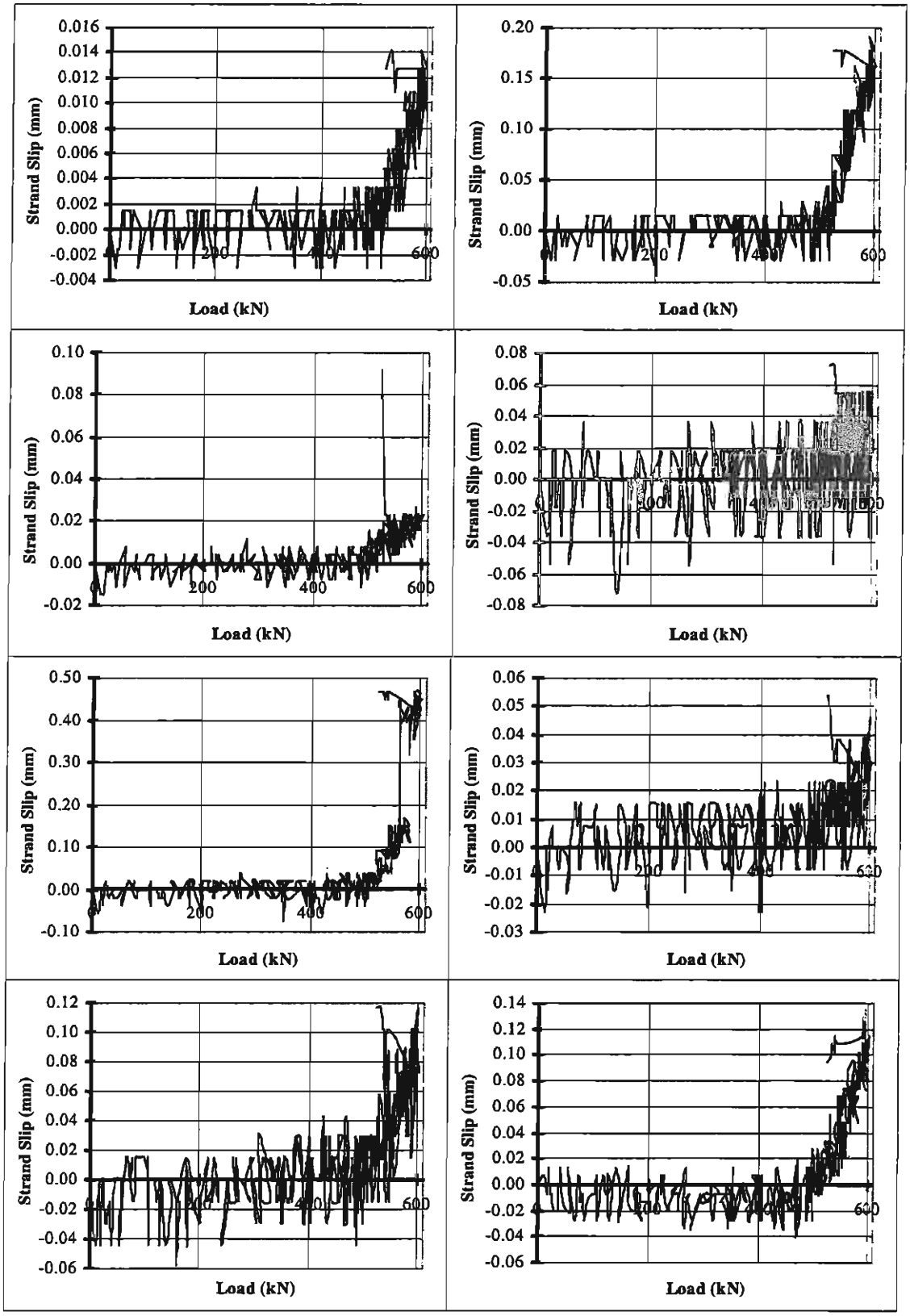

Figure D.1 - Strand Slip Measurements from Test 2-W

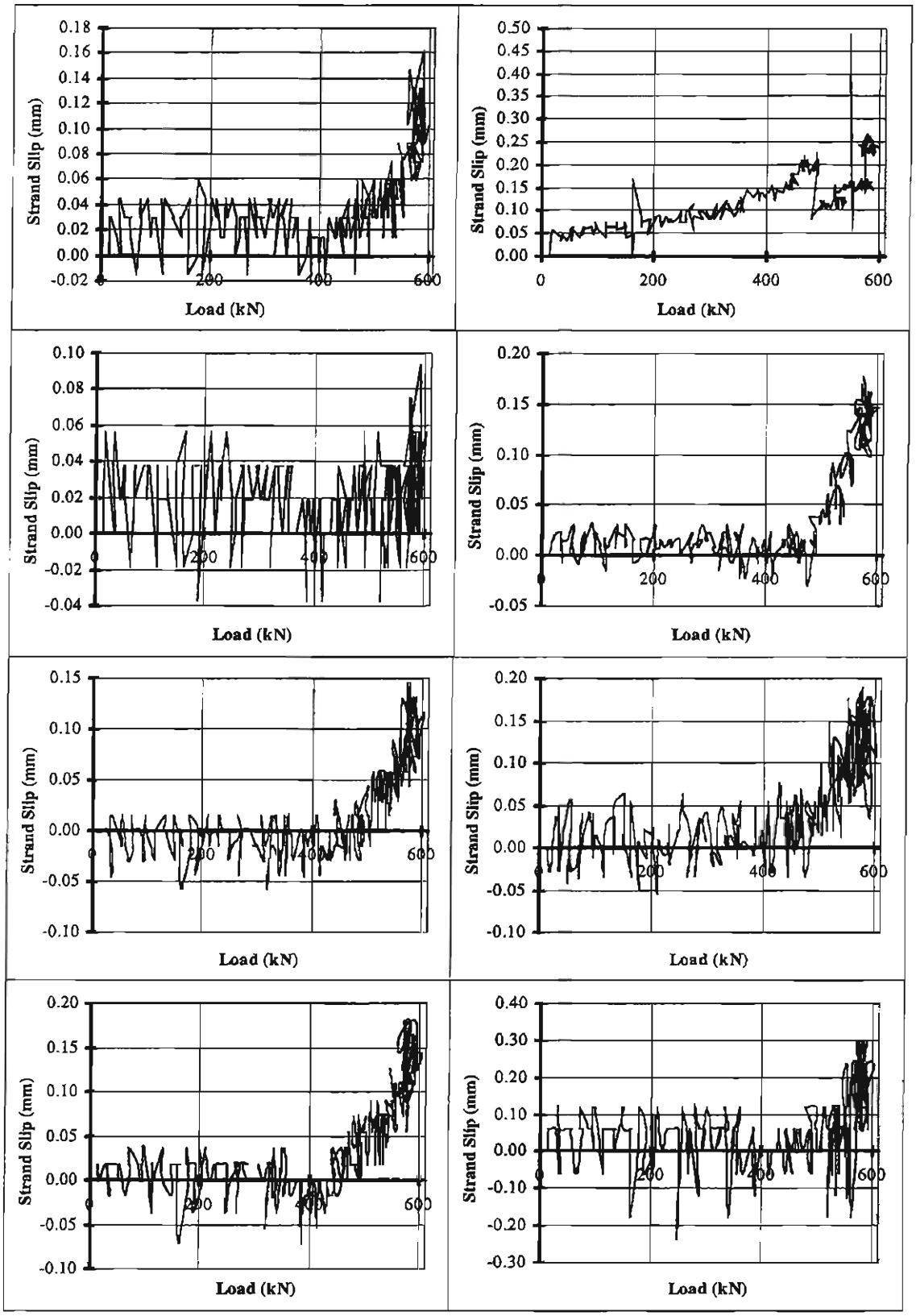

Figure D.2 - Strand Slip Measurements from Test 2-E

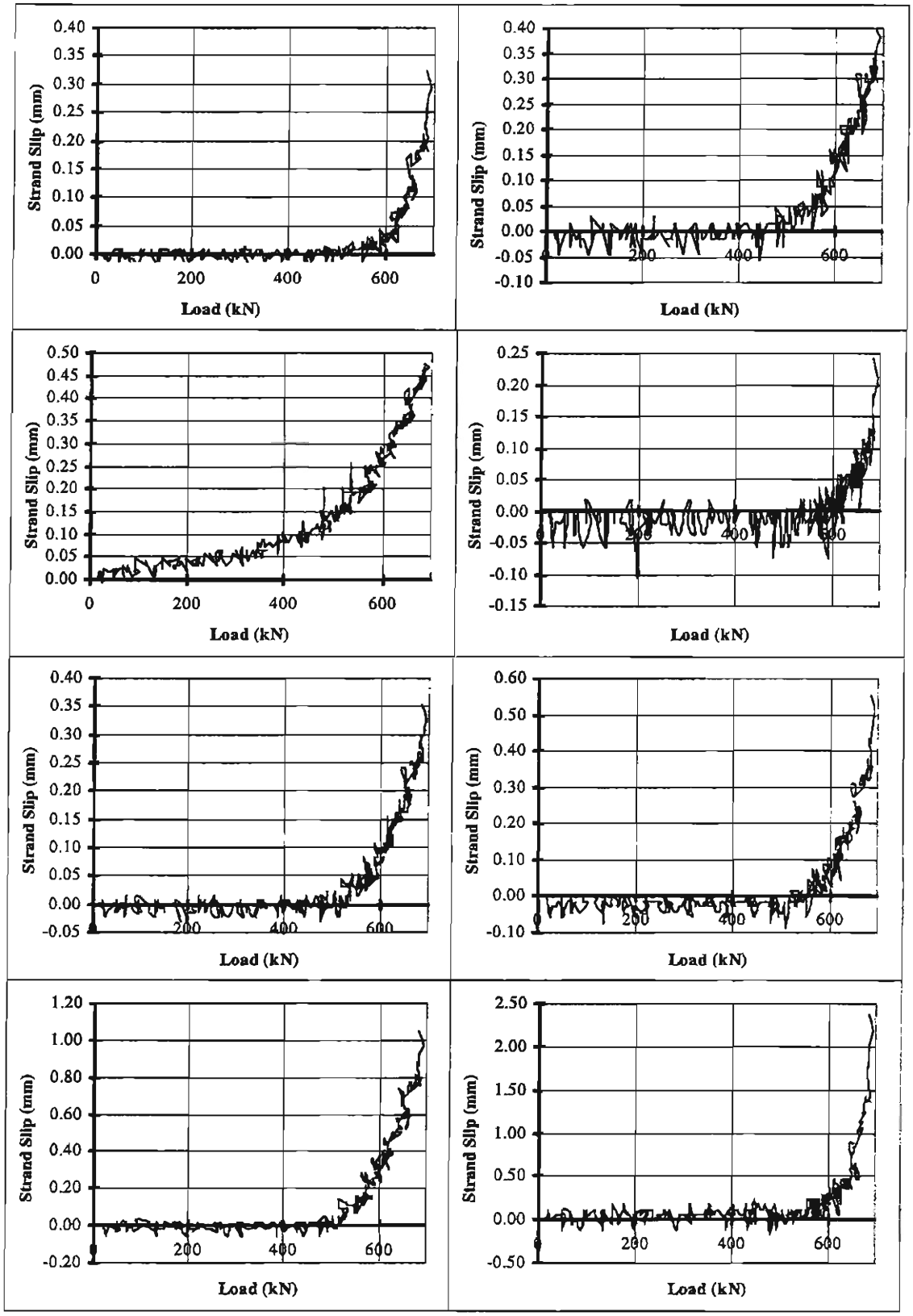

Figure D.3 - Strand Slip Measurements from Test 3-E

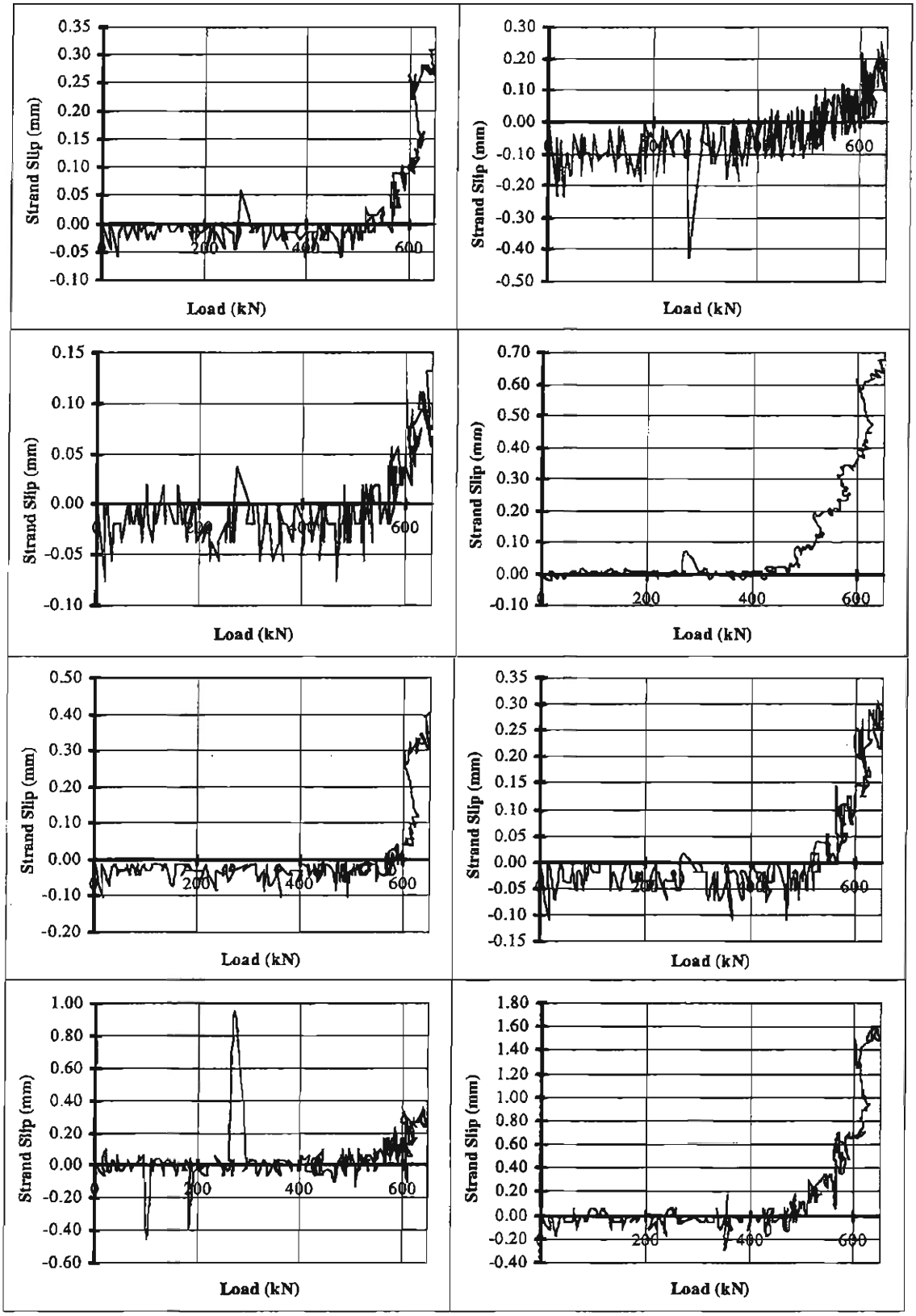

Figure D.4 - Strand Slip Measurements from Test 3-W

APPENDIX E. STRAND CHEMICAL TEST RESULTS

The results of chemical tests performed on samples of strand by Hauser Chemical Research Company are presented in this appendix. These strand samples were taken from the same roll of strand as the strand used in the test girders.

HAUSER®

June 10, 1997
Test Report No. M80011

CLIENT: University of Colorado at Boulder
Department of Civil, Environmental and
Architectural Engineering
Boulder, CO 80309-0428

Attn: Professor P. Benson Shing

MATERIALS: Two coated metal samples received 5/9/97 not labeled, described as:

1. Braided Metal Cable
2. Braided Metal Cable

TESTS: Determine amount of phosphate coating on braided steel cable using the client-supplied method below:

TEST METHOD: The sub-sample was prepared by cutting each of the 7-wire samples received for testing into sections varying from 1 3/16 to 1 3/4" long. The weight of each segment was measured to 0.1 mg.

A stripping solution consisting of 20% (w/w) chromium trioxide was heated to 180 - 200°C. A section of the test wire was weighed to 0.1 mg and its surface area was determined in square inches. The wire was immersed in the hot stripping solution for two minutes. The wire was removed and rinsed promptly in cold running water. The wire was dried by dipping in acetone and holding the wire in front of a fan. The stripped wire was reweighed.

The wire sections were identified as 125-n for Sample #1 and 126-n for Sample #2.

HAUSER CHEMICAL RESEARCH, INC.
5555 Airport Blvd. • Boulder, CO 80301-2339 • Ph: (303) 443-4662 • FAX: (303) 441-5800

The length of each cut section was measured using a dial caliper, The diameters were measured twice, at 90°, and the average was reported. The surface area of the wire was calculated without considering the cut ends.

RESULTS: The results of the stripping operations are given in Tables I and II.

Table I

WIRE SECTION NUMBER	LENGTH	DIAMETER	MASS BEFORE STRIPPING	MASS AFTER STRIPPING	PHOSPHATE, MG/SQ IN.
125-1	1.843	0.1970	7.1483	7.1437	4.034
125-2	1.835	0.1968	6.8906	6.8874	2.821
125-3	1.829	0.1963	7.0802	7.0760	3.724
125-4	1.684	0.1965	6.5120	6.5082	3.655
125-5	1.698	0.1966	6.5703	6.5649	5.151
125-6	1.718	0.1962	6.6288	6.6265	2.172
125-7	1.828	0.1963	7.1001	7.0946	4.880
125-8	1.672	0.2069	7.1635	7.1611	2.208
125-9	1.810	0.2071	7.7635	7.7618	1.444
125-10	1.835	0.1971	7.1364	7.1328	3.169
125-11	1.753	0.1973	6.8026	6.7995	2.854
125-12	1.685	0.1965	6.2710	6.2680	2.884
125-13	1.727	0.2070	7.3919	7.3887	2.849
125-14	1.752	0.1963	6.7104	6.7070	3.147
125-15	1.829	0.1964	7.0768	7.0705	5.584
125-16	1.885	0.1972	6.5873	6.5830	4.120
125-17	1.684	0.1965	6.5202	6.5170	3.078
125-18	1.753	0.1972	6.7851	6.7805	4.237
125-19	1.780	0.1963	6.4993	6.4959	3.097
125-20	1.679	0.1971	6.5558	6.5524	3.271
125-21	1.689	0.1968	6.5108	6.5061	4.501
Averages		0.1982	6.8431	6.8393	3.470
Standard deviations		0.0037	0.3654	0.3655	1.030

Table II

Wire Section Number	Length	Diameter	Mass before stripping	Mass after stripping	Phosphate, mg/sq. in.
126-1	1.390	0.1964	5.4040	5.4022	2.099
126-2	1.306	0.1973	5.4053	5.4007	5.318
126-3	1.451	0.1968	5.6184	5.6143	5.470
126-4	1.769	0.1972	6.8602	6.8556	4.199
126-6	1.425	0.1967	5.4648	5.4607	4.656
126-7	1.737	0.2069	7.4484	7.4463	1.860
126-8	1.424	0.1968	5.4935	5.4899	4.090
126-9	1.742	0.1963	6.7369	6.7331	3.538
126-10	1.736	0.1962	6.7122	6.7093	2.710
126-11	1.754	0.1964	6.8046	6.8004	3.882
126-12	1.467	0.1965	5.6897	5.6865	3.534
126-13	1.460	0.2071	6.2677	6.2653	2.527
126-14	1.492	0.1972	5.8274	5.8236	4.111
126-15	1.733	0.1964	6.7340	6.7286	5.052
126-16	1.393	0.2069	5.9757	5.9738	2.099
126-17	1.392	0.1972	5.4227	5.4195	3.711
126-18	1.491	0.1971	5.8092	5.8056	3.901
126-19	1.478	0.1966	5.7083	5.7054	3.178
126-20	1.421	0.1965	5.4894	5.4855	4.446
126-21	1.455	0.1973	5.6318	5.6281	4.103
Averages		0.1983	6.0252	6.0217	3.6791
Standard deviations		0.0038	0.6286	0.6286	0.9911

COMMENTS: Section 126-5 was damaged during processing and was deleted from the data set.

WORK PERFORMED BY: Perry Christopher, Technician II

WORK SUPERVISED BY:

Ronald L. Turner
Senior Chemist

REPORT REVIEWED BY:

John Elverum
Staff Chemist